



## Faro Mine Complex NP Study Report

2008/09 Task 18 - FINAL

*Prepared for:*

**DELOITTE & TOUCHE INC.**  
*Interim Receiver of Anvil Range Mining Corporation*  
30 Wellington Street West  
Toronto, ON M5L 1B1

*On behalf of*  
**Faro Project Management Team**



*Prepared by:*



*Project Reference Number:*  
SRK 1CD003.114



**May 2009**

**Faro Mine Complex  
NP Study Report  
2008/09 Task 18 - FINAL**

Report prepared for

**Deloitte & Touche Inc.**

Suite 1900, 30 Wellington Street West  
Toronto, ON M5L 1B1  
Canada

on behalf of  
**Faro Project Management Team**

**SRK Consulting (Canada) Inc.**

Suite 2200, 1066 West Hastings Street  
Vancouver, B.C. V6E 3X2

Tel: 604.681.4196 Fax: 604.687.5532  
E-mail: [vancouver@srk.com](mailto:vancouver@srk.com) Web site: [www.srk.com](http://www.srk.com)

**SRK Project Number 1CD003.114**

**May 2009**

## Executive Summary

---

<u>Title:</u>	Faro Mine Complex: NP Study Report – 2008/09 Task 18- FINAL
<u>Consultant:</u>	SRK Consulting (Canada) Inc.
<u>Status:</u>	Final
<u>Date:</u>	May 2009
<u>Size:</u>	20 Pages of text (including cover, introductory and reference list); 10 Pages of Figures (including one flysheet), 5 Appendices containing 97 pages (including 3 non-standard 11 x 17 pages and 5 flysheets).
<u>Digital File:</u>	PDF format; 6.33 MB

---

### Objectives and Primary Findings:

This report summarizes the results of a study designed to better understand the mineralogical sources of neutralization potential (NP) in Anvil Range waste rock types.

Three Faro waste rock units were evaluated. Samples of the largest waste rock unit (biotite schist- Unit 1D) were found to have calcium and magnesium carbonate contents that agreed well with laboratory measurements of NP. Samples of Unit 3D (calc-silicate schist (the second largest waste rock unit)) were found to have a component of measured NP that was derived from silicate minerals. However, almost all samples of Unit 3D were also found to have sufficient calcium and magnesium carbonate content to maintain neutral pH conditions over the long term. A third, and volumetrically less important, Faro waste rock unit (Unit 10E- hornblende quartz diorite) was evaluated, with results indicating that a portion of the measured NP for this unit was derived from silicate minerals. If the silicates are not considered to be an effective source of neutralization potential, a somewhat larger portion of Unit 10E waste could be potentially acid generating than indicated by previous interpretations of ABA data.

Four Grum waste rock units were evaluated (Unit 3G0, Unit5A0, Unit 5B0, and Unit 5D). For all four units, calcium and magnesium carbonate minerals were found to be the source of nearly all of the laboratory measured NP.

One Vangorda waste rock unit was evaluated (Unit 3G0). Both measured NP and calcium and magnesium carbonate content were low in all samples, with the results suggesting that a portion of the measured NP was derived from silicate minerals. The results are somewhat inconclusive, as analytical uncertainty can be significant for samples with low NP and carbonate mineral abundance.

### Future Work Recommendations:

Based on the findings of this study, no further work on refining the understanding of neutralization potential in Faro Mine Complex waste rock is recommended.

# Table of Contents

Executive Summary .....	i
<b>1 Introduction .....</b>	<b>1</b>
1.1 Background .....	1
1.2 Testing Program Design .....	1
<b>2 Methods .....</b>	<b>2</b>
2.1 Sample Collection .....	2
2.2 Laboratory Testing .....	3
2.2.1 ABA .....	3
2.2.2 Elemental Content .....	3
2.3 Mineralogical Characterization .....	3
2.3.1 Sample Selection .....	3
2.3.2 Petrographic Analysis .....	3
2.3.3 Quantitative XRD .....	3
2.3.4 Electron Microprobe Analysis .....	3
<b>3 Results .....</b>	<b>4</b>
3.1 Laboratory Testing .....	4
3.1.1 ABA .....	4
3.1.2 Elemental Content .....	4
3.2 Mineralogical Characterization .....	5
3.2.1 Petrographic Analysis .....	5
3.2.2 Quantitative XRD .....	5
3.2.3 Electron Microprobe Analysis .....	6
<b>4 Discussion .....</b>	<b>7</b>
4.1 Neutralization Potential .....	7
4.1.1 Comparison of NP and Inorganic Carbon Content .....	7
4.1.2 Comparison of NP with Calcium and Magnesium Carbonate Content .....	8
4.2 Implications for ARD Classification of Waste Rock .....	11
4.2.1 Faro .....	11
4.2.2 Grum .....	12
4.2.3 Vangorda .....	12
<b>5 Conclusions and Recommendations .....</b>	<b>13</b>
<b>6 References .....</b>	<b>16</b>



## List of Tables

Table 1:	Summary of Samples Collected .....	2
Table 2:	Carbonate Content Reported from Petrographic Analysis.....	5
Table 3:	Carbonate Content Determined by Rietveld XRD .....	6
Table 4	Average Compositions of Carbonate Minerals in Anvil Range Waste Rock Samples Studied in 2008.....	9
Table 5:	Availability of NP.....	10

## List of Figures

Figure 1	NP vs. AP by Rock Type- Faro (2008 and Historical Data)
Figure 2	NP vs. AP by Rock Type- Grum (2008 and Historical Data)
Figure 3	NP vs. AP by Rock Type- Vangorda (2008 and Historical Data)
Figure 4	Ternary Diagram of Faro Carbonate Mineral Composition
Figure 5	Ternary Diagram of Grum Carbonate Mineral Composition
Figure 6	Ternary Diagram of Vangorda Carbonate Mineral Composition
Figure 7	Comparison of NP and TIC
Figure 8	Comparison of $IC_{Ca,Mg}$ and NP
Figure 9	Comparison of NP:AP and $(NP*0.55):AP$ for the Historical ABA database

## List of Appendices

Appendix A	ABA Results
Appendix B	Elemental Content
Appendix C	Optical Petrography
Appendix D	X-ray Diffraction Results
Appendix E	Electron Microprobe Analyses

# 1 Introduction

## 1.1 Background

In March 2007, the Independent Peer Review Panel (IPRP) issued their final report “Review of Remediation Alternatives for the Anvil Range Mine Complex” (IPRP 2007). One of the recommendations made by the IPRP was to conduct additional test work to better understand the forms and availability of neutralization potential (NP) in waste rock. Specific recommendations made by the IPRP with respect to this issue included:

- *“conducting additional test work to better estimate the magnitude of the neutralizing potential (NP) and the time to the onset of acidity”; and*
- *“Quantitative mineralogy, along with Modified Sobek NP, should be conducted on a representative set of samples for each waste rock type to estimate the magnitude of the contribution of the iron and manganese carbonates and relatively un-reactive silicates to the results of the modified Sobek NP procedure. Detailed quantitative mineralogical analysis could also be used to check assumptions regarding minerals contributing to other test results.”*

The basis for these recommendations is that the proportion of non-potentially acid generating rock may be overestimated or that the time to onset of acidic conditions may be overestimated due to potential overestimation of the effective NP in test samples. NP can be overestimated in some test procedures and in some samples due to the presence of poorly reactive silicate minerals, overly aggressive amounts of acid addition, or insufficient oxidation of iron during the back-titration step of the NP test for samples that contain iron and manganese carbonates. The Modified Sobek procedure for NP determination provides a more consistent target for acid addition. Additionally, Jambor (2003) has shown that the Modified Sobek procedure accounts for both the initial neutralization provided by iron and manganese carbonates and the subsequent acidity released when the ferrous iron or manganese II are oxidized. However, the relative contribution of silicate and carbonate minerals can only be definitively resolved through mineralogical studies.

Historical and more recent characterization programs have not specifically examined the mineralogical forms of NP in the waste rock. To address the IPRP recommendations, some further work to determine the mineralogical forms and availability of NP was proposed, and the results of that work form the basis of this report.

## 1.2 Testing Program Design

The NP study included identification and quantification of carbonate mineral phases in all of the major non-sulphide waste rock units. The specific composition of the carbonate minerals was also identified through electron microprobe analyses. The study consisted of two phases:

- Representative samples were collected from each of the major non-sulphide units and submitted for an initial phase of ABA and elemental analyses. The results were compared to the historical database to establish whether they were representative of the larger dataset, and were used to inform selection of a subset of samples for the detailed mineralogical characterization.
- A subsequent phase of investigations was planned consisting of petrographic analysis, determinations of mineral phase and abundance by x-ray powder diffraction, and determination of carbonate mineral species using electron microprobe analysis.

As calcium and magnesium carbonate minerals are likely to be the major source of neutralization under near-neutral weathering conditions, particular emphasis was placed on the determination of calcium and magnesium carbonate content of the Anvil Range waste rock samples.

Massive and semi-massive sulphide waste units were excluded from the study as these units do not contain appreciable amounts of NP.

## 2 Methods

### 2.1 Sample Collection

Rock samples collected in 2002 were no longer available for testing, therefore additional rock samples were collected from the mine site for this study. A total of 39 samples were collected by SRK staff from 8 different rock types (Table 1). Grab samples were collected from pit walls or from waste rock dumps during site visits in 2007 and 2008.

**Table 1: Summary of Samples Collected**

Rock Code	Lithological Description	No. of Samples	Mine Area
1D	Biotite schist	11	Faro
3D	Amphibolite and calc-silicate schist	6	Faro
10E	Hornblende biotite quartz diorite	2	Faro
10F	Quartz feldspar porphyry	1	Faro
3G0	Non-calcareous phyllite	3	Grum
5A0	Carbonaceous phyllite	3	Grum
5B0	Calcareous phyllite	7	Grum
5D	Chlorite phyllite	3	Grum
3G0	Non-calcareous phyllite	3	Vangorda

## **2.2 Laboratory Testing**

### **2.2.1 ABA**

Cantest Ltd. (Burnaby, BC) conducted ABA tests including: paste pH, sulphate-sulphur and NP (Modified method; MEND, 1991). Total carbon and total sulphur were determined by LECO furnace at Acme Analytical Laboratories Ltd. (Vancouver, BC). Inorganic carbon was determined at Acme by direct Leco furnace determination of C evolved as CO<sub>2</sub> following addition of HCl.

### **2.2.2 Elemental Content**

Determination of elemental content of the samples was reported by Cantest Ltd. (Burnaby, BC). Analyses were conducted at Global Discovery Labs (Vancouver, BC) using *aqua regia* digestion with ICP-MS/ES finish.

## **2.3 Mineralogical Characterization**

### **2.3.1 Sample Selection**

Based on initial laboratory testing results, a subset of 22 samples was chosen for detailed mineralogical characterization. Samples for mineralogical characterization were selected to best represent the range of ABA characteristics for each rock type given the available samples.

### **2.3.2 Petrographic Analysis**

Polished thin sections were prepared from coarse fragments in crushed samples by Vancouver Petrographics (Langley, BC). Petrographic analysis of the samples was conducted by Dr. Craig Leitch (Salt Spring Island, BC).

### **2.3.3 Quantitative XRD**

Quantitative mineral phase determinations were carried out using x-ray powder diffraction analyses followed by Rietveld refinement. XRD analyses were carried out at the University of British Columbia's Department of Earth and Ocean Sciences (Vancouver, BC) under the direction of Dr. Mati Raudsepp.

### **2.3.4 Electron Microprobe Analysis**

A total of 17 samples had sufficient carbonate content (based on XRD results) to warrant analysis of carbonate grains by electron microprobe. Approximately 20 carbonate grains were analyzed per sample. Analyses were reported by Mineral Services Canada (Vancouver, BC), with electron microprobe determinations carried out at the University of British Columbia's Department of Earth and Ocean Sciences (Vancouver, BC) by Dr. Mati Raudsepp.

## 3 Results

### 3.1 Laboratory Testing

#### 3.1.1 ABA

NP and AP results for the 2008 samples are provided in Appendix A and are summarized along with the historical data in Figures 1, 2 and 3. NP and TIC data for the samples selected for subsequent mineralogical analyses are presented and discussed in Section 4.1.1.

Figure 1 compares the historical data for Faro with the characteristics of the 2008 samples. For all three main rock groups evaluated, NP values in the 2008 samples ranged from 2 to 60 kg CaCO<sub>3</sub>/tonne and appear to be distributed around the median values of the historical data. For all three rock groups, the highest NP values in the historical data are up to 4 times higher than the maximum NP values returned for the 2008 samples. It should be noted that data for Units 10E and 10F are combined, as a significant number of the records in the historical database do not differentiate between these two intrusive units.

Figure 2 compares the historical data for Grum with the characteristics of the 2008 samples. Overall, the NPs of the 2008 samples span most of the NP range displayed in the historical samples, however it appears that the lithology of some of the samples may have been misclassified (in particular, the 2008 samples of Unit 3G0, with NP values around 180 kg CaCO<sub>3</sub>/tonne, do not correlate well with the historic data). The likely explanation is that rock units at Grum consist of a range of phyllite lithologies, and distinguishing between the various lithologies is based on subtle variations between some of the units. This would also have been a factor for classification of historical samples. Overall, the 2008 Grum samples provide a good range of NP content for evaluation; application of the findings of this study needs to consider the effects of possible lithological misclassification.

Assessment of the Vangorda lithologies received less focus, as nearly all of the Vangorda waste rock is already acidic or is likely to generate acid in the future. As such only 3 samples of Vangorda rock were collected. As discussed for Grum, it can be very difficult to distinguish between the various lithologies at Vangorda. All three of the 2008 samples appear to belong to unit 3G0, while all of the historical data that could be logged to a specific rock type was from units 5A or 5B. Figure 3 compares the historical data for Vangorda with the characteristics of the 2008 samples. The NP values for the 2008 samples ranged from 1.7 to 6.8 kg CaCO<sub>3</sub>/tonne, which is at the low end of the range displayed by the historical samples.

#### 3.1.2 Elemental Content

Complete results are provided in Appendix B. 3G0 samples from Vangorda had much higher metals concentrations compared to all other samples. Metals analyses were carried out for characterization purposes only, and are not considered in further detail in this report.

## 3.2 Mineralogical Characterization

### 3.2.1 Petrographic Analysis

Carbonate mineral species and abundance reported from petrographic examinations are summarized in Table 2. The detailed petrographic report is included as Appendix C.

**Table 2: Carbonate Content Reported from Petrographic Analysis**

Sample ID	Rock Type (Logged)	Optical Report Description*	Abundance (Visual Estimate)	Mine Area
FNP-08	1D	no carbonate noted	0%	Faro
FNP-13	1D	ankerite/siderite	3%	Faro
FNP-14	1D	no carbonate noted	0%	Faro
GS 7	1D	dolomite, trace ankerite	3%	Faro
GS 8	1D	dolomite/ankerite	25%	Faro
FNP-01	3D	dolomite/ankerite	<1%	Faro
FNP-02	3D	mainly ankerite, minor calcite	3%	Faro
FNP-04	3D	ankerite	2%	Faro
FNP-06	3D	ankerite	5%	Faro
FNP-17	10E	no carbonate noted	0%	Faro
FNP-18	10E	calcite	<1%	Faro
GS 3	3G0 - Grum	dolomite	20%	Grum
GS 5	3G0 - Grum	ankerite, veinlet dolomite	15%	Grum
GS 2	5A0	ankerite, minor siderite	20%	Grum
GNP-05	5A0	mainly ankerite	5%	Grum
GNP-06	5B0	dolomite, ankerite	7-8%	Grum
GNP-07	5B0	dolomite, ankerite	7-8%	Grum
GNP-09	5B0	mainly dolomite	20%	Grum
GNP-11	5B0	dolomite, ankerite	25%	Grum
GNP-02	5D	calcite, dolomite, ankerite	20%	Grum
GNP-03	5D	calcite, dolomite	20%	Grum
VNP-02	3G0- Vang	ankerite/siderite	1%	Vangorda

Note: \*Specific types of carbonate minerals cannot be reliably identified through optical mineralogy. Tentative identifications shown in Table 2 were made on the basis of colour and reactivity of hand samples to 10% HCl.

### 3.2.2 Quantitative XRD

X-ray diffraction analyses (Table 3) indicated that calcite, dolomite, ankerite, and siderite were present. The complete XRD results are included as Appendix D. XRD does not reliably differentiate between ankerite and dolomite, therefore the XRD results for these species are considered ambiguous and can be combined to yield an 'ankerite/dolomite' category.

**Table 3: Carbonate Content Determined by Rietveld XRD**

Sample ID	Rock Type (Logged)	Calcite (%)	Siderite (%)	Ankerite (%)	Dolomite (%)	Mine Area
FNP 08	1D	-	2.6	-	-	Faro
FNP 13	1D	-	5.8	-	-	Faro
FNP 14	1D	-	-	-	-	Faro
GS 7	1D	1.4	-	-	-	Faro
GS 8	1D	-	7.4	-	0.9	Faro
FNP 01	3D	0.8	-	-	-	Faro
FNP 02	3D	3.6	-	-	-	Faro
FNP 04	3D	3.4	-	-	-	Faro
FNP 06	3D	1.6	-	-	-	Faro
FNP 17	10E	0.4	-	-	-	Faro
FNP 18	10E	1.1	-	-	-	Faro
GS 3	3G0- Grum	1.4	-	17.8	-	Grum
GS 5	3G0- Grum	3.9	0.6	-	-	Grum
GS 2	5A0	0.5	4.6	19.9	-	Grum
GNP 05	5A0	-	6.8	-	-	Grum
GNP 06	5B0	4.6	0.4	-	-	Grum
GNP 07	5B0	4.1	-	-	-	Grum
GNP 09	5B0	6.9	-	-	-	Grum
GNP 11	5B0	6.8	-	-	-	Grum
GNP 02	5D	8.5	-	-	0.5	Grum
GNP 03	5D	8.4	-	-	-	Grum
VNP 02	3G0- Vang	-	0.4	-	-	Vangorda

Note: ankerite and dolomite cannot be readily distinguished from each other by this method and should be grouped as an "ankerite-dolomite" category in any subsequent interpretations.

### 3.2.3 Electron Microprobe Analysis

Electron microprobe analyses are presented in Figures 4, 5 and 6. Complete results are provided in Appendix E.

Results for Faro are presented in Figure 4. The major element compositions of 120 carbonate mineral grains from nine samples were determined. The majority of the grains were classified as calcite (80), followed by siderite (22) and by grains with ankerite/dolomite composition (18 (including 7 grains that are technically classified as magnesite but which have similar composition to ankerite/dolomite as shown in Figure 4).

Results for Grum are presented in Figure 5. The compositions of 200 carbonate mineral grains from ten samples were determined. The majority of the grains were classified as calcite (116), followed by siderite (51), and 'ankerite/dolomite + similar magnesite' (33) (Figure 5).

Results for Vangorda are presented in Figure 6. The compositions of 9 carbonate mineral grains from a single sample were determined. The majority of the grains were classified as siderite (8) with one grain identified as ankerite/dolomite (1) (Figure 6).

## 4 Discussion

### 4.1 Neutralization Potential

#### 4.1.1 Comparison of NP and Inorganic Carbon Content

The acid base accounting results include both an analytical measurement of NP, and a measurement of total inorganic carbon (TIC). The analytical NP is a measurement of the total buffering capacity of the sample in the presence of a relatively strong acid. The inorganic carbon content (TIC) measures the carbonate content of the sample. Carbonates may provide more effective buffering of acidity, but there are forms of carbonate that do not provide any buffering. Correlations between analytical NP and TIC are typically interpreted as follows:

- Samples with NP greater than TIC are interpreted as having some NP in the form of silicate minerals. Silicate minerals are generally less reactive than carbonate NP. At some sites, the contribution of silicate minerals toward maintaining neutral pH conditions is conservatively discounted. At sites with predominantly calcium and/or magnesium carbonate minerals, TIC is used as a surrogate for the reactive NP. At other sites, “unavailable” NP (often determined from correlations of paste pH and NP) is subtracted from all the NP measurements.
- Samples with good 1:1 correspondence between NP and TIC are interpreted as having NP in the form of calcium and/or magnesium carbonate minerals, which are considered to be both reactive and capable of maintaining pH conditions in the neutral to slightly alkaline pH range.
- Samples with NP less than TIC are interpreted as having some TIC in the form of iron or manganese carbonates. Information in the literature (e.g. Jambor 2003) suggests that iron and manganese carbonates should not contribute appreciably to the Modified Sobek measurement of NP because it provides sufficient opportunity for any dissolved ferrous iron to oxidize (Jambor 2003).

Figure 7 provides a comparison of NP with TIC for the test samples expressed in equivalent units of kg CaCO<sub>3</sub> equivalent/ tonne of rock (kg CaCO<sub>3</sub>/t).

For approximately one third of the samples, NP exceeded TIC. The difference was greatest for samples with low TIC (< 10 kg CaCO<sub>3</sub>/t), and suggests that dissolution of silicates contributes a small absolute amount to measured NP values. Observations for those samples for which NP exceeds TIC include:

- All three samples from the Faro intrusive rocks (units 10E and 10F) had NP>TIC and low TIC (< 10 kg CaCO<sub>3</sub>/t); and



- All six samples of Faro calc-silicate (Unit 3D) had NP>TIC by an average of about 17 kg CaCO<sub>3</sub>/t. Three of these samples had low TIC (< 10 kg CaCO<sub>3</sub>/t), and the TIC accounted for only 20 to 30% of the NP. The other three samples had TIC > 20 kg CaCO<sub>3</sub>/t, and for these samples TIC accounted for approximately 60 to 70% of the NP.

Nearly all Grum samples (from units 3G0, 5A0, 5B0 and 5D) had excellent agreement between NP and TIC (Figure 7). The exception was one sample of unit 5A0, which had much higher TIC (82 kg CaCO<sub>3</sub>/t) than NP (11 kg CaCO<sub>3</sub>/t).

TIC was significantly greater than NP for all samples of Faro schist (unit 1D) with TIC > 10 kg CaCO<sub>3</sub>/t and all three samples of unit 3G0 (non-calcareous phyllite) from Vangorda. This reflects the contribution of iron carbonates to the TIC, and is consistent with the observation of iron carbonates in these samples as presented in Section 3.2.3.

In conclusion, the correlations between NP and TIC indicate that measurement and interpretation of NP data is complicated by the presence of silicate minerals in some rock units and by the presence of iron carbonates in others. Further understanding of these issues can be gained through the mineralogical analyses, as discussed in the following section.

#### 4.1.2 Comparison of NP with Calcium and Magnesium Carbonate Content

The calcium and magnesium carbonates are considered to be a reliable indication of the effective NP in most types of rock. Quantification of the calcium and magnesium carbonates can be made through direct mineralogical analyses (i.e. Rietveld XRD), or through a combination of inorganic carbon analyses and mineralogical analyses (also Rietveld XRD). In this study, the microprobe analyses allowed further refinement of carbonate speciation by providing direct measurement of the calcium, magnesium, iron and manganese content of the different types of carbonate minerals in each sample.

Combining the XRD results (which provide estimates of carbonate mineral abundance) and the EMPA results (which provide estimates of the composition of the carbonate mineral species) allows an estimation of the neutralization potential contained in calcium and magnesium carbonate minerals (represented as IC<sub>Ca,Mg</sub>). The following steps summarize how IC<sub>Ca,Mg</sub> was determined.

1. Average compositions were calculated for calcite, ankerite/dolomite, and siderite for waste rock samples tested in this study. Table 4 shows the stoichiometric formulas that resulted of these calculations, along with the corresponding formula weights for each mineral.
2. The XRD-indicated percent abundances of calcite, ankerite/dolomite, and siderite were used together with the respective stoichiometric formulas (Table 4) to calculate the fraction of the total XRD-indicated carbonate associated with calcium and magnesium for each sample.

The general form of this calculation is:

$$f_{Ca,Mg} = \{\sum(x_{Ca,m} + x_{Mg,m})IC_m\}/TIC_{XRD}$$

where:

$IC_m$  is the carbonate content indicated by QXRD associated with each mineral (m);

$x_{Ca,m}$  and  $x_{Mg,m}$  are the mole proportions of calcium and magnesium in each mineral indicated by microprobe; and

$TIC_{XRD}$  is the total inorganic carbon content as calculated from XRD-indicated calcite, ankerite/dolomite, and siderite abundance.

3. The  $f_{Ca,Mg}$  values were then multiplied by the analytically-determined TIC values to arrive at a value for  $IC_{Ca,Mg}$  for each sample.

**Table 4 Average Compositions of Carbonate Minerals in Anvil Range Waste Rock Samples Studied in 2008**

Mineral	Average Formula	Formula Weight (g/mole)
Calcite	$Ca_{0.97}Mg_{0.01}Fe_{0.01}Mn_{0.01}CO_3$	100.2
Ankerite-Dolomite	$Ca_{1.07}Mg_{0.62}Fe_{0.29}Mn_{0.01}(CO_3)_2$	195.2
Siderite	$Ca_{0.11}Mg_{0.26}Fe_{0.62}Mn_{0.01}CO_3$	105.8

As calcium- and magnesium-bearing carbonate minerals dissolve readily, comparing  $IC_{Ca,Mg}$  to the Modified Sobek NP values provides an indication of the proportion of NP that is readily soluble (or ‘available’). This comparison is presented graphically in Figure 8, and Table 5 presents the calculated availability of analytically-measured NP for the samples evaluated in this study.

The comparison of NP and  $IC_{Ca,Mg}$  for the two main Faro rock types (1D and 3D) and one minor Faro rock type (10E) each showed that different proportions of the measured NP are derived from calcium and magnesium carbonates in each rock type.

- Five samples of rock type 1D (biotite schist) typically showed  $IC_{Ca,Mg} > NP$ , with a median ‘Percent Availability’ of 109% and a range from 0 to 153%. The dominant carbonate mineral in these samples was siderite, which contains an average of 44% calcium and magnesium carbonate. It is possible that the  $IC_{Ca,Mg}$  is greater than the Modified Sobek NP because of incomplete reaction of the iron carbonates in the NP titration. In this case, the Modified Sobek NP provides a more conservative indication of effective NP.
- Four samples of rock type 3D (calc-silicate) showed  $NP > IC_{Ca,Mg}$ , with a median ‘Percent Availability’ of 61% and a range from 29 to 70%. This rock type contained no significant iron carbonate component (see Section 3.2.2 and Figure 4), and it is likely that silicate minerals contributed to the laboratory-determined NP. In this case, the  $IC_{Ca,Mg}$  provides a more conservative indication of the effective NP.
- Two samples of rock type 10E (quartz diorite) showed  $NP > IC_{Ca,Mg}$ , with ‘Percent Availability’ ranging from 35 to 44% for the two samples evaluated. However, the

absolute values of both NP and  $IC_{Ca,Mg}$  were low for both Unit 10E samples. For both samples, calcite was the only carbonate mineral detected by QXRD, and it is likely that silicate minerals contribute to the laboratory-determined NP. As discussed for Unit 3G0, the  $IC_{Ca,Mg}$  provides a more conservative indication of the effective NP of Unit 10E. Since no iron carbonates were identified, TIC also provides a good measure of effective NP for this rock type.

**Table 5: Availability of NP**

Sample ID	Rock Type	TIC <sup>1</sup> (kg CaCO <sub>3</sub> /t)	NP <sup>2</sup> (kg CaCO <sub>3</sub> /t)	$IC_{Ca,Mg}$ <sup>3</sup> (kg CaCO <sub>3</sub> /t)	Percent Availability <sup>4</sup>		
					( $IC_{Ca,Mg}/NP$ ) * 100%	Average for Rock Type	Range for Rock Type
FNP-13	1D	60	22	22	100%	99%	0 to 153%
FNP 08	1D	31	11	12	109%		
FNP 14	1D	5	9	0	0%		
GS 7	1D	32	24	31	132%		
GS 8	1D	97	27	41	153%		
FNP-02	3D	37	56	36	65%	55%	29 to 70%
FNP 01	3D	6	20	6	29%		
FNP-04	3D	43	60	42	70%		
FNP-06	3D	22	39	22	56%		
FNP 17	10E	2	6	2	35%	39%	35 to 44%
FNP 18	10E	8	17	8	44%		
GS 3	3G0 - Grum	201	185	172	93%	93%	93 to 94%
GS 5	3G0 - Grum	78	75	71	94%		
GS 2	5A0	233	179	178	100%	188%	100 to 277%
GNP-05	5A0	82	11	30	277%		
GNP-06	5B0	62	51	57	112%	107%	103 to 112%
GNP-07	5B0	36	34	35	104%		
GNP-09	5B0	68	65	67	103%		
GNP-11	5B0	147	129	144	111%		
GNP-02	5D	101	95	99	104%	99%	93 to 104%
GNP-03	5D	76	80	75	93%		
VNP-02	3G0 - Vang	11	7	4	62%	62%	62%

Notes:

1. 'TIC' is Total Inorganic Carbon (determined analytically as part of ABA testing, and included here for comparative purposes)
2. 'NP' indicates NP derived analytically using the MEND (1991) method
3. ' $IC_{Ca,Mg}$ ' indicates calcium and magnesium carbonate neutralization potential calculated from TIC, XRD and EMPA results
4. 'Percent Availability' indicates the proportion of measured NP derived from calcium and magnesium carbonate (calculated as ( $IC_{Ca,Mg}/NP$ )\*100%)

The comparison of NP and  $IC_{Ca,Mg}$  for the four main Grum rock types showed that the measured NP values are generally reflective of calcium and magnesium carbonates content (typical availability ranging from 93 to 112%).

- Five of ten Grum samples evaluated by XRD contained detectable iron-bearing carbonate minerals (see Section 3.2.2), and there was good agreement between NP and  $IC_{Ca,Mg}$ . This indicates that either the Modified Sobek method or the mineralogical method is suitable for estimating the effective NP content.
- One Grum sample (GNP-05, Unit 5A0) had  $IC_{Ca,Mg} \gg NP$ , with a calculated 'Percent Availability' of 277%. XRD characterization of this sample showed 6.8% siderite, and no XRD-detectable calcium- or magnesium-bearing carbonate minerals. However, EMPA results showed that siderite from this sample typically consisted of around 30% magnesium carbonate and 5% calcium carbonate (Figure 5). The excess of  $IC_{Ca,Mg}$  over NP could be due to incomplete digestion of the iron carbonate minerals in the NP determination. However, it is also possible that there was an analytical error in the NP or TIC analyses.

Only a single Vangorda rock sample was evaluated (VNP-02). This sample had low values for both NP (7 kg  $CaCO_3$ /t) and  $IC_{Ca,Mg}$  (4 kg  $CaCO_3$ /t), with  $NP > IC_{Ca,Mg}$  (Percent Availability 62%). These results suggest that the  $IC_{Ca,Mg}$  would provide a more conservative indication of NP availability. However, since there is only one sample, and both measurements are close to detection limits, these results are considered inconclusive.

## 4.2 Implications for ARD Classification of Waste Rock

### 4.2.1 Faro

Biotite schist at Faro (Unit 1D) was found to have  $NP < IC_{Ca,Mg} < TIC$ . These results reflect:

- the presence of iron carbonate as a component of the overall carbonate population in this unit (indicated by  $IC_{Ca,Mg} < TIC$ );
- the effectiveness of the NP determination method in oxidizing ferrous iron released through iron carbonate dissolution (indicated by  $NP < IC_{Ca,Mg}$ ).

As such, the historical laboratory-determined NP values are a conservative indication of the net available carbonate neutralization potential for Unit 1D. Therefore, the existing ARD classification (based on NP:AP ratios) is appropriate.

Calc-silicate schist at Faro (Unit 3D) was found to have  $IC_{Ca,Mg} \sim TIC < NP$ . These results reflect:

- the lack of iron carbonate as a significant component of the carbonate population in this unit (indicated by  $IC_{Ca,Mg} \sim TIC$ );
- the contribution of silicates to laboratory-determined measurements of NP (indicated by  $IC_{Ca,Mg} < NP$ ).

Typical historical Unit 3D samples had an excess of neutralization potential over acid potential, and reducing NP values to account for non-carbonate NP will not significantly change the ARD classification. For illustrative purposes, Figure 9 shows NP and AP values for Unit 3D samples from

historical studies (on which the current ARD classifications are based), along with a revised set of NP values that reflect the average ‘percent availability’ calculated for the four Unit 3D samples tested as part of this study (calculated as  $NP * 0.55$ ). For almost all samples in the historical database, applying this correction did not change the ARD classification. It is important to note that the results of this NP correction have been presented to show how discounting a large portion of measured NP for Unit 3D does not significantly change the ARD classification of the samples in the historical ABA database. It is not intended that the ‘Percent Availability’ calculated in this study be used as a rigorously-determined NP correction factor for Unit 3D. The samples characterized in this study represent the lower-NP portion of the Unit 3D population in the historical ABA database, and an appropriate correction factor would be lower for materials with higher NP.

Hornblende quartz diorite at Faro (Unit 10E) was found to have  $IC_{Ca,Mg} \sim TIC < NP$ . As discussed above for Unit 3D, these results reflect:

- the lack of iron carbonate as a significant component of the carbonate population in this unit (indicated by  $IC_{Ca,Mg} \sim TIC$ );
- the contribution of silicates to laboratory-determined measurements of NP (indicated by  $IC_{Ca,Mg} < NP$ ).

The Unit 10E samples tested in this study had NP values well below the median of the intrusive samples in the historical ABA database. As noted in the Unit 3G0 discussion above, the relative contribution of silicates is greater at lower absolute NP values, and it is therefore not appropriate to apply a broad ‘percent availability’ type of correction factor to the historical NP values. Given that the median NP value for the intrusive rocks (Units 10E and 10F) in the historical database is low (around 10 kg  $CaCO_3$ /tonne), any correction for ‘unavailable’ NP would cause a change in ARD classification for a portion of the intrusive waste rock. With the information at hand, there is no approach to reclassification that can realistically achieve a more accurate classification. Since the intrusive rocks represent a minor portion of the overall waste, it is SRK’s opinion that this aspect should be addressed as an uncertainty rather than refined through additional study.

#### 4.2.2 Grum

For all four Grum rock types evaluated, laboratory-determined NP values generally showed good agreement with  $IC_{Ca,Mg}$  values (Figure 8). This generalization held despite a range of iron carbonate content in the samples tested.

Overall, laboratory NP determinations for Grum rocks appear to be reflective of calcium and magnesium carbonate content. Therefore, the existing ARD classification (based on NP:AP ratios) is appropriate.

#### 4.2.3 Vangorda

Results from a single test suggest that measured NP in Unit 3G0 at Vangorda may overestimate the effective neutralization capacity. As discussed in Section 4.1, the results of this study are

inconclusive due to the limited number of samples characterized in this study. However, since most of the rock at Vangorda is already acid generating or is predicted to be acid generating, there is no need to complete further work on this material.

## 5 Conclusions and Recommendations

The laboratory and mineralogical characterization carried out in this study allowed determination of calcium and magnesium carbonate content of the samples tested. As calcium and magnesium carbonate minerals are the most reactive neutralizing agents in geological materials, the proportion of these minerals provides a conservative estimate of the neutralization potential of a given waste rock unit.

Previous geochemical characterization of waste rock at the Anvil Range mines has made use of NP:AP ratios to assign ARD classification. Comparison of the mineralogically-determined calcium and magnesium carbonate content with laboratory-determined NP for the main waste rock units provides a basis for assessing whether the previously-assigned ARD classifications should be revised to account for a portion of the laboratory-determined NP that may not be as effective at maintaining circum-neutral pH under field conditions. This study does not provide any evidence to support or discount the potential importance of silicate minerals in buffering acidity. The decision to discount the silicate NP in the overall interpretation of ARD potential is considered conservative.

For Unit 1D (Faro biotite schist), Unit 3G0 (Grum non-calcareous phyllite), Unit 5A0 (Grum carbonaceous phyllite), Unit 5B0 (Grum calcareous phyllite) and Unit 5D (Grum chloritic phyllite) the laboratory-determined NP values appear to be a good measure of the neutralization potential represented by calcium and magnesium carbonates. The results of this study also show that the MEND (1991) method of NP determination adequately accounts for acidity generated by dissolution of iron carbonates.

For Unit 3D (Faro calc-silicate schist) and Unit 10E (hornblende quartz diorite), measured NP values were found to consist of a carbonate and a non-carbonate component. For Unit 3D, calcium and magnesium carbonates accounted for an average of 55% of the measured NP for Unit 3D samples tested in this study. The existing ARD classifications were examined to determine whether revising Unit 3D NP values by a factor of 55% would result in significant reclassification, and it was found that reclassification would be minimal due to the large excess of NP in the calc-silicate rock.

In contrast to Unit 3D, the historical NP values for intrusive rocks (a compilation of Unit 10E and 10F, including altered and unaltered variants) were generally lower, and ARD classification of samples in the historical ABA database ranges widely from acid generating to not potentially acid generating. The Unit 10E results from the present study indicate that discounting measured NP values to reflect only the contribution from calcium and magnesium carbonate minerals would increase the proportion of intrusive waste rock that was classified as potentially acid generating. Given the broad variability of ABA characteristics for intrusive rocks in the historical data set, the

lack of a clear approach to defining an 'effective NP' for these rocks at this time, the comparatively low sulphur contents, and the relatively small proportion of intrusive rocks to the overall tonnage of waste rock at Faro, it is recommended that the potential overestimation of available NP be addressed as an uncertainty rather than attempting to refine the understanding through additional study.

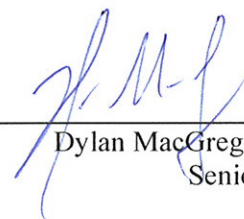
Limited testing of Vangorda waste rock was conducted as the available samples contained little neutralization potential. Results from a single sample classified as Unit 3G0 suggested that measured NP may overestimate available NP by a factor of 2. However, these results are not conclusive due to the small number of samples tested and the analytical uncertainty associated with the low values of NP and TIC in this sample. Given the presently and potentially acid generating nature of the Vangorda waste rock, it is recommended that the potential overestimation of available NP be addressed as an uncertainty rather than attempting to refine the understanding through additional study.

This report, "1CD003.114 – Faro Mine Complex- NP Study Report: 2008/09 Task 18– FINAL",  
was prepared by SRK Consulting (Canada) Inc.

**Prepared by**



for Madeleine Corriveau, EIT/GIT (B.C.)  
Staff Geochemist



Dylan MacGregor, GIT (B.C.)  
Senior Geochemist

**Reviewed by**



Kelly Sexsmith, P.Geo. (B.C.)  
Principal Environmental Geochemist

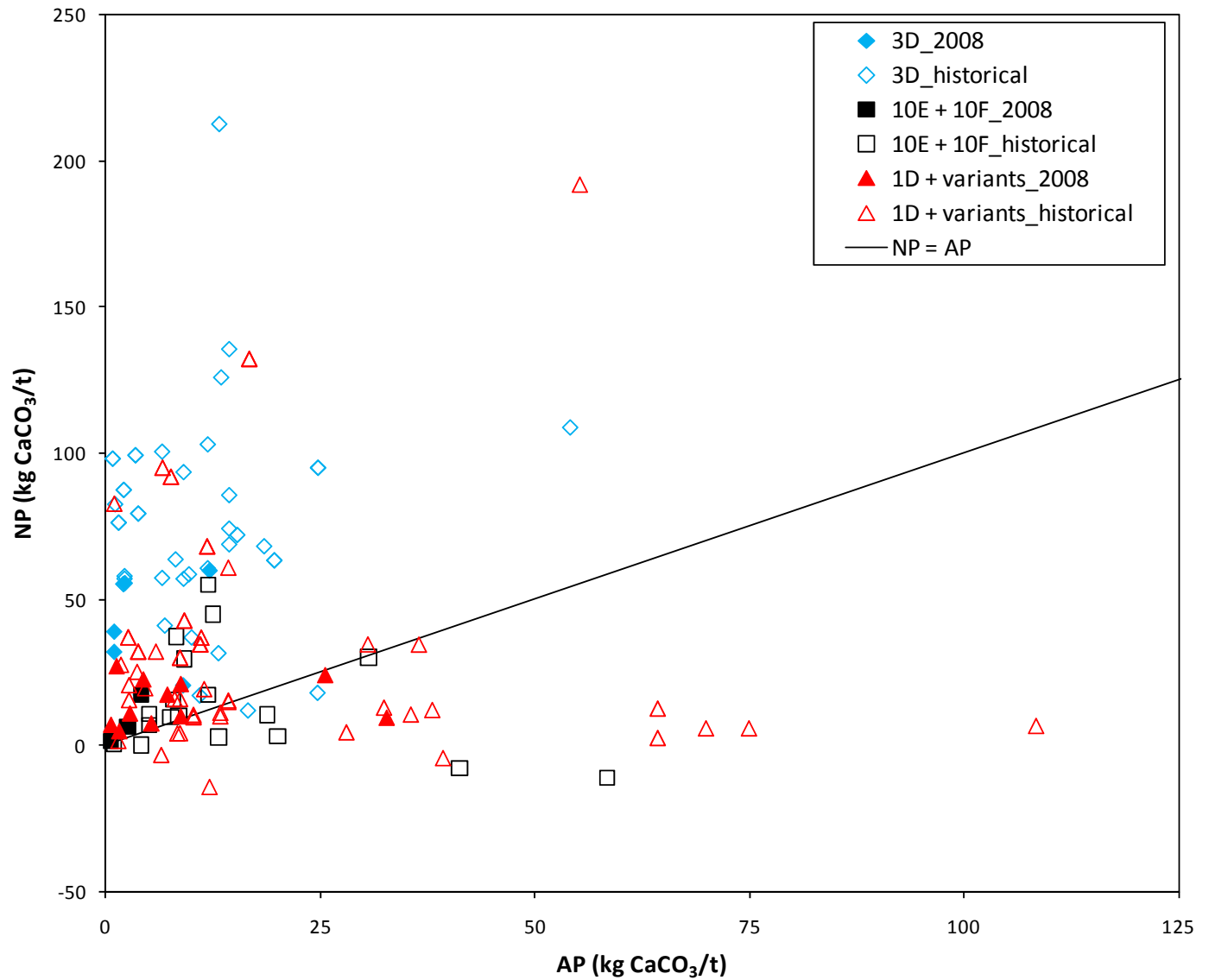


## 6 References

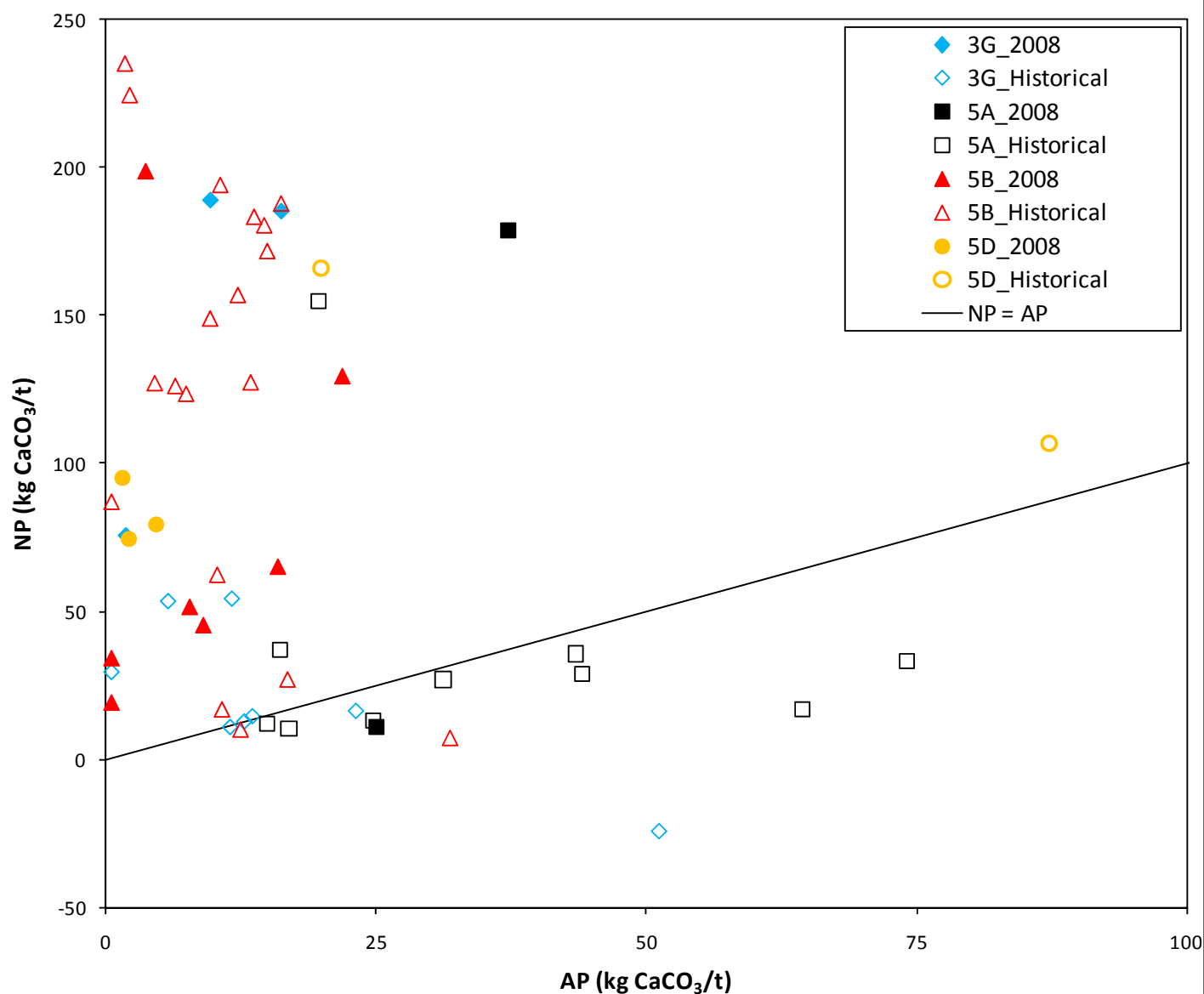
- Jambor, J. 2003. Chapter 6. Mine-waste Mineralogy and Mineralogical Perspectives of Acid-Base Accounting. *In* Jambor, J.L., Blowes, D.W. and Ritchie, A.I.M (eds.). Environmental Aspects of Mine Wastes, Mineralogical Association of Canada Short Course Series Volume 31, pp. 117-145.
- IPRP (Independent Peer Review Panel) 2007. Review of Remediation Alternatives for the Anvil Range Mining Complex- Final Report. Report prepared for Deloitte & Touche, Faro Mine Closure Planning Office, Indian and Northern Affairs Canada, Yukon Government, Selkirk First Nation, and the Kaska Tribal Council. March 2007.
- MEND (Mine Environment Neutral Drainage Program). 1991. Acid Rock Drainage Prediction Manual, MEND Project 1.16.1 (b). Prepared by Coastech Research Inc., North Vancouver, B.C. March 1991.
- SRK Consulting. 2004. Geochemical Studies Of Waste Rock At The Anvil Range Mining Complex, Phase 3 Report. Report prepared for Deloitte & Touche, June 2004.

**Figures**

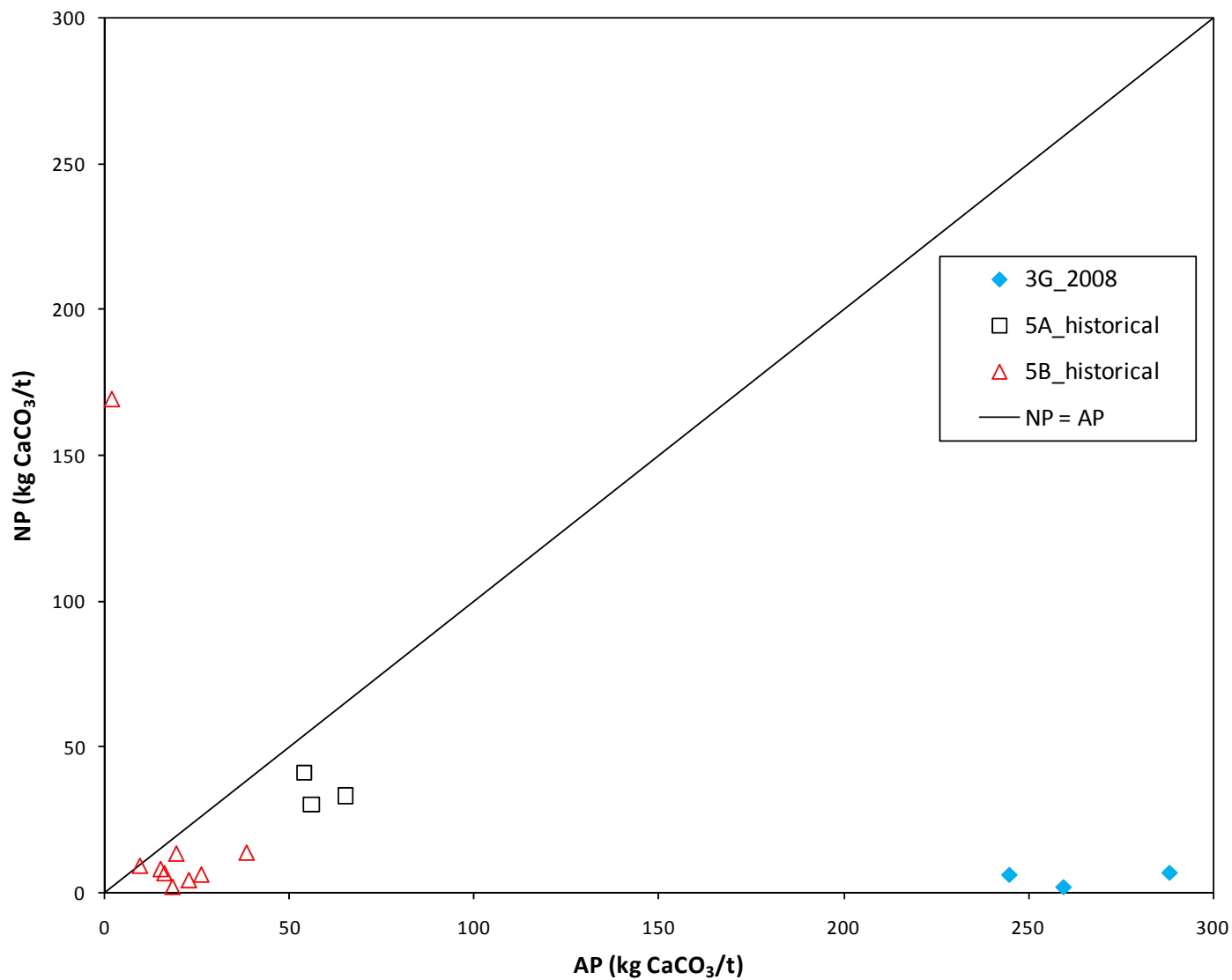
## Faro NP vs. AP- 2008 and Historical

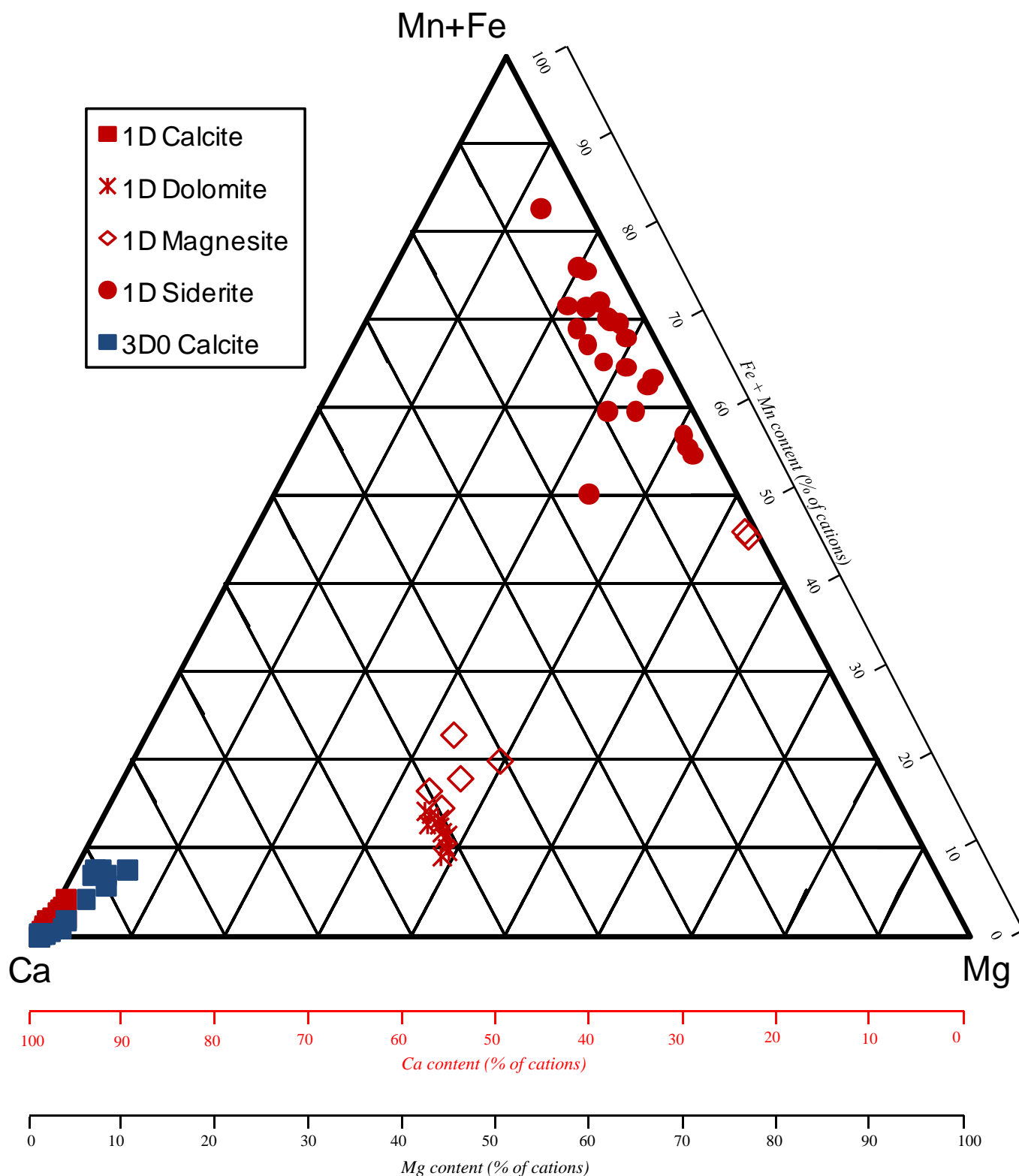


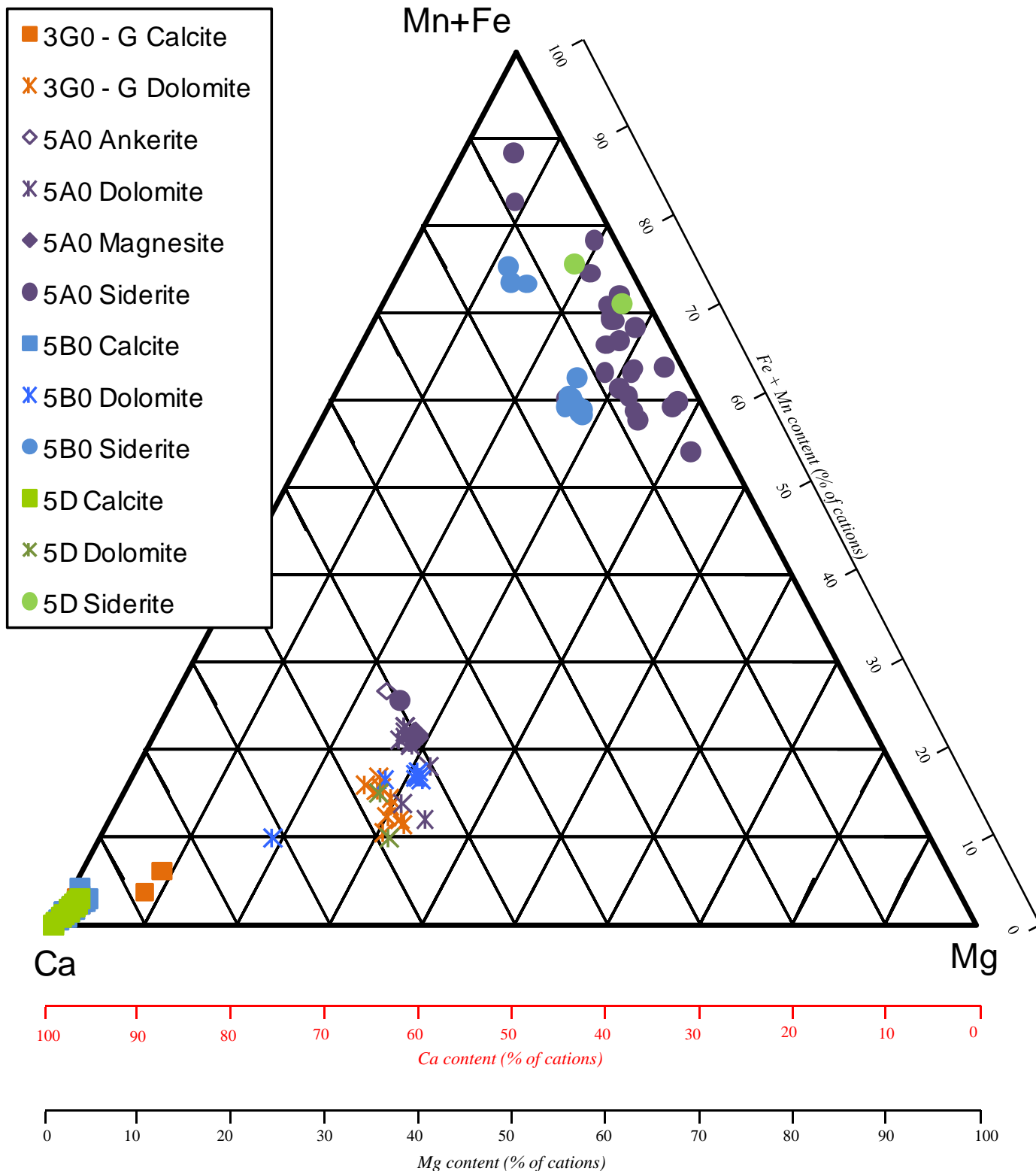
## Grum NP vs. AP- 2008 and Historical

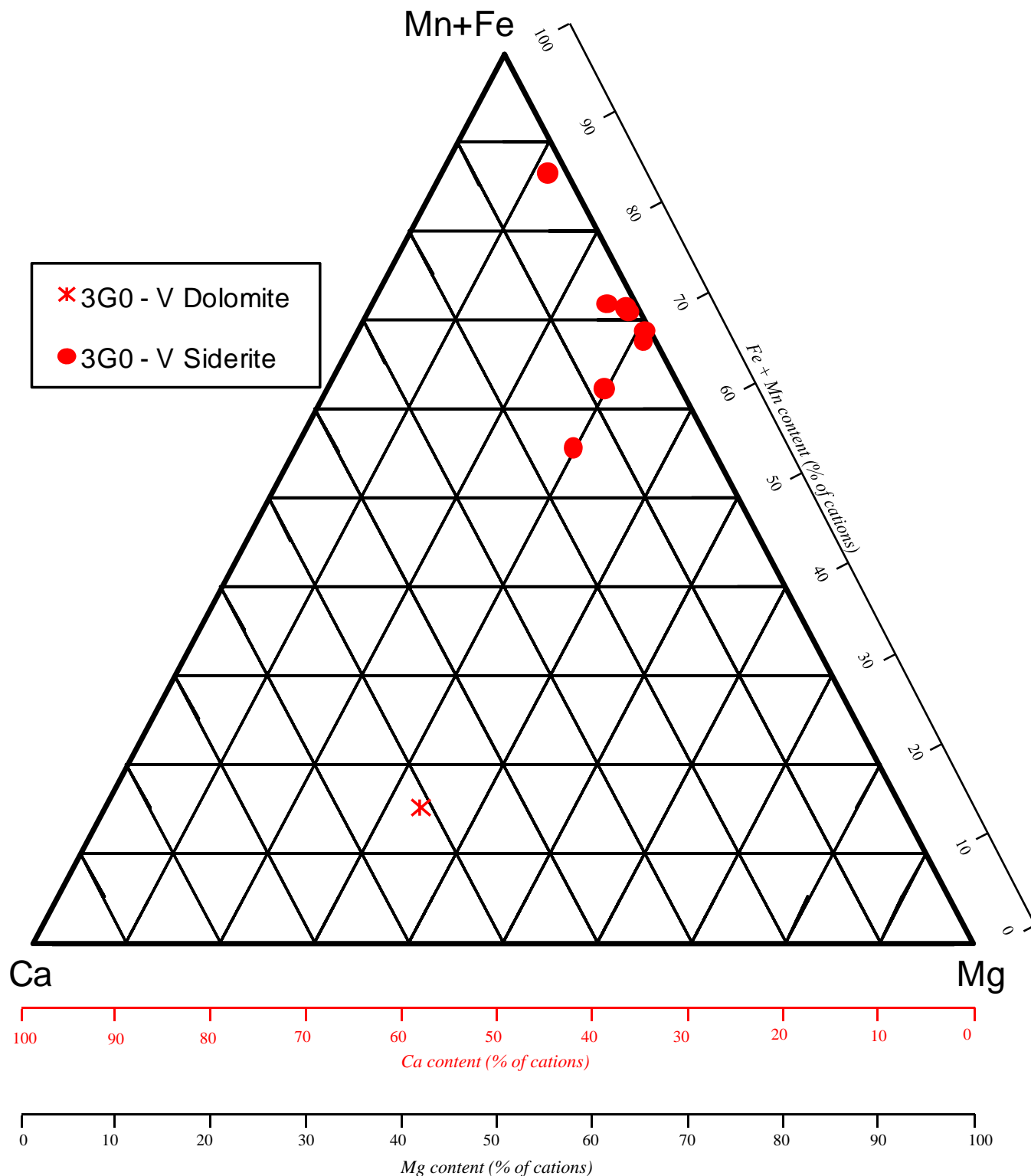


## Vangorda NP vs. AP- 2008 and Historical

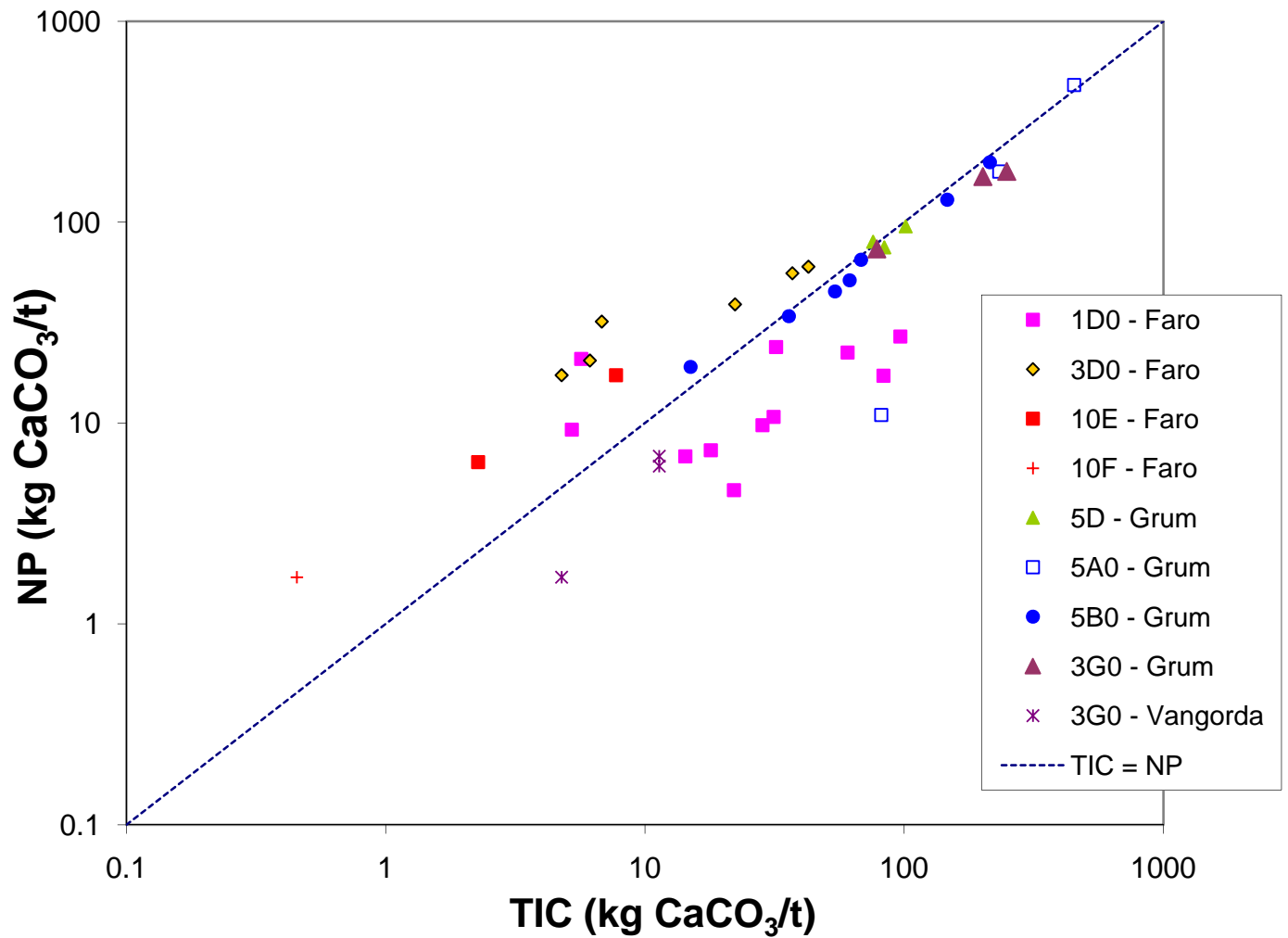




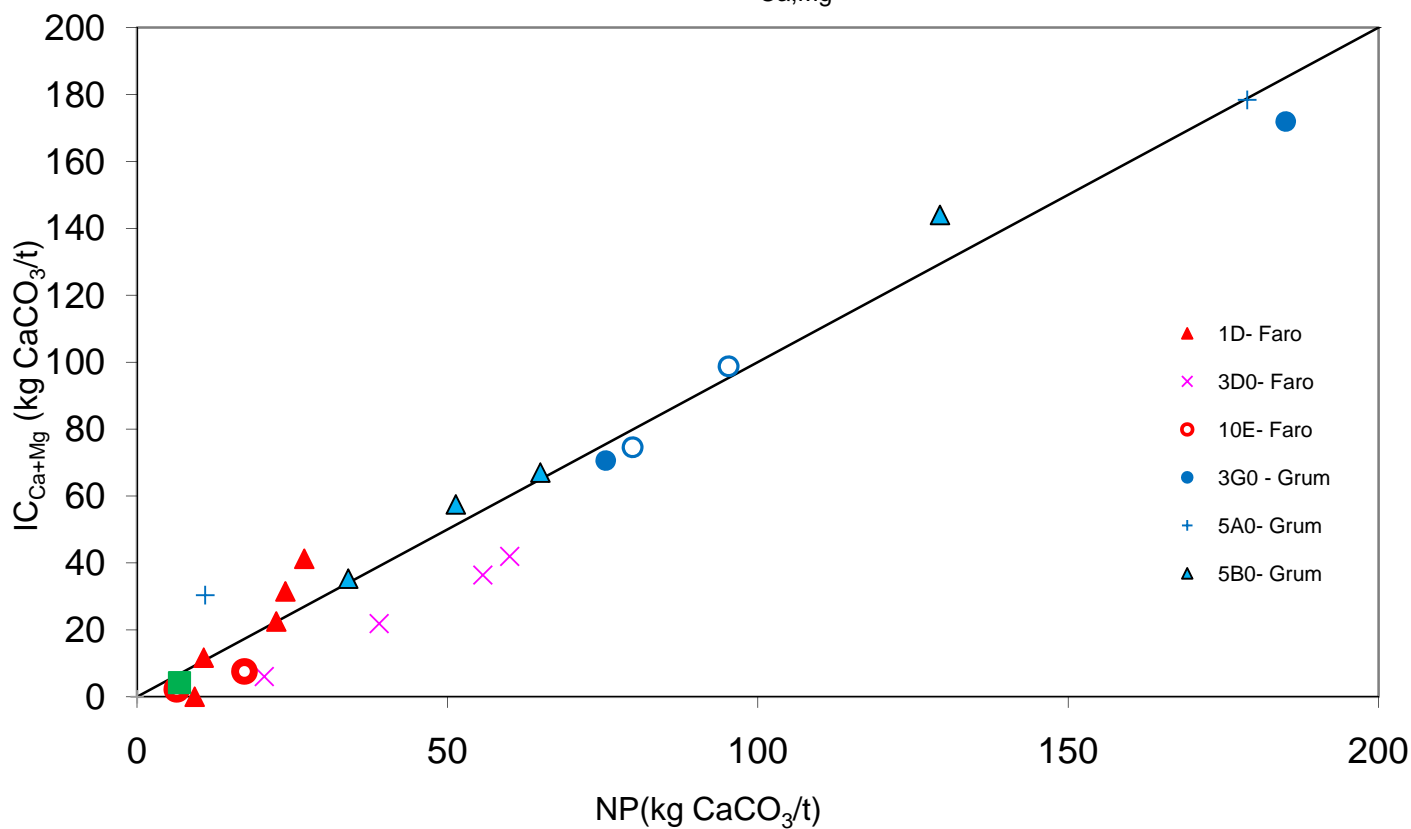




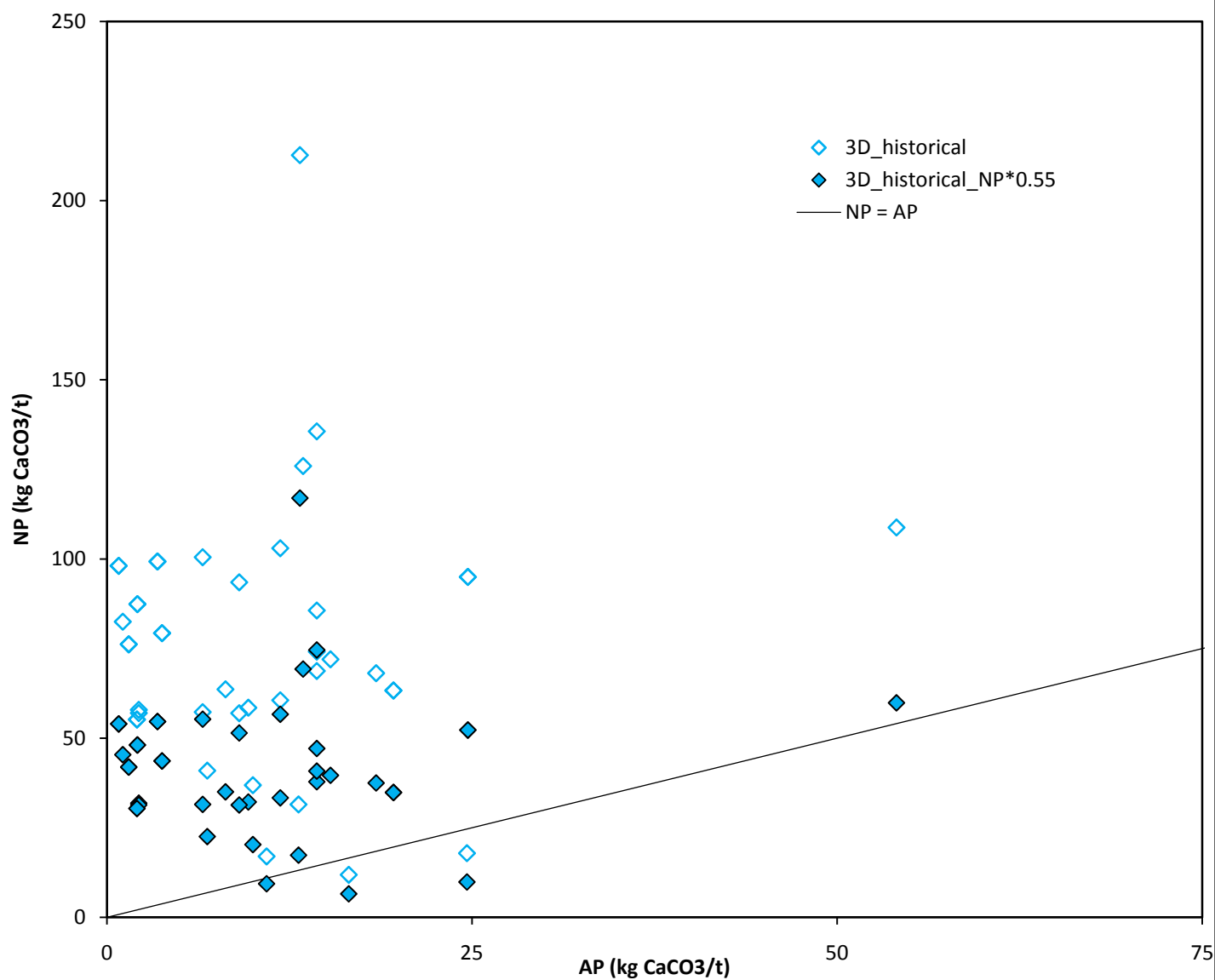




# Anvil Range Comparison of $IC_{Ca,Mg}$ and NP



# Faro Unit 3D NP vs. AP- Historical and Adjusted Historical (NP \* 0.55)



## **Appendices**

## **Appendix A**

### **ABA Results**



CANTEST Ltd. 4606 Canada Way, Burnaby, BC, Canada V5G 1K5 Tel: 604 734 7276 Fax: 604 731 2386 www.cantest.com

SRK Consulting, Anvil Range Mining, 28-May-08  
Page 1 of 4

Table 1: ABA Test Results for 38 Anvil Range Mining Samples - June 2008

S. No.	Sample ID	Paste pH	CO2 (Wt.%)	CaCO3 Equiv. (Kg CaCO3/Tonne)	Total Sulphur (Wt.%)	Sulphate Sulphur (Wt.%)	Sulphide Sulphur* (Wt.%)	Maximum Potential Acidity** (Kg CaCO3/Tonne)	Mod. ABA NP	Net Neutralization Potential (Kg CaCO3/Tonne)	Fizz Rating
									Neutralization Potential (Kg CaCO3/Tonne)		
1	GS 1	8.1	19.89	452.0	0.91	0.05	0.86	26.9	482.1	455.2	Strong
2	GS 2	8.3	10.24	232.7	1.20	0.01	1.19	37.2	178.8	141.6	Strong
3	GS 3	8.4	8.85	201.1	0.59	0.07	0.52	16.3	185.0	168.8	Strong
4	GS 4	8.7	10.94	248.6	0.33	0.02	0.31	9.7	188.7	179.1	Strong
5	GS 5	8.2	3.45	78.4	0.09	0.03	0.06	1.9	75.5	73.6	Strong
6	GS 6	8.4	0.63	14.3	<0.02	0.01	<0.02	<0.6	6.8	6.8	None
7	GS 7	7.9	1.41	32.0	0.88	0.06	0.82	25.6	23.9	-1.7	Moderate
8	GS 8	8.3	4.25	96.6	0.04	<0.01	0.04	1.3	27.0	25.7	Slight
9	FNP 01	8.9	0.27	6.1	0.29	<0.01	0.29	9.1	20.5	11.4	None
10	FNP 02	8.9	1.63	37.0	0.07	<0.01	0.07	2.2	55.7	53.5	Strong
11	FNP 03	9.2	0.30	6.8	0.03	<0.01	0.03	0.9	32.0	31.1	Slight
12	FNP 04	8.7	1.88	42.7	0.40	0.01	0.39	12.2	60.0	47.8	Strong
13	FNP 05	8.5	0.68	15.5	0.12	0.01	0.11	3.4	20.6	17.2	Slight
14	FNP 06	8.8	0.98	22.3	0.03	<0.01	0.03	0.9	39.0	38.0	Strong
15	FNP 07	9.1	0.21	4.8	0.13	<0.01	0.13	4.1	17.3	13.3	Slight
16	FNP 08	8.4	1.38	31.4	0.09	<0.01	0.09	2.8	10.7	7.9	None
17	FNP 09	8.5	0.02	0.5	<0.02	<0.01	<0.02	<0.6	1.7	1.7	None
18	FNP 10	8.4	3.66	83.2	0.23	<0.01	0.23	7.2	17.2	10.0	None
19	FNP 11	8.5	0.79	18.0	0.17	<0.01	0.17	5.3	7.3	2.0	None
20	FNP 12	8.4	1.25	28.4	0.29	0.01	0.28	8.8	9.8	1.0	None
21	FNP 13	8.3	2.66	60.5	0.15	0.01	0.14	4.4	22.4	18.1	None
22	FNP 14	7.9	0.23	5.2	1.07	0.02	1.05	32.8	9.3	-23.5	None
23	FNP 15	8.7	0.25	5.7	0.29	0.01	0.28	8.8	20.9	12.1	Slight
24	FNP 16	8.6	0.97	22.0	0.05	<0.01	0.05	1.6	4.6	3.1	None
25	GNP 01	9.0	3.69	83.9	0.07	<0.01	0.07	2.2	74.9	72.7	Strong
26	GNP 02	8.4	4.46	101.4	0.06	0.01	0.05	1.6	95.3	93.7	Strong
27	GNP 03	8.5	3.34	75.9	0.16	0.01	0.15	4.7	79.8	75.1	Strong
28	GNP 04	8.9	9.42	214.1	0.12	<0.01	0.12	3.8	198.6	194.9	Strong
29	GNP 05	8.4	3.59	81.6	0.81	0.01	0.80	25.0	11.0	-14.0	None
30	GNP 06	8.8	2.71	61.6	0.25	<0.01	0.25	7.8	51.4	43.5	Strong
31	GNP 07	9.3	1.58	35.9	<0.02	<0.01	<0.02	<0.6	34.0	34.0	Strong
32	GNP 08	9.1	2.38	54.1	0.29	<0.01	0.29	9.1	45.2	36.1	Strong
33	GNP 09	8.9	3.00	68.2	0.51	<0.01	0.51	15.9	65.0	49.0	Strong
34	GNP 10	8.8	0.66	15.0	<0.02	<0.01	<0.02	<0.6	19.0	19.0	Moderate
35	GNP 11	9.0	6.45	146.6	0.71	0.01	0.70	21.9	129.3	107.5	Strong
36	VNP 01	6.5	0.21	4.8	8.33	0.02	8.31	259.7	1.7	-258.0	None
37	VNP 02	6.7	0.50	11.4	9.25	0.02	9.23	288.4	6.8	-281.6	None
38	VNP 03	6.4	0.50	11.4	7.88	0.04	7.84	245.0	6.1	-238.9	None
Detection Limits		0.5	0.02	0.5	0.02	0.01	0.02	0.6			
CANTEST SOP No:		7160	LECO	Calculation	LECO	7410	Calculation	Calculation	7150	Calculation	7150

**Notes:**

Total Sulphur by LECO furnace

\*Based on difference between total sulphur and sulphate-sulphur

\*\*Based on sulphide-sulphur

Reference for Mod ABA NP method (SOP No. 7150): MEND Acid Rock Drainage Prediction Manual, MEND Project 1.16.1b (pages 6.2-11 to 17), March 1991.



CANTEST Ltd. 4606 Canada Way, Burnaby, BC Canada V5G 1K5 Tel: 604 734 7276 Fax: 604 731 2386 www.cantest.com

SRK Consulting, Anvil Range Mining, 18-Aug-08

Page 1 of 4

**Table 1: ABA Test Results for 2 Anvil Range Mining (FARO) Samples - September 2008**

										Mod. ABA NP		
S. No.	Sample ID	Paste pH	Total Carbon (Wt. %)	CO2 (Wt.%)	CaCO3 Equiv. (Kg CaCO3/Tonne)	Total Sulphur (Wt.%)	Sulphate Sulphur (Wt.%)	Sulphide Sulphur* (Wt.%)	Maximum Potential Acidity** (Kg CaCO3/Tonne)	Neutralization Potential (Kg CaCO3/Tonne)	Net Neutralization Potential (Kg CaCO3/Tonne)	Fizz Rating
1	FNP-17	8.1	0.03	0.10	2.3	0.08	<0.01	0.08	2.5	6.4	3.9	None
2	FNP-18	8.7	0.17	0.34	7.7	0.13	<0.01	0.13	4.1	17.3	13.2	Moderate
<i>Detection Limits</i>		0.5	0.02	0.02	0.5	0.02	0.01	0.02	0.6			
CANTEST SOP No:		7160	LECO	LECO	Calculation	LECO	7410	Calculation	Calculation	7150	Calculation	7150

TC is complimentary data

**Notes:**

Total Carbon, Total Sulphur & CO2 by LECO furnace (done at Acme Labs)

\*Based on difference between total sulphur and sulphate-sulphur

\*\*Based on sulphide-sulphur

Reference for Mod ABA NP method (SOP No. 7150): MEND Acid Rock Drainage Prediction Manual, MEND Project 1.16.1b (pages 6.2-11 to 17), March 1991.

## **Appendix B**

### **Elemental Content**



Table 3: Trace Metals Using Aqua Regia Digestion with ICP-MS/ES Finish for 38 Anvil Range Mining Samples - June 2008

S. No:	Sample ID	Ag ppm	Al %	As ppm	Ba ppm	Bi ppm	Ca %	Cd ppm	Co ppm	Cr ppm	Cu ppm	Fe %	Ga ppm	Hg ppb	K %	La ppm	Mg %	Mn ppm	Mo ppm	Na %	Ni ppm	P ppm	Pb ppm	S %	Sb ppm	Sc ppm	Se ppm	Sr ppm	Te ppm	Th ppm	Ti %	Tl ppm	U ppm	V ppm	W ppm	Y ppm	Zn ppm
1	GS 1	0.1	0.3	5	157	0.1	16.22	0.4	10	35.1	42.7	2.82	1.2	<10	0.11	20.3	1.06	577	6.3	0.06	38.3	3402	17	0.86	0.3	3.4	1.4	421	<0.5	6.1	<.005	0.1	2.8	25.6	0.1	18.2	30
2	GS 2	0.3	0.31	2.6	134	0.6	4.56	0.2	16.6	59.2	76.4	4.98	1.2	<10	0.11	8.0	1.72	680	9.9	0.06	48.1	1722	38	1.10	0.5	2.7	1.3	111	<0.5	5.1	<.005	0.2	2.4	30.5	<0.1	10.2	29
3	GS 3	<0.1	0.82	19	206	0.1	4.26	<0.1	16.3	56.5	40.8	3.39	3.3	<10	0.24	37.3	1.99	726	3.6	0.03	39.2	511	8	0.52	0.1	3.4	<0.5	93	<0.5	11.7	<.005	0.2	1.3	16.3	<0.1	11.6	39
4	GS 4	0.3	0.31	14.7	92	0.3	4.93	0.1	19.5	74.2	219.1	3.87	1.3	<10	0.10	6.5	1.92	1265	7.5	0.07	52.1	2974	27	0.49	0.2	2.9	1.4	112	<0.5	5.3	<.005	0.1	1.9	45.7	0.1	16.2	21
5	GS 5	<0.1	2.92	27.6	19	<0.1	2.35	<0.1	46.6	35.9	46.0	5.69	10.9	<10	0.05	11.0	2.73	521	1.8	0.03	31.8	1273	4	0.07	<0.1	14.9	<0.5	91	<0.5	2.2	<.005	<0.1	0.3	129.6	<0.1	6.2	68
6	GS 6	<0.1	2.1	1.9	75	<0.1	0.20	<0.1	23.4	90.3	39.1	5.44	7.9	<10	0.30	6.0	1.21	428	2.4	0.03	42.4	421	9	<0.05	<0.1	6.4	<0.5	6	<0.5	1.9	<.005	0.1	0.3	46.3	<0.1	3.1	287
7	GS 7	0.2	1.93	12.1	138	0.3	0.99	1.0	25.1	89.6	72.8	5.08	6.6	<10	0.21	5.2	1.58	272	4.9	0.06	53.7	1506	70	0.79	0.1	3.0	0.5	33	<0.5	2.7	<.005	0.2	2.2	46.7	<0.1	7.7	226
8	GS 8	0.5	5.16	134.1	25	0.7	0.40	<0.1	55	401.7	113.0	12.09	18.3	<10	0.18	3.2	5.57	567	0.8	0.02	300.1	375	16	<0.05	0.2	10.8	<0.5	12	<0.5	2.4	<.005	<0.1	0.3	132.4	<0.1	5.1	182
9	FNP 01	<0.1	4.31	4.1	273	0.1	2.10	<0.1	18.5	106.2	52.1	3.49	16.8	<10	1.74	22.7	1.24	254	2.8	0.29	44.5	472	42	0.27	0.1	6.9	<0.5	148	<0.5	8.4	0.12	0.4	0.6	49.7	0.1	8.2	77
10	FNP 02	<0.1	4.42	22.9	91	<0.1	3.89	<0.1	12.7	78.8	52.9	1.62	14.3	<10	0.14	21.2	0.65	161	3.1	0.42	33.8	463	21	0.06	0.4	2.3	<0.5	321	<0.5	8.8	0.02	<0.1	0.6	27.2	<0.1	6.8	41
11	FNP 03	<0.1	4.25	3.3	123	<0.1	2.76	<0.1	10	76.3	15.1	1.83	14.7	<10	0.59	25.6	1.00	145	2.2	0.36	24	438	31	<0.05	<0.1	4.0	<0.5	263	<0.5	10.2	0.07	0.1	0.5	33.7	0.1	6.4	58
12	FNP 04	0.1	3.01	1.4	299	0.1	3.39	1.4	13.7	93.5	47.2	2.55	12.0	<10	0.87	29.4	0.99	336	4.1	0.26	37.9	1246	23	0.37	<0.1	5.8	<0.5	174	<0.5	10.9	0.06	0.3	1.2	61.7	0.1	10.2	566
13	FNP 05	0.1	1.98	0.9	396	0.2	1.09	0.1	6.9	40.4	15.2	3.16	9.1	<10	0.94	9.8	0.67	596	3.0	0.15	2.8	654	44	0.28	<0.1	8.2	<0.5	74	<0.5	5.3	0.08	0.7	0.5	61.1	<0.1	10.5	98
14	FNP 06	<0.1	1.72	4.2	33	0.1	1.95	0.4	11.6	61	15.2	1.69	5.6	<10	0.09	31.4	0.76	293	2.2	0.09	28.4	411	35	<0.05	<0.1	2.4	<0.5	61	<0.5	12.8	0.04	<0.1	1.0	20.8	0.2	9.1	105
15	FNP 07	0.6	3.08	1.5	36	0.8	1.71	0.3	14.6	113	99.6	2.77	10.9	<10	0.11	14.8	0.93	209	4.4	0.31	34.4	348	65	0.34	<0.1	1.9	<0.5	112	<0.5	6.2	0.04	<0.1	0.5	37.7	0.1	4.2	107
16	FNP 08	<0.1	1.95	1.7	441	0.3	0.10	<0.1	23.2	96.3	26.0	4.98	8.7	<10	1.84	3.3	0.85	254	2.3	0.04	48	274	7	0.07	<0.1	9.1	<0.5	7	<0.5	1.2	0.15	0.5	0.3	62.7	<0.1	3.7	30
17	FNP 09	<0.1	0.22	1.5	24	<0.1	0.03	0.4	0.9	54.5	122.9	0.62	1.3	<10	0.10	19.5	0.03	49	4.7	0.03	2.2	48	18	<0.05	0.1	1.2	<0.5	3	<0.5	43.0	<.005	0.1	20.0	5.1	0.1	30.9	29
18	FNP 10	<0.1	1.04	2.8	109	0.1	0.18	<0.1	27.5	73.1	67.2	5.42	5.2	<10	0.83	2.5	0.95	440	2.0	0.03	52.6	301	4	0.20	<0.1	6.8	<0.5	6	<0.5	1.5	0.05	0.4	0.4	43.9	<0.1	2.9	36
19	FNP 11	<0.1	2.07	1.2	102	<0.1	0.11	<0.1	17.2	76.5	33.5	5.26	8.4	<10	1.54	3.7	0.85	250	2.1	0.03	42.8	251	4	0.15	<0.1	4.6	<0.5	4	<0.5	1.7	0.10	0.5	0.4	39.4	<0.1	1.6	42
20	FNP 12	0.1	1.56	2.8	227	<0.1	0.17	<0.1	19.2	59.7	34.6	4.75	5.5	<10	1.14	6.7	0.78	642	2.2	0.03	38.3	505	23	0.30	<0.1	3.5	<0.5	5	<0.5	4.8	0.08	1.6	1.6	26.8	<0.1	4.5	66
21	FNP 13	0.4	1.23	1.5	235	<0.1	0.29	<0.1	21.7	67.4	43.0	4.82	5.2	<10	0.88	3.9	0.83	373	2.1	0.03	40.9	609	7	0.14	<0.1	3.6	<0.5	13	<0.5	2.0	0.07	1.6	0.4	31.3	<0.1	3.6	71
22	FNP 14	0.2	2.09	1	183	0.3	0.32	0.1	18.8	113.7	71.6	4.08	11.0	<10	2.15	39.1	1.44	436	4.0	0.04	40.7	457	67	0.99	<0.1	7.8	0.6	9	<0.5	14.4	0.16	0.8	0.9	66	<0.1	10.5	172
23	FNP 15	1.8	0.89	4.1	25	3.8	0.69	1.1	21.1	128.2	27.0	2.08	4.2	<10	0.05	4.1	0.81	317	1.6	0.05	86.1	827	1490	0.23	0.1	4.9	2.6	31	<0.5	0.9	0.01	0.1	<0.1	56.2	<0.1	3.8	203
24	FNP 16	<0.1	1.54	8.7	35	0.2	0.16	<0.1	21.5	72.1	33.2	4.92	6.4	<10	0.18	5.3	0.80	490	2.5	0.02	42.9	299	24	<0.05	<0.1	2.3	<0.5	5	<0.5	2.3	<.005	0.1	0.3	26.8	<0.1	3.4	101
25	GNP 01	<0.1	1.27	12.5	39	<0.1	2.58	<0.1	16.1	45.2	11.6	2.98	3.9	<10	0.09	11.8	1.01	352	1.8	0.02	35.3	284	5	0.06	<0.1	1.5	<0.5	106	<0.5	10.4	<.005	<0.1	0.8	10.9	<0.1	4.3	68
26	GNP 02	<0.1	1.23	4.6	32	0.1	3.35	<0.1	15.7	43.8	23.4	2.91	4.2	<10	0.10	48.0	0.99	414	1.9	0.02	32.9	408	11	0.05	<0.1	1.6	<0.5	119	<0.5	14.9	<.005	<0.1	0.7	10.6	<0.1	10.5	66
27	GNP 03	<0.1	1.96	7.9	47	0.1	2.82	<0.1	20.7	53.7	41.3	4.13	6.7	<10	0.13	58.4	1.38	387	1.4	0.02	45.3	454	7	0.17	<0.1	1.8	<0.5	105	<0.5	18.4	<.005	<0.1	0.8	16.4			



CANTEST Ltd. 4606 Canada Way, Burnaby, BC Canada V5G 1K5 Tel: 604 734 7276 Fax: 604 731 2386 www.cantest.com

SRK Consulting, Anvil Range Mining, 18-Aug-08  
Page 3 of 4

Table 3: Trace Metals Using Aqua Regia Digestion with ICP-MS/ES Finish on 2 Anvil Range Mining (FARO) Samples - September 2008

S. No:	Sample ID	Ag ppm	Al %	As ppm	Ba ppm	Bi ppm	Ca %	Cd ppm	Co ppm	Cr ppm	Cu ppm	Fe %	Ga ppm	Hg ppb	K %	La ppm	Mg %	Mn ppm	Mo ppm	Na %	Ni ppm	P ppm	Pb ppm	S %	Sb ppm	Sc ppm	Se ppm	Sr ppm	Te ppm	Th ppm	Ti %	Tl ppm	U ppm	V ppm	W ppm	Y ppm	Zn ppm
1	FNP-17	0.1	1.72	16	498	0.7	0.52	0.2	7	40.1	85.4	3.06	8.4	10	1.34	15.2	0.67	494	3.6	0.10	1.9	667	4	0.05	<0.1	12.4	0.5	38	<0.05	7.1	0.11	0.4	0.5	76.9	0.9	13.7	51
2	FNP-18	<0.1	2.02	3.7	421	0.1	1.05	0.2	6.8	60.2	30.7	3.24	8.5	22	1.21	14.4	0.74	520	4.7	0.14	1.9	678	18	0.13	<0.1	11.4	<0.5	65	<0.05	6.4	0.13	0.4	1.3	79.9	1.2	14	71
QA/QC																																					
STANDARD MS2		0.3	2.38	21.3	90	5.4	0.10	0.3	12.6	34.3	139.1	3.39	7.8	77	0.37	28.7	0.64	597	12.9	0.04	29.5	579	21.9	<.05	0.1	5.2	<0.5	11	<0.05	10.2	0.06	0.30	2.9	39.9	1	10.4	111
True Values STD MS2		0.2	2.7	22	95.0	4	0.2	0.3	13	40	149	3.2	8.0	74	0.33	28	0.65	570	11	0.04	31	540	21	<.05	0.2	5.5	<0.5	12	<0.05	14	0.07	0.30	3	38	1	11	116
Percent Difference		50.0	-11.9	-3.2	-5.3	35.0	-37.5	0.0	-3.1	-14.3	-6.6	5.9	-2.5	4.1	12.1	2.5	-1.5	4.7	17.3	0.0	-4.8	7.2	4.3	0.0	-50.0	-5.5	0.0	-8.3	0.0	-27.1	-14.3	0.0	-3.3	5.0	0.0	-5.5	-4.3
Detection Limits		0.1	0.01	0.5	1	0.1	0.01	0.1	0.1	1	0.2	0.01	1	0.01	0.01	1	0.01	5	0.1	0.01	0.2	0.001	0.2	0.05	0.1	0.1	0.5	1	0.05	0.2	0.005	0.1	0.1	2	0.1	2	1
Method		1B	1B	1B	1B	1B	1B	1B	1B	1B	1B	1B	1B	1B	1B	1B	1B	1B	1B	1B	1B	1B	1B	1B	1B	1B	1B	1B	1B	1B	1B	1B	1B	1B	1B	1B	1B

**Notes:**  
Analysis done at Global Discovery Labs (Teck Cominco)  
Analytical Methods: ICP-MS Package; 0.5 gram sample digested in hot reverse aqua regia (soil, silt) or hot aqua regia (for rocks).

## **Appendix C**

### **Optical Petrography**

## PETROGRAPHIC REPORT ON 20 SAMPLES (PROJECT SRK-Anvil Range 2-21-90)

Report for: Ivy Rajan  
CANTEST  
4606 Canada Way  
BURNABY, B.C. V5G 1K5 (604) 734-7276

Invoice 080792

Sept. 19, 2008.

### SUMMARY:

Briefly, most of the samples may be divided into weakly to moderately foliated schist/gneiss of variable composition (quartz-pyroxene-biotite-muscovite-chlorite-plagioclase-Kspar±metamorphic indicator minerals such as epidote, amphibole, staurolite, andalusite, or kyanite, and relatively little carbonate), or relatively well foliated, locally crenulated/kink banded, quartz-muscovite-chlorite (rare relict biotite) schist with significant carbonate (up to 20-25%). Accessory sulfides (mainly pyrrhotite, locally altered to pyrite) are commonly partly oxidized to limonite; rutile (rare sphene, ilmenite) is common but minor; apatite and tourmaline are rare, graphite (?) may be present. One sample contains significant barite (?) and one significant pyrite-sphalerite-galena. Capsule descriptions are as follows:

FNP 01: quartz-biotite/sericite/chlorite-Kspar-local amphibole-plagioclase-epidote-andalusite?-pyrite/pyrrhotite/limonite-trace carbonate-sphene-rutile-apatite schist.

FNP 02: quartz-plagioclase-clinopyroxene-Kspar-minor muscovite-biotite schist/gneiss, partly altered to amphibole-carbonate-chlorite-sericite (rare veinlets of zoisite or Kspar), and with accessory sphene-rutile, sulfides, and apatite.

FNP 04: moderately foliated quartz-calcic plagioclase-clinopyroxene-minor Kspar-biotite/phlogopite-muscovite-accessory pyrrhotite-sphene/rutile schist, partly altered to carbonate and minor sericite.

FNP 06: Kspar-clinopyroxene-barite?-muscovite-accessory sphene-ilmenite-pyrrhotite schist/gneiss, partly altered to epidote/zoisite-actinolite-carbonate-chlorite-sericite. Mineralogy is tentative due to fine-grain size and should be confirmed by XRD analysis.

FNP 08: muscovite-biotite-quartz-accessory rutile-trace pyrite schist with local porphyroblastic kyanite? (after staurolite?) partly retrograded to chlorite and sericite, cut by narrow veinlets of Kspar, and partly oxidized to amorphous goethitic limonite along the foliation.

FNP 13: muscovite-quartz-biotite-accessory carbonate?-pyrrhotite-rutile-sphene schist with local porphyroblastic staurolite partly retrograded to chlorite, and partly oxidized to goethitic limonite as pseudomorphs of sulfides, staining adjacent Fe-carbonate, or along the foliation.

FNP 14: well foliated quartz-muscovite/sericite-biotite-accessory pyrite (after pyrrhotite)-rutile schist, cut by veinlets of Kspar, and locally by pyrite (after marcasite?)-chalcopyrite.

GS 2: quartz-carbonate-muscovite/sericite-accessory pyrite, rutile, graphite (?) schist, with sulfides slightly oxidized at rims to limonite. Sulfides are locally in contact with carbonate.

GS 3: quartz-carbonate-muscovite-chlorite-minor (relict) biotite, accessory pyrrhotite, rutile schist/gneiss with coarse blastic quartz and carbonate that contains most of the sulfide.

GS 5: well foliated quartz-chlorite-lesser muscovite-Fe carbonate-accessory rutile schist; foliation-parallel quartz-dolomite (?) veinlets containing rare traces of pyrite (slightly oxidized to limonite). The abundant rutile and chlorite, and presence of Fe carbonate, suggest derivation from a mafic rock.

GS 7: mainly quartz-muscovite-chlorite-accessory rutile-graphite?-pyrite (partly oxidized to limonite) schist, or locally quartz-plagioclase-biotite-staurolite schist retrograded to chlorite-sericite, or carbonate-bearing/veined schist. Carbonate and pyrite do not occur together.

GS 8: relatively coarse, blastic biotite (retrograded to chlorite-muscovite)-carbonate-minor quartz-accessory rutile (partly after former ilmenite?) schist. Carbonate is mostly Fe-bearing dolomite (ankerite?) and chlorite is slightly ferriferous.

GNP 02: strongly foliated/crenulated/kink banded quartz-muscovite-carbonate-chlorite-minor pyrite-rutile schist, locally stained by traces of limonite derived by oxidation of pyrite or Fe carbonate.

GNP 03: well foliated, locally crenulated/kink banded, quartz-muscovite-carbonate-chlorite-accessory pyrrhotite-rutile schist, with minor oxidation of sulfides to limonite along fractures.

GNP 05: moderately foliated, quartz-muscovite-chlorite-minor carbonate-accessory pyrite-rutile-graphite?-apatite schist, with minor oxidation of sulfides to limonite along fractures.

GNP 06: well-foliated, commonly isoclinally or ptygmatically folded, quartz-muscovite-chlorite-minor Fe carbonate-accessory pyrite  $\pm$ pyrrhotite (partly oxidized to limonite)-rutile-possible graphite schist, cut by layer-parallel to locally perpendicular carbonate-quartz veins.

GNP 07: very fine-grained, strongly foliated/locally crenulated/kink banded, almost pure muscovite (minor chlorite, carbonate, possible accessory quartz?-rutile, local tourmaline, trace oxidized pyrite) schist with carbonate present as porphyroblasts, veinlets and layers.

GNP 09: well foliated quartz-muscovite-carbonate-chlorite-minor plagioclase-Kspar-accessory pyrrhotite (trace chalcopyrite)-rutile schist; sulfides are mainly confined to lensy quartz-chlorite-minor carbonate segregations, and are slightly oxidized to limonite along fractures.

GNP 11: strongly foliated, locally crenulated/kink banded/cleaved quartz-muscovite-carbonate-chlorite (accessory pyrrhotite-rutile-possible graphite?) schist, with pyrrhotite mostly confined to layer-parallel/oblique lenses/veinlets, where it is partly encased in carbonate.

VNP 02: strongly mineralized rock, composed mainly of secondary quartz with abundant pyrite, minor muscovite, sphalerite and galena, and traces of rutile and possible graphite (?) although it is difficult to confirm the latter.

Detailed petrographic descriptions and photomicrographs are appended (on CD). If you have any questions regarding the petrography, please do not hesitate to contact me.

FNP 01: QUARTZ-BIOTITE/SERICITE/CHLORITE-KSPAR, LOCAL PLAGIOCLASE-AMPHIBOLE-PYRITE-EPIDOTE-ANDALUSITE?-TRACE CARBONATE-RUTILE SCHIST

Sample consists of small (mainly <2 cm diameter) flat chips of grey slate/phyllite or locally mica schist. The chips are locally slightly magnetic, show no reaction to cold dilute HCl, and only minor stain for K-feldspar in the etched offcut. Modal mineralogy in polished thin section is roughly:

Quartz	40%
Biotite (partly chloritized)	25%
Sericite, muscovite	15%
K-feldspar (partly secondary)	10%
Chlorite	3%
Plagioclase (calcic)	2%
Amphibole (hornblende/actinolitic hornblende?)	2%
Pyrite, pyrrhotite (trace limonite)	1%
Epidote	1%
Andalusite (?)	<1%
Carbonate (dolomite/ankerite?)	<1%
Rutile, sphene, trace apatite	<1%

Most of the chips in this sample consist mainly of quartz and phyllosilicates (mica, including biotite and lesser sericite, local chlorite) plus lesser K-feldspar, local amphibole, plagioclase, epidote, pyrite or pyrrhotite, and traces of carbonate, sphene and rutile. Typically a strong foliation is developed by alignment of sheet silicates, sub-parallel to ribbons of quartz-minor feldspar rich rock.

Quartz forms mainly ragged, sub- to anhedral interlocking crystals <0.35 mm in diameter, but locally in irregular to lenticular aggregates up to almost 1 mm long. The crystals are commonly elongated/flattened in the plane of foliation (length:width ratios up to 3:1) and show signs of moderate to strong strain such as undulose extinction, sub-grain development, and local suturing of grain boundaries. Locally, the quartz occurs in rounded blastic clots up to 1.2 mm in diameter, or lenses/segregations up to 3 mm long, in places containing epidote as ragged subhedra up to 1.5 mm long (lack of pleochroism suggests low Fe content).

Biotite forms mainly euhedral to subhedral flakes up to about 0.3 mm in diameter, with medium reddish brown pleochroism except where they are partly chloritized, turning them pale brownish green and lowering the birefringence. In places the biotite is completely replaced by chlorite as subhedral flakes up to 0.25 mm in diameter, with optical characteristics (very pale green pleochroism, near-zero to weakly anomalous blue-purple, length-slow birefringence) indicative of Fe:Fe+Mg, or F:M, ratio around 0.5 (?). Sericite interleaved or intergrown with biotite and relict biotite forms sub- to euhedral flakes up to 0.1 mm. K-feldspar occurs as subhedral crystals mostly <50 microns, both in thin ribbons along the foliation (typically surrounding micas and separating them from quartz in adjacent ribbons) and in thin veinlets <0.1 mm thick cross-cutting the foliation.

In some chips, amphibole forms sub/euhedral crystals up to 1 mm long with very pale green pleochroism and small extinction angle around 16 degrees suggestive of hornblende or actinolitic hornblende (?). The crystals are commonly in elongated aggregates distributed along foliation, and are intergrown with what appears to be calcic plagioclase (subhedral, rarely twinned crystals to 0.25 mm with strong positive relief against adjacent quartz). In one chip, elongated bladed euhedral crystals up to 1 mm long of what may be andalusite (?) are tentatively identified on the basis of strong positive relief, low first-order birefringence and length-fast character. Very minor sulfides (mainly pyrite or pyrrhotite, subhedra to 0.3 mm, locally partly oxidized at rims to limonite) are locally intergrown with amphibole or epidote, or less commonly with Kspar and biotite as lenses <0.1 mm thick. Traces of carbonate as subhedra mostly <0.1 mm (likely dolomite or ankerite), sphene as euhedra to 0.1 mm and rutile, forming pale brown euhedra <30 um long, plus rare apatite to 0.1 mm, are intergrown with biotite/sericite and quartz/plagioclase respectively.

In summary, this sample is quartz-biotite/sericite/chlorite-Kspar-local amphibole-plagioclase-epidote-andalusite?-pyrite/pyrrhotite/limonite-trace carbonate-sphene-rutile-apatite schist.

**FNP 02: QUARTZ-PLAGIOCLASE-CLINOPYROXENE-KSPAR-AMPHIBOLE-MUSCOVITE-BIOTITE SCHIST/GNEISS ALTERED TO CARBONATE-CHLORITE-SERICITE; ACCESSORY SPHENE-RUTILE-SULFIDES-APATITE, RARE ZOISITE, KSPAR VEINLETS**

Sample consists of flat, angular chips mostly <2 cm in diameter of pale grey, fine-grained, mostly schistose rock. The rock is not magnetic, but shows minor reaction to cold dilute HCl, and minor stain for K-feldspar in the etched outcut. Modal mineralogy in polished thin section is approximately:

Quartz	30%
Plagioclase (calcic?)	25%
Clinopyroxene (salite?)	20%
K-feldspar	10%
Amphibole	5%
Mica (muscovite, biotite, sericite)	3%
Carbonate (mainly ankerite, minor calcite?)	3%
Chlorite	2%
Sphene, trace rutile, apatite	1-2%
Pyrrhotite, trace chalcopyrite	<1%
Zoisite (veinlets)	<1%

This sample is composed mainly of crudely defined, irregular, alternating layers <2 mm thick rich in either quartz-feldspar(s) partly altered to sericite, or pyroxene (altered to amphibole around margins, or locally to carbonate or chlorite), with accessory mica, carbonate, sphene/rutile, sulfides, rare apatite. Layers containing mica are relatively rare (mainly euhedral flakes of muscovite or biotite up to 0.5 mm, locally chloritized). Rare veinlets <0.1 mm thick consist of zoisite subhedra <0.15 mm.

In the felsic layers, quartz forms ragged, sub- to anhedral, interlocking crystals mostly <0.25 mm in diameter, generally intimately intergrown with feldspars (plagioclase and lesser K-feldspar) plus accessory sphene/rutile. Somewhat elongated shapes (length:width up to 3:1) sub-parallel to foliation indicate flattening during metamorphism. The quartz is typically only weakly strained (shows minor undulose extinction) but displays corroded/overgrown margins, especially on the larger crystals, suggestive of secondary quartz activity. Plagioclase forms ragged subhedra mostly <0.2 mm with positive relief compared to quartz, suggestive of a highly calcic composition (twinning is mostly absent), and are typically partly to locally strongly altered to fine-grained sericite (randomly oriented flakes mostly <15 microns). K-feldspar forms rounded to ragged subhedra up to as much as 1 mm in size that locally poikilitically enclose other silicates. Kspar also occurs in rare narrow veinlets. Rare apatite forms stubby euhedra to 0.1 mm.

In the more mafic layers, ragged rounded to elongate aggregates of clinopyroxene have irregular outlines up to 3 mm in diameter. Large extinction angle near 43 degrees and pale brownish colour suggest a salitic composition (between diopside and hedenbergite?). In places the crystals are altered around the margins to a fuzzy, ill-defined mineralogy that appears to include amphibole (fibrous subhedra <0.15 mm, possibly tremolite-actinolite?) and carbonate (either fine-grained, brownish ankerite or coarser, relatively clear calcite/dolomite as subhedra to 0.6 mm). Minor chlorite forming ragged subhedral flakes <0.15 mm (with very pale green colour, weakly anomalous blue length-slow to weakly anomalous green, length-fast birefringence indicative of F:M around 0.5) is also likely after former pyroxene; they are locally interleaved with minor sericite <0.1 mm in size.

Sphene is common as slender euhedra to 0.2 mm long or ragged aggregates to 0.1 mm composed of small subhedra mostly <30 microns in diameter commonly cored by slender acicular rutile <20 microns long. Relatively rare sulfides occur as elongated blebs up to 1 mm long sub-parallel to the schistosity, composed of sub/euhedral pyrrhotite up to 0.2 mm and rare chalcopyrite as subhedra <0.1 mm, associated with chlorite but not with carbonate.

In summary, this appears to be quartz-plagioclase-clinopyroxene-Kspar-minor muscovite-biotite schist/gneiss, partly altered to amphibole-carbonate-chlorite-sericite (rare veinlets of zoisite or Kspar), and with accessory sphene-rutile, sulfides, and apatite.

**FNP 04: QUARTZ-PLAGIOCLASE-CLINOPYROXENE-KSPAR-BIOTITE/PHLOGOPITE-MUSCOVITE-MINOR CARBONATE-SERICITE PYRRHOTITE-SPHENE/RUTILE SCHIST**

Sample consists of flattish, angular chips mostly <2 cm in diameter of dark grey schistose rock. The rock is locally weakly magnetic, shows only trace reaction to cold dilute HCl, and only minor stain for K-feldspar in the etched offcut. Modal mineralogy in polished thin section is approximately:

Quartz	30%
Plagioclase (calcic, sericitized)	30%
Clinopyroxene	25%
K-feldspar	5%
Mica (biotite/phlogopite, minor muscovite)	5%
Carbonate (ankerite?)	2%
Sericite (after plagioclase)	1%
Pyrrhotite, trace pyrite	1%
Sphene, rutile	1%

This sample is similar to FNP 02, composed of alternating lensy layers mostly <1-2 mm thick composed of either quartz-feldspar(s) rich or clinopyroxene-rich rock, the former showing alteration to traces of sericite and carbonate and the latter minor alteration to carbonate, mainly at the margins. Accessory pyrrhotite and sphene are mostly associated with local layers enriched in mica (pale biotite or phlogopite, minor muscovite).

In the felsic layers, quartz is about as abundant as plagioclase, and Kspar is subordinate. Quartz forms sub- to anhedral interlocking crystals rarely over 0.35 mm in diameter, although commonly in aggregates up to almost 1 mm long (typically elongated in the plane of foliation or layering). The crystals are generally only weakly strained (show minor undulose extinction). Plagioclase forms subhedral somewhat skeletal, ragged crystals up to about 0.2 mm long, commonly strongly aligned with the foliation forming a ribbon-like texture, and locally showing vague, poorly defined twinning; extinction on 010 up to 30 degrees and positive relief compared to quartz suggest a calcic composition, likely above An50. Most plagioclase is incipiently altered to sericite as minute randomly oriented flakes mostly <15 microns in diameter. K-feldspar is typically finer-grained and interstitial to quartz and plagioclase, forming subhedra mostly <0.1 mm in size.

In the mafic layers, clinopyroxene forms stubby to rounded subhedra up to about 0.5 mm in diameter, but locally in stringer-like aggregates that are optically semi-continuous for up to several mm along the foliation. Extinction angle is large (40+ degrees) and colour is neutral to pale brownish, although the latter is most pronounced where carbonate alteration is strongest. The crystals tend to be ragged and commonly corroded around the margins by alteration to carbonate (interlocking sub/anhedra <0.1 mm, locally with a fibrous texture suggestive of development after amphibole such as tremolite/actinolite?). Carbonate also occurs in irregular veinlets <0.1 mm thick oblique to foliation.

Layers rich in mica consist of pale to very pale brown, possibly biotitic-phlogopitic, mica, locally with colourless muscovite, as ragged sub- to euhedral flakes mostly <0.2 mm in diameter, not always aligned with the foliation/layering (locally oblique, especially where the layers bend around clots of quartz or sulfide). Most sulfide is pyrrhotite, forming sub/euhedra to 0.5 mm long in blebby aggregates up to 2 mm long, aligned with the foliation and locally partly oxidized at the rims to FeSx phases or replaced by possible marcasite (rare pyrite is euhedral/skeletal, <0.1 mm). Accessory sphene, forming sub/euhedral crystals or aggregates up to 0.15 mm long partly cored by rutile as acicular euhedra <25 microns long, is associated with pyrrhotite or occurs included within pyroxene- or phlogopite-rich layers.

In summary, this is moderately foliated quartz-calcic plagioclase-clinopyroxene-minor Kspar-biotite/phlogopite-muscovite-accessory pyrrhotite-sphene/rutile schist, partly altered to carbonate and minor sericite.



**FNP 06: KSPAR-CLINOPYROXENE-BARITE-MUSCOVITE-MINOR SPHENE-ILMENITE-PYRRHOTITE SCHIST, ALTERED TO EPIDOTE/ZOISITE-ACTINOLITE-CARBONATE-CHLORITE-SERICITE**

Sample consists of flat angular chips up to almost 3 cm in diameter of medium grey, finely layered/banded or locally schistose rock (break is not always parallel to foliation/layering). The rock is not magnetic, and shows only local reaction to cold dilute HCl, but there is strong stain for K-feldspar in the etched offcut. Modal mineralogy in polished thin section is (very approximately):

K-feldspar	40%
Epidote (clinozoisite?), zoisite	15%
Barite (?), partly plucked out	10%
Amphibole (actinolite, after pyroxene?)	10%
Relict clinopyroxene	5%
Carbonate (ankerite?)	5%
Mica (mainly muscovite)	5%
Chlorite	5%
Sericite (after feldspar)	3-4%
Sphene, ilmenite	<1%
Pyrrhotite, trace sphalerite	<<1%

This sample is composed of mostly intimately intergrown, very fine-grained minerals that are difficult to distinguish and identify petrographically; it would benefit from XRD analysis. However, it appears to be composed of chips of rock that range from relatively fine-grained, somewhat foliated Kspar plus epidote/amphibole/carbonate/chlorite (all likely after pyroxene, which remains in some layers) to layers of coarser-grained barite (?) or mica (mainly muscovite).

K-feldspar rich layers mostly <1 mm thick are composed of interlocking ragged subhedra mostly <0.25 mm in diameter, with random to somewhat aligned orientations (sub-parallel to the layering). The feldspar is locally incipiently to strongly altered to fine-grained sericite as randomly oriented flakes mostly <25 microns in diameter.

Mafic-rich interlayers are also up to about 1 mm thick, but commonly discontinuous and irregular, <0.25 mm thick. They are partly composed of relict clinopyroxene, forming bladed to rounded subhedra up to 2 mm long, generally aligned within the layering/foliation. Extinction angle around 45 degrees and general lack of colour (except where altered, particularly at margins, to epidote-group minerals, amphibole and carbonate) suggests it may be diopside. Progressive alteration replaces or pseudomorphs the pyroxene with either amphibole (radiating rosettes of fine-grained fibrous needle-like crystals mostly <0.2 mm long with pale green pleochroism and small extinction angle, typical of actinolite) or epidote-group mineral that forms either subhedra mostly <0.5 mm in diameter with pale yellow-green pleochroism (clinozoisite, or Fe-poor epidote) or euhedral bladed crystals with anomalous blue birefringence and no pleochroism (zoisite?). In places further alteration is to carbonate (likely ankerite to judge by the lack of reaction in hand specimen, forming ragged subhedra rarely over 0.25 mm) and chlorite (sub/euhedral flakes to 0.2 mm with weakly blue anomalous to green anomalous birefringence suggestive of F:M around 0.5?).

In some layers, coarse blastic barite (?) forming subhedral crystals mostly <0.5, but locally to 1 mm, occurs in rounded aggregates up to 3 mm long that overgrown mafic layers, and are partly to largely plucked out by section preparation. The crystals are strained/recrystallized (show undulose extinction). Some layers are mostly muscovite as strongly aligned flakes <1 mm in diameter.

Sphene, forming ragged subhedra mainly <50 microns long, is difficult to distinguish except in reflected light; it is locally associated with minor ilmenite as tabular euhedra mostly <25 microns long. Rare sulfide is mainly pyrrhotite, forming subhedra mostly <35 microns in diameter, and rarely associated with trace sphalerite (colourless, i.e. low Fe, <20 microns in diameter).

In summary, this appears to be Kspar-clinopyroxene-barite?-muscovite-accessory sphene-ilmenite-pyrrhotite schist/gneiss, partly altered to epidote/zoisite-actinolite-carbonate-chlorite-sericite. Mineralogy is tentative due to fine-grain size and should be confirmed by XRD analysis.

**FNP 08: MUSCOVITE-BIOTITE-QUARTZ-ACCESSORY RUTILE-TRACE PYRITE SCHIST, PORPHYROBLASTIC KYANITE? (AFTER STAUROLITE?) RETROGRADED TO CHLORITE-SERICITE, CUT BY KSPAR AND LIMONITE VEINLETS**

Sample consists of flat chips up to 3 cm in diameter of pale grey-brown (slightly weathered and oxidized), medium-grained micaceous schist. The rock is not magnetic, shows no reaction to cold dilute HCl, and very minor stain for K-feldspar in the etched offcut (mainly along very narrow irregular veinlets cutting the schistosity, i.e. secondary). Modal mineralogy in polished thin section is approximately:

Muscovite, minor sericite, clay?/sericite	50%
Biotite	20%
Quartz	20%
K-feldspar (mainly secondary)	5%
Kyanite (?), after relict staurolite (?)	2%
Chlorite (magnesian?), after kyanite (?)	1%
Limonite	1%
Rutile	<1%
Pyrite	<<1%

This appears to be a mica-quartz schist, with minor high-grade (amphibolite facies) metamorphic indicator minerals (kyanite after staurolite?) as local porphyroblasts, partly retrograded to magnesian chlorite. Minor limonite may be derived by oxidation of accessory pyrite, traces of which remain.

Most of the chips are composed of well-foliated mica schist, comprising strongly aligned flakes of muscovite (up to about 1 mm in diameter) mixed with lesser, less perfectly aligned, deep reddish brown flakes of biotite of similar or smaller size, alternating with irregular segregations of quartz up to 1.5 mm thick.

Quartz forms interlocking, ragged sub/anhedral crystals up to about 0.5 mm in diameter, mostly with weak to moderate strain indicated by undulose extinction, minor sub-grain development, and rare suturing of grain boundaries

Locally, large porphyroblastic crystals of kyanite (?) up to 3 mm long, oriented oblique to foliation, appear to be pseudomorphous after staurolite (?) that occurs as minor small (<0.2 mm) remnants within the porphyroblasts. Kyanite (?) is tentatively identified on the basis of low (length-slow) birefringence, strong positive relief against quartz, extinction about 30 degrees to longitudinal cleavage, and poikilitically included relics of staurolite (?) which show pale yellow pleochroism and also appear to be length-slow, with positive relief against kyanite (?). The kyanite (?) is altered to fine-grained sub/euhedral flakes of chlorite mostly < 35 microns in diameter, with optical properties (almost colourless, weak first-order grey, length-fast birefringence) suggestive of a slightly magnesian composition (F:M 0.4-0.5?), or locally sericite (subhedral flakes <45 microns in size).

Kspar is mainly controlled along narrow irregular veinlets <0.5 mm thick sub-perpendicular or sub-parallel to foliation, where it forms irregular sub/anhedral crystals mostly <0.25 mm in diameter. It is slightly altered to minute flakes of clay?/sericite mostly <10 microns in diameter.

Scattered crystals of accessory rutile occur as dark brown, acicular euhedra up to 0.12 mm long, generally aligned with the mica flakes. Rare pyrite forms skeletal euhedra up to 0.3 mm in diameter, associated with mica but in contact with quartz. The pyrite is slightly oxidized around the rims to a coating of limonite, and some limonite is locally found staining adjacent mica flakes.

Along the foliation, minor limonite occurs as (mostly transported) amorphous red-brown stains or locally narrow veinlets <0.1 mm thick (likely mostly goethite). It may be derived by oxidation of pyrite.

In summary, this is muscovite-biotite-quartz-accessory rutile-trace pyrite schist with local porphyroblastic kyanite? (after staurolite?) partly retrograded to chlorite and sericite, cut by narrow veinlets of Kspar, and partly oxidized to amorphous goethitic limonite along the foliation.

**FNP 13: MUSCOVITE-QUARTZ-BIOTITE-MINOR FE CARBONATE?-PYRRHOTITE-TRACE CHALCOPYRITE-RUTILE/SPHENE SCHIST, PORPHYROBLASTIC STAUROLITE ALTERED TO CHLORITE; LIMONITE AFTER SULFIDES, CARBONATE**

Sample is similar to the previous sample (FNP 08) and consists of flat chips mostly <2.5 cm in diameter of pale orange-brownish grey, slightly oxidized and weathered (trace stains of limonite). The rock is weakly magnetic, but shows no reaction to cold dilute HCl, and no stain for K-feldspar in the etched offcut. Modal mineralogy in polished thin section is approximately:

Muscovite	40%
Quartz	30%
Biotite	20%
Carbonate (ankerite/siderite?)	3%
Staurolite (relict)	2%
Pyrrhotite, trace chalcopryrite	1-2%
Limonite (after sulfide, carbonate)	1-2%
Rutile, sphene	1%
Chlorite (magnesian?), after staurolite	1%

This appears to be a mica-quartz schist, with minor high-grade (amphibolite facies) metamorphic indicator minerals (staurolite) as local porphyroblasts, partly retrograded to chlorite. Minor limonite is likely derived by oxidation of accessory pyrrhotite and stains adjacent carbonate and mica along the foliation.

Most chips are composed of well-foliated mica-quartz schist, comprising strongly aligned flakes of muscovite (up to about 1 mm in diameter but locally semi-continuous optically for up to 3 mm) mixed with lesser, aligned to oblique, pale to medium reddish brown flakes of biotite of similar or smaller size, alternating with irregular segregations of quartz up to slightly over 1.5 mm thick.

Quartz forms interlocking, mostly subhedral crystals <0.35 mm in diameter, mostly with only weak to moderate strain indicated by undulose extinction, minor sub-grain development, and rare suturing of grain boundaries

Rarely, porphyroblastic crystals of staurolite (pale yellow pleochroism, length-slow, with positive relief against quartz) up to 1.5 mm long, oriented oblique to foliation, appear to be partly to largely pseudomorphed by chlorite mostly < 35 microns in diameter, with optical properties (almost colourless, weak first-order grey, but variable, length-fast/slow birefringence) suggestive of a slightly magnesian composition (F:M 0.4-0.5?). Inclusions of minute opaques mark the cores of some of the relict staurolite crystals, suggestive of former andalusite (?). Biotite intergrown around the margins contains local sub/euhedral crystals of dark brown/opaque rutile or colourless sphene, both up to 50 microns in diameter but locally aggregating to 0.15 mm.

Local pyrrhotite forms sub/euhedra up to 0.3 mm in diameter in aggregates up to several mm long (rarely with inclusions of chalcopryrite to 0.1 mm), commonly coated with what appears to be Fe-carbonate (ankerite or siderite) as subhedra mostly <0.1 mm, although it is difficult to distinguish from sphene, which forms similar sized sub/euhedra in aggregates to 0.2 mm locally containing cores of rutile as euhedra to 0.1 mm long. The pyrrhotite is partly (or locally completely) oxidized around the rims to a coating of limonite, and limonite occurs staining adjacent carbonate (?) and mica flakes. Minor limonite also occurs as (mostly transported) amorphous red-brown stains or locally narrow veinlets <0.1 mm thick (likely mostly goethite), along the foliation. It appears to be derived by oxidation of pyrrhotite.

In summary, this is muscovite-quartz-biotite-accessory carbonate?-pyrrhotite-rutile-sphene schist with local porphyroblastic staurolite partly retrograded to chlorite, and partly oxidized to goethitic limonite as pseudomorphs of sulfides, staining adjacent Fe-carbonate, or along the foliation.

**FNP 14: QUARTZ-MUSCOVITE/SERICITE-BIOTITE-ACCESSORY PYRITE (AFTER PYRRHOTITE?)-RUTILE SCHIST, VEINLETS OF KSPAR AND PYRITE-CHALCOPYRITE**

Sample consists of flat, well foliated chips mostly <2.5 cm in diameter of dark grey (but locally slightly limonite-stained) schist. The rock is locally weakly magnetic, shows minor reaction to cold dilute HCl, and minor stain for K-feldspar in the etched offcut (commonly along narrow veinlets, indicating a secondary origin). Modal mineralogy in polished thin section is approximately:

Quartz	40%
Muscovite, sericite	30%
Biotite	20%
K-feldspar (largely secondary)	5-7%
Pyrite (mainly after pyrrhotite?), trace chalcopyrite	2-3%
Rutile	1%

Most of the chips in this sample consist of interlayered, alternating quartz-rich or mica-rich rock, the former locally with clotty texture (metamorphic “sweats” or segregations) and the latter with accessory sulfides and rutile, locally cut by narrow veinlets of Kspar.

Quartz forms somewhat ragged, locally irregular, sub- to anhedral crystals up to 0.5 mm in diameter, typically with only minor strain indicated by relatively weak undulose extinction and minor sub-grain development. Scattered aggregates to about 1 mm of the coarser-grained quartz suggest that the finer-grained matrix quartz could be developed by crushing and granulation, or that the coarse aggregates may represent former quartz “eyes” in a volcanic rock (?).

Micas are typically intimately intermixed, forming sub- to euhedral flakes mostly <0.25, but locally up to 0.5, mm in diameter. Biotite shows pale to bright red-brown pleochroism. Both biotite and muscovite are commonly aligned along or oblique to the foliation, suggesting development of a crenulation cleavage on top of the foliation. In places the micas are relatively fine-grained and difficult to separate (biotite and “sericite”); these zones have the appearance of having replaced former zones similar to the clinopyroxene-rich layers in other samples of this suite.

K-feldspar occurs both as narrow (<0.1 mm thick) irregular veinlets cutting or oblique to foliation, or as irregular, poorly defined zones up to 0.5 mm thick sub-parallel to foliation, in which the Kspar forms ragged subhedra mostly <0.1 mm in diameter, typically interstitial to quartz and mixed with biotite and fine-grained muscovite (sericite).

Sulfides appear to be mostly pyrite (in part possibly after marcasite?), likely after pyrrhotite to judge by the locally porous, secondary texture and the weak magnetism of the sample. Pyrite forms either relatively coarse, ragged, skeletal sub/euhedra up to 0.5 mm, or else fine-grained, acicular or bladed euhedra <0.1 mm long that are suggestive of former marcasite (?), commonly developed after pyrrhotite; the latter also occur along narrow irregular veinlets <0.1 mm thick, with traces of chalcopyrite as subhedra <0.1 mm. The sulfides are intergrown with quartz and biotite. Rutile occurs as aggregates up to 0.1 mm long of dark brown, rounded stubby subhedra mostly <20 microns long, or as minute dust-like particles <3 microns in size, both typically concentrated as wispy foliae within biotite, although in places similar aggregates of rutile occur in quartz.

In summary, this is well foliated quartz-muscovite/sericite-biotite-accessory pyrite (after pyrrhotite)-rutile schist, cut by veinlets of Kspar, and locally by pyrite (after marcasite?)-chalcopyrite.

## GS 2: QUARTZ-CARBONATE-SERICITE/MUSCOVITE-ACCESSORY PYRITE-RUTILE-GRAPHITE? SCHIST; PYRITE SLIGHTLY OXIDIZED TO LIMONITE

No hand sample material remains, but etched offcut shows that the sample consists of flat chips of dark grey, fine-grained, well foliated schist up to 2.5 cm in diameter. The rock is not magnetic, shows only trace reaction to cold dilute HCl, and no stain for K-feldspar in the etched offcut. Modal mineralogy in polished thin section is approximately:

Quartz	65%
Carbonate (ankerite, minor siderite?)	20%
Sericite, muscovite	10%
Pyrite	2%
Rutile	1%
Graphite (?)	1%
Limonite (after sulfides)	<1%

The chips in this sample are composed of crudely segregated lenses or layers of quartz and carbonate, separated by wispy foliae of mica-minor carbonate-accessory graphite-sulfides. Foliation varies from weak to strong. Some carbonate is heavily Fe-stained.

Quartz forms tightly interlocking, mostly subhedral crystals <0.2 mm in diameter (locally in rounded to irregular-shaped aggregates up to 0.5 mm across). The quartz crystals typically show moderate to locally strong undulose extinction, minor sub-grain development, and suturing of grain boundaries, indicative of strain. They are also intergrown around their margins with the adjacent interstitial carbonate and sericite/muscovite.

Carbonate occurs as either relatively coarse-grained sub/euhedra up to 0.5 mm (in local blastic aggregates as much as 1 mm across), or as relatively fine-grained sub/anhedra mostly <0.1 mm in size, interstitial to quartz and associated with the muscovite/sericite. Most of the carbonate is relatively clear to slightly brownish, but lacks reaction to HCl in hand specimen, and so may be ankeritic, but some is distinctly brown and/or limonite-stained, and may be siderite (?).

Muscovite/sericite typically forms euhedral flakes up to about 0.2 mm, or ragged, subhedral flakes mostly <0.1 mm, respectively, that vary from strongly aligned in the plane of foliation, to locally oblique to it.

Sulfides, as in FNP 14, are mainly pyrite, forming ragged sub- to euhedral crystals up to 1 mm in diameter but locally aggregating to 2 mm. The crystals are fractured and appear to be partly oxidized at the rims to limonite (locally readily visible at petrographic scale of observation). In places, a relict porous texture is suggestive of replacement of former pyrrhotite (?). In most cases, the coarser-grained sulfide does not actually make contact with the carbonate, but locally minor fine-grained pyrite is contained within the carbonate.

In the mica-rich foliae, minor rutile (subhedra mostly <5, locally up to 20 microns long) and possible graphite (flakes mostly <5 microns) are intimately mixed with the mica, making their identification difficult to confirm even at very high magnification (250x).

In summary, this is quartz-carbonate-muscovite/sericite-accessory pyrite, rutile, graphite (?) schist, with sulfides slightly oxidized at rims to limonite. Sulfides are locally in contact with carbonate.

### GS 3: QUARTZ-CARBONATE-MUSCOVITE-CHLORITE (RELICT BIOTITE)-ACCESSORY PYRRHOTITE-RUTILE SCHIST/GNEISS WITH COARSE BLASTIC QUARTZ-CARBONATE

Sample consists of elongated, flattish chips up to 3 cm long of light grey, fine-grained, quartz-mica schist similar to the previous sample (GS 2). The rock is weakly magnetic, shows minor slow reaction to cold dilute HCl, and no stain for K-feldspar in the etched offcut. Modal mineralogy in polished thin section is approximately:

Quartz	60%
Carbonate (dolomite?)	20%
Muscovite, sericite	10%
Chlorite (magnesian)	5%
Biotite	3%
Pyrrhotite	1-2%
Rutile	<1%

This sample consists mainly of chips of weakly foliated, quartz-carbonate rich gneiss or schist with lesser muscovite and chlorite (partly after relict biotite) in thin wispy foliae, locally associated with accessory pyrrhotite and trace rutile. In these foliae, muscovite or sericite forms sub- to euhedral flakes up to 0.35 mm in diameter, but locally optically continuous for up to 3 mm, that are mixed with variable amounts of chlorite (mainly euhedral flakes up to 0.2 mm, but in aggregates up to 0.4 mm, with very weak green pleochroism and green anomalous, length-fast birefringence indicative of F:M around 0.4). In places minor relict biotite with pale brown pleochroism, forming ragged relict flakes <0.15 mm, suggests some chlorite may be after biotite. Most chlorite is intimately intergrown with carbonate, suggesting replacement of former mafic minerals.

Quartz occurs mainly in lensey segregations or layers up to about 1 mm thick in which it forms tightly interlocking, rounded subhedral to locally irregular anhedral crystals mostly <0.25 mm in diameter, with moderate strain indicated by undulose extinction, some sub-grain development, and local suturing of grain boundaries. Locally however quartz also occurs as coarse-grained blastic megacrystals or aggregates up to 2 mm across in which strong strain is indicated by more abundant undulose extinction, sub-grain development, and suturing of grain boundaries. These aggregates are intergrown with coarse-grained carbonate.

Coarse-grained carbonate occurs in aggregates up to 5 mm across, composed of interlocking sub/euhedra up to 2 mm in diameter that are likely dolomite (the clear crystals) or brownish ankerite (?) to judge by the slow reaction or lack of reaction to HCl in hand specimen. Fine-grained rims on some of the brownish crystals could be siderite (?). These areas contain most of the sulfides (mainly pyrrhotite) in the sample. Carbonate also occurs along irregular, locally vuggy vein-like areas up to almost 1 mm thick, oblique to the weak foliation.

Pyrrhotite occurs as aggregates to 0.2 mm of interlocking euhedra mostly <50 microns in size, commonly completely encased in carbonate. Traces of rutile (slender acicular euhedra to 25 microns) occur aligned with the foliation, included in muscovite that locally wraps around the margins of coarse carbonate crystals.

In summary, this is quartz-carbonate-muscovite-chlorite-minor (relict) biotite, accessory pyrrhotite, rutile schist/gneiss with coarse blastic quartz and carbonate that contains most of the sulfide.

**GS 5: QUARTZ-CHLORITE-CARBONATE-MUSCOVITE-ACCESSORY RUTILE SCHIST  
WITH FOLIATION-PARALLEL VEINLETS OF QUARTZ-DOLOMITE-TRACE PYRITE  
(PARTLY OXIDIZED TO LIMONITE)**

Sample consists of greenish-grey, very flat, “paper schist” fragments up to 2.5 cm in diameter set in epoxy (no other sample material remains). The rock is weakly magnetic, shows minor reaction to cold dilute HCl (mostly along veinlets, where powdered), and no stain for K-feldspar in the etched offcut. Modal mineralogy in polished thin section is approximately:

Quartz	35%
Chlorite (magnesian)	35%
Carbonate (ankerite, veinlet dolomite?)	15%
Muscovite, sericite	13%
Rutile	1-2%
Limonite (partly after carbonate)	<1%
Pyrite	trace

This sample consists essentially of paper-thin, strongly foliated fragments of quartz-chlorite-minor mica- Fe carbonate-rutile schist, cut by foliation-parallel or -oblique veinlets of carbonate and quartz.

Quartz occurs mostly as small, commonly somewhat flattened/elongated subhedral crystals <0.2 mm long (length:width ratios up to 2.5:1), with only weak to moderate undulose extinction indicative of weak strain and possible later annealing. However, in the veinlets and local lensy segregations, quartz occurs as larger, sub- to anhedral interlocking crystals up to 0.35 mm in size, with somewhat stronger strain indicated by undulose extinction, minor sub-grain development and suturing of grain boundaries.

Chlorite is abundant, forming mostly euhedral flakes <0.2 mm in diameter, strongly aligned in and defining the foliation. Optical properties (very pale green pleochroism, weakly anomalous green, length-fast birefringence) indicate a somewhat magnesian composition (F:M around 0.4?)

Lesser muscovite is intimately intergrown with or included in the chlorite, forming similar size (mostly <0.15 mm) euhedral flakes also sub-parallel to the well-developed foliation.

Minor carbonate forming sub/anhedral crystals mostly <50 microns in diameter (rarely to 0.1 mm) is intergrown with the phyllosilicates and quartz, commonly in irregular, poorly defined aggregates <0.1 mm thick, roughly along the foliation. Much of this carbonate is partly to strongly stained by limonite as amorphous red- to orange-brown material; taken with the general lack of reaction to HCl in hand specimen, this suggests this carbonate may be ankerite (?). It is commonly associated with accessory rutile as aggregates mostly <0.15 mm long, composed of euhedral acicular crystals <30 microns long.

In the veinlets, however, carbonate (forming sub- to euhedral crystals up to almost 1 mm long) is relatively clear or slightly brownish, lacks Fe stain, and reacts more readily to HCl in hand specimen, suggesting it may be dolomite (?). The veinlets also contain rutile similar to that in the matrix (likely accidental inclusions) and traces of pyrite (euhedra <0.12 mm) that are slightly oxidized to limonite at the rims, contributing some limonite that is transported into stains along grain boundaries in adjacent quartz and carbonate. Pyrite is in contact with quartz and carbonate.

In summary, this is strongly foliated quartz-chlorite-lesser muscovite-Fe carbonate-accessory rutile schist, with foliation-parallel quartz-dolomite (?) veinlets containing rare traces of pyrite (slightly oxidized to limonite). The abundant rutile and chlorite, and presence of Fe carbonate, suggest derivation from a mafic rock (?).

GS 7: QUARTZ-MUSCOVITE-CHLORITE-MINOR PYRITE-RUTILE-GRAPHITE? SCHIST, LOCAL BLASTIC BIOTITE-STAUROLITE/CHLORITE SCHIST, CARBONATE VEINS

Sample consists mostly of very pale buff- to greenish-grey, fine-grained, very flat, “paper schist” fragments up to 4 cm in diameter; a few chips are slightly coarser-grained. The rock is not magnetic, shows no reaction to cold dilute HCl except in some chips (where powdered only), and no stain for K-feldspar in the etched offcut. Modal mineralogy in polished thin section is approximately:

Quartz	35%
Muscovite, sericite	35%
Chlorite	15%
Plagioclase (relict, partly sericitized)	3%
Carbonate (dolomite, trace ankerite?)	3%
Biotite (relict)	3%
Staurolite	2%
Pyrite (partly after pyrrhotite?)	2%
Rutile, graphite (?), minor ilmenite, sphene	1-2%
Limonite (after sulfides)	<1%

Most of the chips in this sample consist of lensey aggregates or segregations of quartz, separated by thinner, locally wispy foliae of muscovite/chlorite/accessory rutile (possible graphite?), with scattered sulfides partly oxidized to limonite. A few chips consist of porphyroblastic biotite and staurolite, both partly retrograded to chlorite and sericite, and some contain significant carbonate (partly along the foliation, partly as veinlets perpendicular to foliation).

In most of the chips, quartz occurs in lensey layers up to 1.5 mm thick, composed of interlocking ragged subhedra mostly <0.4 mm in diameter that generally display only slight flattening and elongation in the plane of foliation (length:width ratios mainly <1.5:1, rarely to 2:1). The crystals show slight strain (weak undulose extinction, rare sub-grain development or suturing of grain boundaries). Muscovite, forming mainly euhedral, strongly aligned flakes <0.5 mm in diameter, is locally intimately mixed with chlorite as sub/euhedral flakes mostly <0.2 mm in diameter, in places after relict biotite or phlogopite (?) with very pale brown pleochroism. Most chlorite has very weak to weak green pleochroism and near-zero to slightly length-slow (?) birefringence, suggesting F:M around 0.5. Minute opaques, including pale to dark brown rutile and possibly graphite (?), mostly <20 and <3 microns in diameter respectively, are concentrated in wispy foliae that show isoclinal folding in the micaceous layers. Sulfides appear to be mostly pyrite, forming ragged, skeletal subhedra to 0.5 mm or occur as narrow (<0.1 mm thick) veinlets along foliation, with local bladed crystals shapes suggestive of former marcasite (?) itself likely after original pyrrhotite (?). In places, some of the sulfides are partly oxidized at rims and along fractures to minor limonite, some of which is transported into adjacent silicates as amorphous stains.

In some chips, quartz (much as described above) is mixed with lesser, mostly interstitial, finer-grained (sub/anedral, <0.1 mm) feldspar (likely plagioclase since no stain for Kspar in etched offcut; possibly albitic since it displays negative relief compared to quartz). In places the plagioclase is incipiently to locally completely altered to sericite as randomly oriented, subhedral flakes mostly <35  $\mu$ m. These chips also contain porphyroblastic sub/euhedral crystals of pale yellow staurolite up to 0.7 mm long, and biotite up to 1 mm long, both partly retrograded to chlorite with distinct green pleochroism, and length-slow anomalous blue birefringence suggestive of more Fe-rich composition (F:M around 0.6-0.7?), or in places sericite; biotite contains ilmenite to 0.2 mm long. In other chips, carbonate is abundant as ragged, irregular aggregates up to 1.2 mm thick along the foliation (mixed with sericite and chlorite), associated with foliation-perpendicular veinlets <0.5 mm thick of similar carbonate (subhedra to 0.25 mm, mainly clear, dolomite at the core, flanked by limonite-stained ankerite?). In the envelopes to these veins, rutile is partly altered to sphene (subhedra to 40 microns).

In summary, this is mainly quartz-muscovite-chlorite-accessory rutile-graphite?-pyrite (partly oxidized to limonite) schist, or locally quartz-plagioclase-biotite-staurolite schist retrograded to chlorite-sericite, or carbonate-bearing/veined schist. Carbonate and pyrite do not occur together.



# GS 8: CHLORITE-FE STAINED CARBONATE-MUSCOVITE-MINOR QUARTZ-ACCESSORY RUTILE (PARTLY AFTER ILMENITE?) SCHIST

Sample consists of somewhat rounded to flattish chips of medium grained, buff- to pale greenish-grey coloured, schistose rock. The rock is weakly magnetic, shows no reaction to cold dilute HCl (except in veins where powdered), and no stain for K-feldspar in the etched offcut).

Modal mineralogy in polished thin section is approximately:

Chlorite (largely after relict biotite?)	45%
Carbonate (dolomite/ankerite?)	25%
Muscovite	20%
Quartz	7%
Rutile (partly sagenitic, in chlorite)	2-3%
Limonite	<1%

Relatively few of the chips in this sample survived the section preparation process; however, most are composed of what appear to be relatively coarse euhedral blastic biotite largely retrograded to chlorite and muscovite, with variable carbonate, accessory quartz, abundant sagenitic rutile or scattered coarser-grained pseudomorphs of tabular ilmenite, and partly stained by limonite (mainly in Fe-carbonate).

Relict blastic biotite (?) crystals have euhedral to somewhat corroded-looking outlines (with ragged terminations) up to 2.5 mm in diameter. They have pale brownish-green colour where chloritized and less coloured where replaced by muscovite, although the two form sub/euhedral flakes up to about 1.5 mm in diameter that are generally so intimately interleaved as to make distinction difficult. Distinct but weak pleochroism and length-slow, weak anomalous blue birefringence in the chlorite suggests a somewhat ferriferous composition (F:M around 0.5-0.6?). Carbonate occurs as ragged, irregular aggregates grading to blastic subhedra up to 1 mm in size composed of granular sub/euhedral crystals mostly < 0.15 mm in diameter that vary from pale to dark brown (weakly to strongly limonite stained; could be dolomite/ankerite?). Quartz occurs as scattered aggregates to 0.5 mm of subhedra mostly <0.2 mm in size, mostly with only minor undulose extinction indicative of minor strain. Rutile occurs as minute extremely slender needles mostly <1-2 by up to 100 microns in size with random orientations contained in the relict biotite sites, or as aggregates of euhedra mostly <20 microns that appear to pseudomorph former tabular ilmenite crystals up to 0.2 mm long. Sulfides are absent, so most of the minor limonite present appears to be derived by the oxidation of iron in the Fe carbonate.

In summary, this appears to represent relatively coarse, blastic biotite (retrograded to chlorite-muscovite)-carbonate-minor quartz-accessory rutile (partly after former ilmenite?) schist. Carbonate is mostly Fe-bearing dolomite (ankerite?) and chlorite is slightly ferriferous.

## GNP 02: FOLIATED/CRENULATED, QUARTZ-MUSCOVITE-CARBONATE-CHLORITE-ACCESSORY PYRITE-RUTILE-LIMONITE SCHIST

No sample material remains, but offcut shows flat tabular chips of pale grey, fine-grained, schistose rock up to at least 2.5 cm in diameter. The rock is not magnetic, shows minor reaction to cold dilute HCl (especially where powdered), and no stain for K-feldspar in the etched offcut. Modal mineralogy in polished thin section is approximately:

Quartz	40%
Muscovite	30%
Carbonate	20%
Chlorite (magnesian?)	8-10%
Pyrite	<1%
Rutile	<1%
Limonite	<1%

Most of the chips in this sample consist of extremely well foliated, crenulated (locally kink banded) layers of muscovite alternating with layers of granular quartz or quartz-carbonate-minor muscovite-chlorite-trace sulfides-rutile. Some of the carbonate, especially along layer-parallel zones or veinlets, is strongly limonite-stained.

Quartz forms somewhat ragged to irregular, an- to subhedral crystals mostly <0.2 mm in diameter that lack significant flattening/elongation even in these well-foliated rocks. Minor strain is indicated by weak undulose extinction and only rare sub-grain development or suturing of grain boundaries.

Muscovite forms mainly euhedral to subhedral, commonly wavy, bent flakes <0.5 mm in diameter but commonly optically semi-continuous for up to several mm in the muscovite-rich layers that are up to 2 mm thick. Crenulation and kink banding are on a scale of about 0.5 to 1.0 mm. Commonly the mica is interleaved with, or included within, chlorite forming mainly euhedral flakes up to about 0.2 mm in diameter with optical properties (very pale green colour, no pleochroism, greenish anomalous length-fast birefringence) suggestive of a slightly magnesian composition (F:M possibly around 0.4?).

Carbonate occurs intergrown with quartz or in lensey layers/segregations up to 1.5 mm thick, composed of interlocking subhedral crystals mostly <1 mm long (length:width up to 3:1, generally elongated/flattened sub-parallel to foliation). Most of this carbonate is relatively clear and likely represents calcite and dolomite (?), but in places (especially around the margins of the masses or where carbonate is present along narrow layer/foliation parallel zones or veinlets <0.2 mm thick composed of interlocking sub/anhedra <50 microns in diameter) it is strongly limonite-stained (could be ankerite?).

Minute rutile crystals, mostly euhedral or acicular prisms <20 but locally up to 50 microns long, are scattered in the phyllosilicates (chlorite and muscovite), commonly aligned with the foliation.

Relatively rare pyrite, forming sub/euhedral crystals up to 0.2 mm long, is commonly entirely enclosed within carbonate, and partly altered to limonite around rims, and along microfractures that are parallel to foliation. In places, transported limonite stains spread out from the pyrite crystals into adjacent carbonate.

In summary, this is strongly foliated/crenulated/kink banded quartz-muscovite-carbonate-chlorite-minor pyrite-rutile schist, locally stained by traces of limonite derived by oxidation of pyrite or Fe carbonate.

GNP 03: FOLIATED, LOCALLY CRENULATED QUARTZ-MUSCOVITE-CARBONATE-CHLORITE-ACCESSORY PYRRHOTITE-RUTILE SCHIST (TRACE LIMONITE)

No hand specimen material remains, but offcut shows flat chips up to 2.5 cm in diameter of pale grey, fine-grained, strongly foliated schist. The rock is locally weakly magnetic, shows local vigorous reaction to cold dilute HCl or slow reaction until powdered, and no stain for K-feldspar in the etched offcut. Modal mineralogy in polished thin section is approximately:

Quartz	40%
Muscovite	30%
Carbonate (calcite, dolomite?)	20%
Chlorite	8-10%
Pyrrhotite	1%
Rutile	<1%
Limonite (mainly after sulfides)	<1%

Most chips in this sample consist of interlaminated foliae of quartz-rich or mica-rich rock, commonly <0.2 mm thick but locally reaching 1mm, and alternating with layers rich in carbonate and quartz, or less commonly chlorite and muscovite. Much of the chlorite is so intimately interleaved with muscovite that it is difficult to distinguish.

Quartz forms somewhat ragged to irregular, sub- to anhedral crystals mostly <0.2 mm in diameter that lack significant flattening/elongation even in such well-foliated rocks (length:width ratios rarely over 1.5:1). Minor strain is indicated by weak undulose extinction and only rare sub-grain development or suturing of grain boundaries. Locally, lenses of quartz up to 2 mm long, aligned with the foliation, are composed of more coarsely crystalline (0.75 mm), more strongly strained and granulated (recrystallized) quartz.

Muscovite forms mainly euhedral to subhedral flakes <0.25 mm in diameter but commonly optically semi-continuous for up to several mm in the muscovite-rich layers that are up to at least 3 mm thick. Vague, weakly developed to locally well developed crenulation and kink banding are on a scale of 1-2 mm or 0.5-1 mm respectively. Commonly (except in the thick muscovite-rich layers) the mica is interleaved with, or included within, chlorite forming mainly euhedral flakes up to about 0.25 mm in diameter with optical properties (almost colourless to very pale green colour, no pleochroism, near-zero to weakly greenish anomalous length-fast birefringence) suggestive of a slightly magnesian composition (F:M possibly around 0.4-0.5?).

Carbonate occurs intergrown with quartz or in lensey layers/segregations up to at least 3 mm thick, composed of interlocking subhedral crystals mostly <1 mm long (length:width up to 4:1, generally elongated/flattened sub-parallel to foliation, and locally intergrown with euhedral bladed quartz of similar elongation and orientation). Most of this carbonate is relatively clear and likely represents calcite and dolomite (?). Carbonate is also locally present along narrow layer/foliation parallel zones or perpendicular veinlets <0.5 mm thick composed of interlocking, bladed sub/euhedra <0.25 mm long).

Most sulfides are pyrrhotite, forming sub/euhedral crystals up to 0.5 mm in diameter but locally in vein-like aggregates up to several mm long, sub-parallel to foliation, where it is intergrown mostly with quartz, but locally also with chlorite or the carbonate, which may partly mantle it. In places the pyrrhotite occurs in thin irregular veinlets perpendicular to foliation, and in these it is partly oxidized to limonite around the margins and along fractures.

Minor rutile is common as minute acicular euhedra mostly <20 microns long, especially within the muscovite-rich layers; locally these rutile needles form aggregates to 50 microns.

In summary, this is well foliated, locally crenulated/kink banded, quartz-muscovite-carbonate-chlorite-accessory pyrrhotite-rutile schist, with minor oxidation of sulfides to limonite along fractures.

GNP 05: MODERATELY FOLIATED QUARTZ-MUSCOVITE-CHLORITE-CARBONATE-MINOR PYRITE (PART OXIDIZED TO LIMONITE)-GRAPHITE?-RUTILE-APATITE SCHIST

No hand specimen material remains, but offcut shows flat chips up to almost 3 cm in diameter of dark grey, fine-grained, strongly foliated schist. The rock is not magnetic, shows no reaction to cold dilute HCl even when powdered, and no stain for K-feldspar in the etched offcut. Modal mineralogy in polished thin section is approximately:

Quartz (locally secondary)	60%
Muscovite	25%
Chlorite (slightly magnesian?)	5%
Carbonate (mainly ankerite?)	5%
Pyrite	1-2%
Graphite (?)	1-2%
Limonite	1%
Rutile	<1%
Apatite	<<1%

This sample consists mainly of alternating, either quartz-rich (minor muscovite, chlorite, carbonate, apatite) or muscovite-rich (lesser quartz, minor chlorite, carbonate, rutile, possible graphite (?), local pyrite partly oxidized to limonite) rock. Quartz rich layers are lensey, locally forming coarser-grained segregations that resemble metamorphic “sweats”. Thinner, wispy, muscovite-rich foliae are less well-defined and are locally anastomose, oblique to layering/foliation, and contain minute opaques.

Quartz forms somewhat ragged, sub- to anhedral interlocking crystals in three size ranges: mostly <50 microns, that lack significant flattening/elongation even in such well-foliated rocks (length:width ratios mainly 1:1), mostly <0.2 mm long, with length:width ratios in the 2:1 to locally 3:1 range, and up to 0.35 mm, in the metamorphic sweats that form rounded lens-like aggregates to 1.5 mm long sub-parallel to foliation, associated with sulfides. Minor strain is indicated in all three types of quartz by weak undulose extinction and only rare sub-grain development or suturing of grain boundaries; inclusions are most abundant in the finest-grained type. Rare thin (<0.25 mm) irregular veinlets of recrystallized (secondary) quartz are perpendicular to foliation. Traces of apatite as stubby euhedral prisms <40 microns long are present in quartz-rich layers.

Muscovite forms mainly subhedral, somewhat ragged flakes <0.25 mm in diameter but locally optically semi-continuous for up to 1 mm. Locally (except in the more muscovite-rich foliae) the mica is intimately interleaved with chlorite forming mainly euhedral flakes mainly <0.15 mm in diameter with optical properties (almost colourless to very pale green colour, no pleochroism, near-zero to weakly greenish anomalous length-fast birefringence) suggestive of a slightly magnesian composition (F:M possibly around 0.4-0.5?).

Carbonate occurs as separate crystals or aggregates intergrown with quartz, or locally in lensey layers/segregations <0.5 mm thick, composed of interlocking subhedral crystals mostly <0.25 mm in size. Most of this carbonate is brownish and since it does not react to HCl in hand specimen, likely represents ankerite (?), especially where it is strongly limonite stained (or the latter may represent siderite?).

Most sulfide is pyrite, forming sub/euhedral crystals up to 2.5 mm in diameter but locally in vein-like aggregates up to 1 cm or so long, sub-parallel to foliation, where it is intergrown mostly with quartz, but locally also with muscovite. The pyrite also occurs in extremely thin (<0.1 mm thick) irregular veinlets parallel to foliation. In both of these it is partly oxidized to (pseudomorphed by) bright red-brown, likely goethitic, limonite around the margins and along fractures.

Minor rutile is common as minute acicular euhedra mostly <20 microns long, especially within the muscovite-rich layers; locally these rutile needles may be mixed with graphite (?) as minute flakes too small to identify, along wispy opaque foliae <20 microns thick.

In summary, this is moderately foliated, quartz-muscovite-chlorite-minor carbonate-accessory pyrite-rutile-graphite?-apatite schist, with minor oxidation of sulfides to limonite along fractures.

**GNP 06: STRONGLY FOLIATED/FOLDED QUARTZ-MUSCOVITE-CHLORITE-CARBONATE MINOR PYRITE/PYRRHOTITE-LIMONITE-GRAPHITE?-RUTILE SCHIST, LOCAL THIN CARBONATE-QUARTZ VEINLETS**

No hand specimen material remains, but offcut shows flat chips up to at least 3 cm in diameter of dark grey, fine-grained, strongly foliated schist. The rock is locally slightly magnetic, shows slow reaction to cold dilute HCl except when powdered, and no stain for K-feldspar in the etched offcut. Modal mineralogy in polished thin section is approximately:

Quartz	50%
Muscovite	25%
Chlorite (magnesian)	15%
Carbonate (dolomite, ankerite?)	7-8%
Pyrite, trace pyrrhotite	<1%
Limonite (after sulfides, carbonate)	<1%
Graphite (?)	<1%
Rutile	<1%

Most of the chips in this sample consist of strongly foliated, isoclinally folded or crumpled, quartz-mica (muscovite/chlorite)-carbonate schist with wispy foliae of opaque matter (local pyrite, pyrrhotite both partly oxidized to limonite, trace rutile, possible graphite too fine to identify).

Quartz forms somewhat ragged, sub- to anhedral interlocking crystals in two main size ranges: mostly <0.1 mm long, with significant flattening/elongation sub-parallel to folded foliation (length:width ratios mainly in the 2:1 to locally 3:1 range), and up to 0.35 mm, in the metamorphic schists that form rounded lens-like aggregates to 1.5 mm long sub-parallel to foliation, associated with sulfides. Minor strain is indicated in both types of quartz by weak undulose extinction and only rare sub-grain development or suturing of grain boundaries. Rare bladed euhedral quartz to 0.25 mm long occurs in ptgmatitically folded carbonate veins up to 0.3 mm thick.

Muscovite forms mainly subhedral, somewhat ragged flakes <0.15 mm in diameter but locally optically semi-continuous for up to 2 mm. Locally (except in the most muscovite-rich layers that are up to 0.5 mm thick) the mica is intimately interleaved with chlorite forming mainly euhedral flakes also mainly <0.15 mm in diameter with optical properties (almost colourless to very pale green colour, rare pleochroism, near-zero to weakly greenish anomalous length-fast birefringence) suggestive of a slightly magnesian composition (F:M possibly around 0.4?).

Carbonate occurs as separate ragged subhedral crystals <0.1 mm in size or slightly larger aggregates mainly intergrown with quartz, or locally in lensey layers/segregations <0.5 mm thick, composed of interlocking subhedral crystals mostly <0.3 mm in size. Most of this carbonate is brownish and since it does not react to HCl in hand specimen, likely represents ankerite (?), especially where it is strongly limonite stained (or the latter may represent siderite?), but in some of the segregations and local cross-cutting/ptgmatitically folded veinlets it is relatively clear, and could be calcite or dolomite (?).

Pyrite forms scattered small cubic crystals mostly <0.25 mm in diameter, commonly encased in or at least closely associated with limonite-stained (ankeritic?) carbonate. Rare pyrrhotite forms local subhedra <0.1 mm in diameter, also partly enclosed by limonite-stained carbonate (some of this limonite comes from oxidation of adjacent pyrrhotite). Rutile occurs as minute stubby prismatic euhedra mostly <20 microns long, generally associated with or included within limonite-stained (ankeritic) carbonate. There may be minor graphite or sub-graphitic carbon present in the thin (<0.1 mm thick) opaque foliae that are mainly concentrated in and along wispy muscovite-rich layers.

In summary, this is well-foliated, commonly isoclinally or ptgmatitically folded, quartz-muscovite-chlorite-minor Fe carbonate-accessory pyrite  $\pm$  pyrrhotite (partly oxidized to limonite)-rutile-possible graphite schist, cut by layer-parallel to locally perpendicular carbonate-quartz veins.

**GNP 07: FINE-GRAINED, STRONGLY FOLIATED, LOCALLY CRENULATED MUSCOVITE-MINOR CHLORITE SCHIST WITH CARBONATE AS PORPHYROBLASTS, LENSES, AND VEINLETS; ACCESSORY QUARTZ?-RUTILE-TOURMALINE-PYRITE/LIMONITE**

Sample consists of flat, somewhat curved chips <4 cm in diameter of fine-grained, dark greenish grey, well foliated, crenulated schist. The rock is not magnetic, shows local minor reaction to cold dilute HCl only where powdered, and no stain for K-feldspar in the etched offcut. Modal mineralogy in polished thin section is approximately:

Muscovite	75%
Chlorite (slightly magnesian)	15%
Carbonate (dolomite, ankerite?)	7-8%
Quartz (?)	1-2%?
Rutile	<1%
Tourmaline (intermediate dravite-schorl?)	<1%
Pyrite (mainly pseudomorphed by limonite)	<1%

Apart from local coarser-grained, foliation-parallel veins of carbonate, or local coarser layers of muscovite, this sample is very fine-grained, apparently composed mainly of muscovite (sericite), chlorite, possibly very little quartz, accessory rutile and tourmaline. Although chlorite is really only identifiable in the coarser layers (with rutile, and tourmaline) it is assumed to exist in the very fine-grained rock in similar proportions. Scattered small euhedral porphyroblasts of Fe-carbonate (?) are locally present. Traces of pyrite (subhedra to 0.1 mm) are mainly pseudomorphed by limonite.

Muscovite/sericite, forming the bulk of the sample, occurs as completely aligned, parallel, mainly euhedral flakes <50 microns in diameter in most of the layers, or up to 0.1 mm in the coarser layers. Slight crenulation is evident, with the development of mostly weak (but locally very strong) kink banding up to 1 mm thick. In the fine-grained layers, darker colour of the section when foliation is parallel to the lower polar suggests significant chlorite is probably present although it is not distinguishable optically even at highest magnification (500x). Similarly, there is probably microcrystalline quartz present although not resolvable optically; XRD analysis would be required to confirm these assumptions. In places, fine-grained carbonate (partly limonite stained, especially around the margins, suggesting dolomite surrounded by ankerite?) occurs as aggregates with irregular outlines up to 2 mm long composed of mainly fibrous, laminated crystals <40 microns long, oriented sub-parallel to foliation. The scattered relict Fe carbonate (?) porphyroblasts have mainly euhedral outlines up to 0.25 mm in diameter, but in some cases are so altered to limonite (particularly at margins, suggesting ankerite or siderite composition?) that the identification is locally tentative. Minute rutile crystals are rarely over 20 microns long, oriented sub-parallel to foliation.

In the coarser layers, chlorite forms mainly euhedral flakes up to 0.1 mm in diameter, with optical properties (pale green pleochroism, weak anomalous green, length-fast birefringence) typical of weakly magnesian composition (F:M around 0.4?). Tourmaline forms euhedral prisms up to 0.2 mm long, with greenish-brown pleochroism suggestive of intermediate dravite-schorl composition (F:M possibly around 0.6-0.7?). Rutile occurs as stubby pale brown euhedra mostly <30 microns long, locally in aggregates to 50 microns.

In the layer/foliation parallel carbonate veinlets and patches, which are up to 1.5 mm thick, crystals are mainly euhedral to subhedral and up to 1 mm in diameter; they are mainly clear and likely represent dolomite.

In summary, this is very fine-grained, strongly foliated/locally crenulated/kink banded, almost pure muscovite (minor chlorite, carbonate, possible accessory quartz?-rutile, local tourmaline, trace oxidized pyrite) schist with carbonate present as porphyroblasts, veinlets and layers.

GNP 09: FOLIATED QUARTZ-MUSCOVITE-CARBONATE-CHLORITE-MINOR FELDSPAR-PYRRHOTITE-RUTILE SCHIST; LENSY PYRRHOTITE-QUARTZ-CHLORITE-CARBONATE

Sample consists of flat, somewhat curved chips <3 cm in diameter of fine-grained, dark greenish grey, well foliated, weakly crenulated schist. The rock is distinctly magnetic, shows local reaction to cold dilute HCl only where powdered, and trace stain for K-feldspar in the etched offcut. Modal mineralogy in polished thin section is approximately:

Quartz	35%
Muscovite, minor sericite (after feldspar)	25%
Carbonate (mainly dolomite?)	20%
Chlorite (magnesian)	10%
Plagioclase (albite?)	5%
Pyrrhotite, trace chalcopyrite, limonite	3%
K-feldspar	1%
Rutile, trace sphene	<1%

This is a fairly typical quartz-muscovite-carbonate-minor chlorite-feldspar, accessory pyrrhotite, rutile schist, roughly segregated into generally coarser-grained, locally lens like quartz-carbonate (local pyrrhotite) layers and thinner, strongly foliated, muscovite-chlorite-rutile rich layers.

Quartz occurs mainly as tightly interlocking, subhedral crystals <0.25 mm in maximum dimension, with length:width ratios up to 2:1 and general elongation/flattening sub-parallel to foliation, but only minor undulose extinction. In coarse-grained, quartz-rich segregations, quartz forms ragged subhedra up to bladed subhedra to 1.2 mm long, oblique to foliation, also with relatively weak undulose extinction, sub-grain development, rare suturing of grain boundaries; some carbonate also occurs in these lensy aggregates. Locally, minor feldspar is present as subhedra <0.1mm in size, distinguishable only where twinning is present in plagioclase (extinction on 010 up to 16 degrees and relief negative compared to quartz suggests an albitic composition), or where it is slightly sericitized. Minor Kspar is also indicated by stain in etched offcut, but is difficult to identify with certainty in thin section since the plagioclase is commonly untwinned and also has negative relief compared to quartz.

Muscovite forms mainly sub- to euhedral flakes up to 0.15 mm in diameter (but locally optically continuous for up to several mm where closely aligned). In places the muscovite-rich foliae, which are up to 1.5 mm thick, are strongly crenulated or severely kink-banded, with the development of a new cleavage slightly oblique to foliation. In some layers, chlorite is definitely identifiable, intimately intermixed with the muscovite, forming sub/euhedral flakes up to 0.15 mm in size with optical properties (pale green pleochroism, anomalous green, length-fast birefringence) typical of weakly magnesian composition (F:M around 0.4). Accessory rutile (and possible sphene?) are typically present as minute, mostly <15 micron long, sub/euhedra in the micaceous layers.

Carbonate is widespread, mainly as small (<0.15 mm) subhedra that like quartz show slight elongation/flattening in the plane of foliation (length:width ratios up to about 2:1). Most of this is likely dolomite since it is clear in thin section, and reacts only when scratched in hand specimen. Carbonate-rich segregations or lensy layers up to 1 mm thick are composed of interlocking subhedra mostly <1 mm long (likely mostly dolomite, elongated in plane of foliation).

Pyrrhotite occurs in relatively coarse-grained, lensy aggregates up to 6 mm long composed of interlocking subhedra mostly <0.5 mm. In general, the pyrrhotite is in contact only with coarse quartz (to 0.25 mm), muscovite (to 0.5 mm), and chlorite (also magnesian, porphyroblastic subhedra up to 1 mm long), or rarely carbonate (dolomite subhedra to 0.2 mm). Only minor oxidation is present, with traces of limonite along microfractures in the pyrrhotite. Traces of chalcopyrite also occur separately as subhedra <0.1 mm in size, locally in contact with carbonate and muscovite.

In summary, this is well foliated quartz-muscovite-carbonate-chlorite-minor plagioclase-Kspar-accessory pyrrhotite (trace chalcopyrite)-rutile schist; sulfides are mainly confined to lensy quartz-chlorite-minor carbonate segregations, and are slightly oxidized to limonite along fractures.

# GNP 11: FOLIATED QUARTZ-MUSCOVITE-CARBONATE-CHLORITE-PYRRHOTITE-RUTILE SCHIST WITH LENSES/VEINS OF PYRRHOTITE-QUARTZ-CARBONATE

Sample consists of flat, somewhat curved chips <2.5 cm in diameter of fine-grained, dark grey, well foliated, weakly crenulated schist with local segregations of carbonate. The rock is weakly magnetic, shows local reaction to cold dilute HCl mainly where powdered, and no stain for K-feldspar in the etched offcut. Modal mineralogy in polished thin section is approximately:

Quartz	40%
Muscovite	25%
Carbonate (dolomite, ankerite?)	25%
Chlorite (slightly magnesian?)	7-8%
Pyrrhotite, trace pyrite/arsenopyrite?, limonite	1-2%
Rutile	<1%
Graphite (?)	<1%

Most of the chips in this sample consist of strongly foliated, or locally strongly crenulated, quartz-muscovite-carbonate-chlorite (accessory pyrrhotite, rutile, possible graphite?) schist, locally with lensey or irregular segregations of quartz or carbonate, although most carbonate is intergrown with quartz in quartz-rich layers, and most sulfide occurs in foliation-parallel or oblique layers or lenses of quartz-carbonate.

Quartz mostly occurs as sub- to anhedral crystals <0.1 mm in size, generally lacking any strong elongation or preferred orientation, although rarely bladed crystals up to 0.25 mm long (length:width up to 3:1) are oriented parallel to kink banded muscovite flakes, or small lensey segregations up to 1 mm long composed of interlocking subhedra to 0.5 mm in length, also with length:width ratios in the 2:1 or 3:1 range, are also sub-parallel to kink bands.

Muscovite forms mainly sub- to euhedral, strongly aligned flakes <0.2 mm in diameter but locally semi-continuous optically over areas up to 1.5 mm thick by several mm long where layers are almost massive muscovite. Faint crenulation and kink banding are evident in these, but are not as strongly developed as in alternating, quartz-carbonate rich and muscovite-rich rock where a crenulation cleavage perpendicular to foliation is strongly developed. In places, especially where the mica is somewhat coarser grained, or is intergrown with quartz and/or carbonate, chlorite is recognizable as sub/euhedral flakes to 0.15 mm with optical properties (very weak green pleochroism, weakly anomalous green, length-fast birefringence) typical of weakly magnesian composition (F:M around 0.4-0.5?).

Carbonate, likely mostly dolomite as relatively clear or pale brownish, irregular subhedral crystals mostly <0.75 microns in size, is intergrown around the margins with darker brown, generally limonite-stained ragged crystals <20 microns in size that could be ankerite (?).

Pyrrhotite occurs as sub/euhedral crystals mostly <0.25 mm in size, rarely containing traces of euhedral pyrite/arsenopyrite (?) <5 microns in size. The pyrrhotite shows traces of oxidation to limonite along microfractures or rims, mostly <3 microns thick. Pyrrhotite occurs partly in fine-grained disseminations (where it is commonly partly encased by carbonate) or locally in veinlets of carbonate up to 0.3 mm thick, oblique to foliation, where it may also be enclosed in carbonate.

Rutile is concentrated in micaceous layers as either minute acicular euhedra mostly <15 microns long, or rare stubby euhedra up to 40 microns in diameter. In some of these layers, minute (<5 micron) graphite (?) may accompany the rutile, but it is difficult to be sure.

In summary, this is strongly foliated, locally crenulated/kink banded/cleaved quartz-muscovite-carbonate-chlorite (accessory pyrrhotite-rutile-possible graphite?) schist, with pyrrhotite mostly confined to layer-parallel/oblique lenses/veinlets, where it is partly encased in carbonate.



## VNP 02: STRONGLY MINERALIZED QUARTZ-PYRITE-MINOR MUSCOVITE-SPHALERITE-GALENA-TRACE FE CARBONATE-RUTILE ROCK

Sample consists of angular, fine-grained, dark/light grey, sulfide-rich rock chips mostly <1 cm (but up to 3 cm) in diameter. The rock is not magnetic, shows no reaction to cold dilute HCl, and no stain for K-feldspar in the etched offcut. Narrow veins are locally present cutting the weak foliation in some chips. Modal mineralogy in polished thin section is approximately:

Quartz (partly/largely secondary)	60%
Pyrite	25%
Muscovite	10%
Sphalerite	2-3%
Galena	1%
Fe-carbonate (ankerite/siderite?)	1%
Rutile, graphite?	<1%
Chalcopyrite (?), in sphalerite only	trace

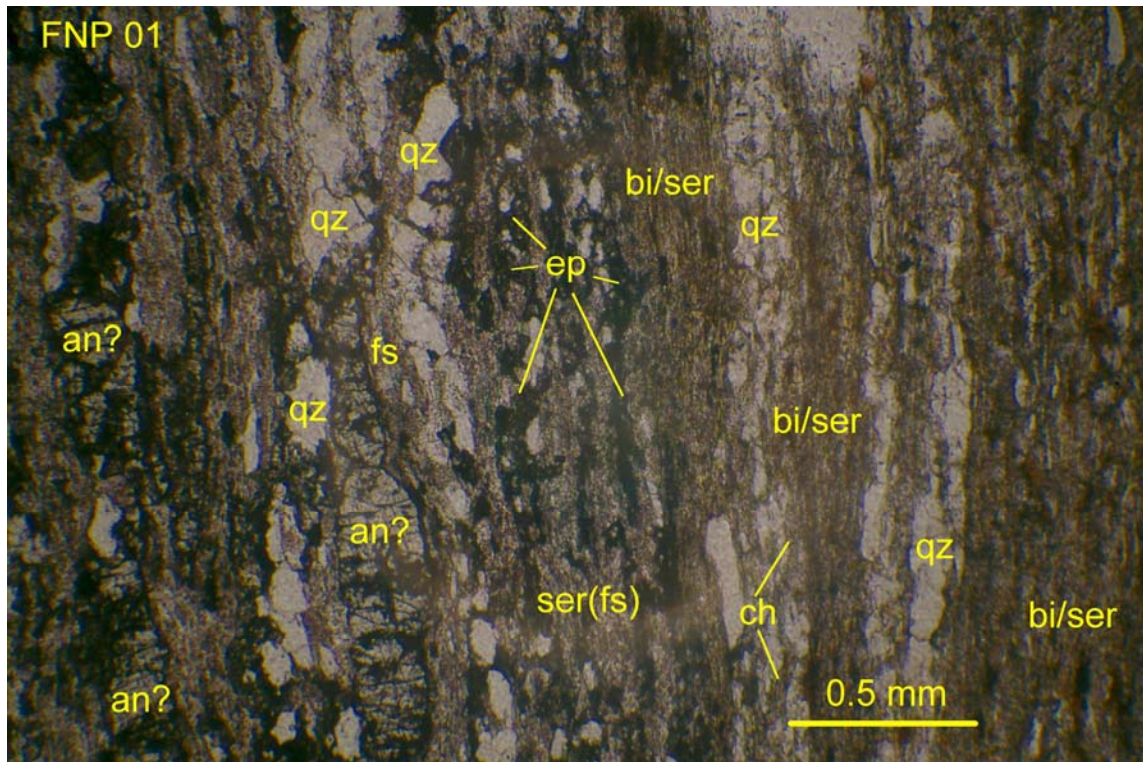
Most of the chips in this sample consist mainly of quartz (largely secondary?) and sulfides (mainly pyrite; minor sphalerite, galena), with only modest amounts of muscovite, and traces of Fe carbonate and rutile.

In most of the chips (that are sulfide-rich), quartz occurs as ragged, irregular sub/anhedra up to about 0.75 mm in diameter, with strong indications of strain (strong undulose extinction, sub-grain development, local suturing of grain boundaries, plus local development of planar features or sheeted networks of healed microfractures). Local veins up to 0.5 mm thick composed of similar textured quartz contain pyrite. In a few chips, which are sulfide-poor, the quartz is finer-grained and sucrosic, forming interlocking subhedra mostly <0.15 mm in maximum dimension, with distinct but not pronounced flattening/elongation defining a weak foliation (length:width ratios up to about 2:1).

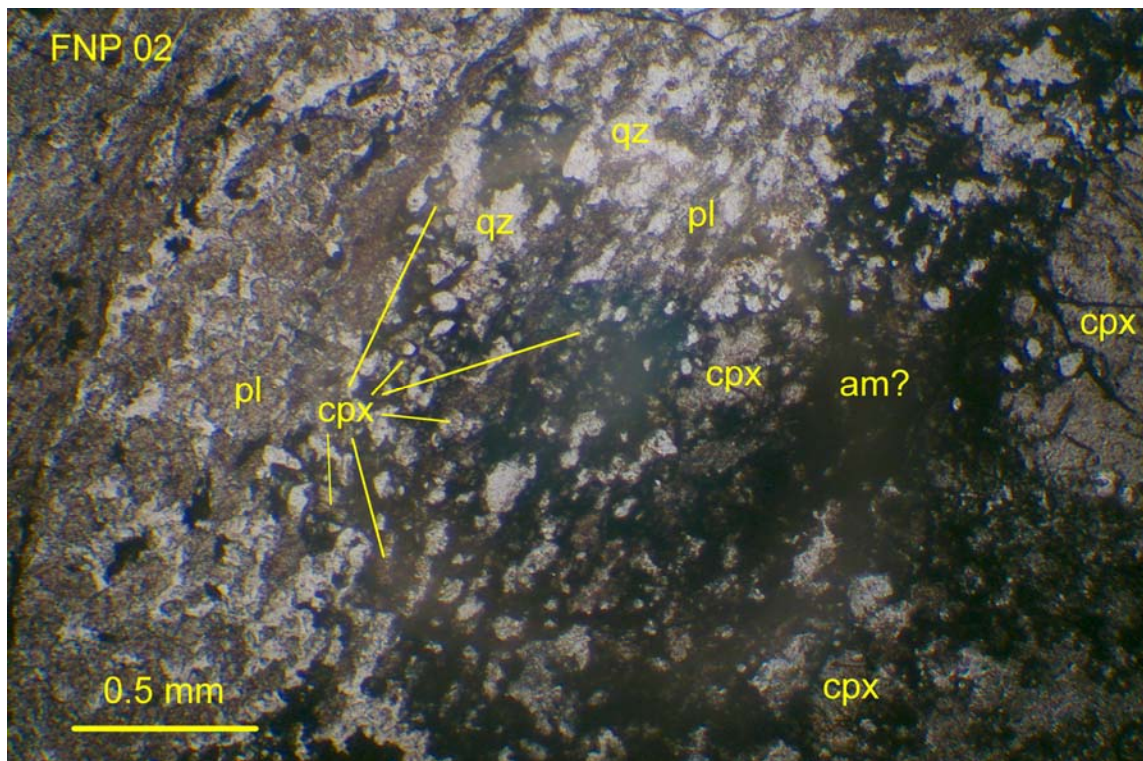
In the former (sulfide-rich) chips, pyrite is abundant as interlocking, locally somewhat skeletal, euhedral crystals up to about 0.5 mm in diameter, typically interstitial to quartz and intergrown with the sphalerite and galena, which occur peripheral to pyrite and also interstitial to quartz. Sphalerite, which has strong red-brown colour, and so is likely moderately Fe-rich, forms mainly sub/euhedral crystals up to about 0.25 mm in diameter, but aggregates to 0.5 mm. Galena forms subhedra up to about 0.15 mm. Both sphalerite and galena occur as smaller inclusions within the pyrite. Chalcopyrite appears to be restricted to minute (<5 micron) inclusions in sphalerite. Galena also occurs as <50 micron sized inclusions within sphalerite.

In the latter type of chip (fine-grained, foliated) the foliation is also marked by aligned flakes of muscovite, mostly sub/euhedral and up to 0.15 mm in diameter, interstitial to the quartz. There is locally minor carbonate associated with this mica, forming small (<0.1 mm thick) lensey aggregates of ragged subhedra <35 microns in size that are generally strongly limonite-stained, suggestive of Fe-rich composition (ankerite or siderite?). Also, sub-parallel to the foliation, wispy concentrations of minute opaques (mostly <5 microns in size) could be rutile and/or graphite (?) but are mostly too small to resolve (some do appear to be rutile). Pyrite disseminated in this type of chip forms euhedral crystals mostly <40 microns in diameter. Very little of the pyrite is actually in contact with the (relatively uncommon) Fe carbonate crystals.

In summary, this sample appears to represent strongly mineralized rock, composed mainly of secondary quartz with abundant pyrite, minor muscovite, sphalerite and galena, and traces of rutile and possible graphite (?) although it is difficult to confirm the latter.

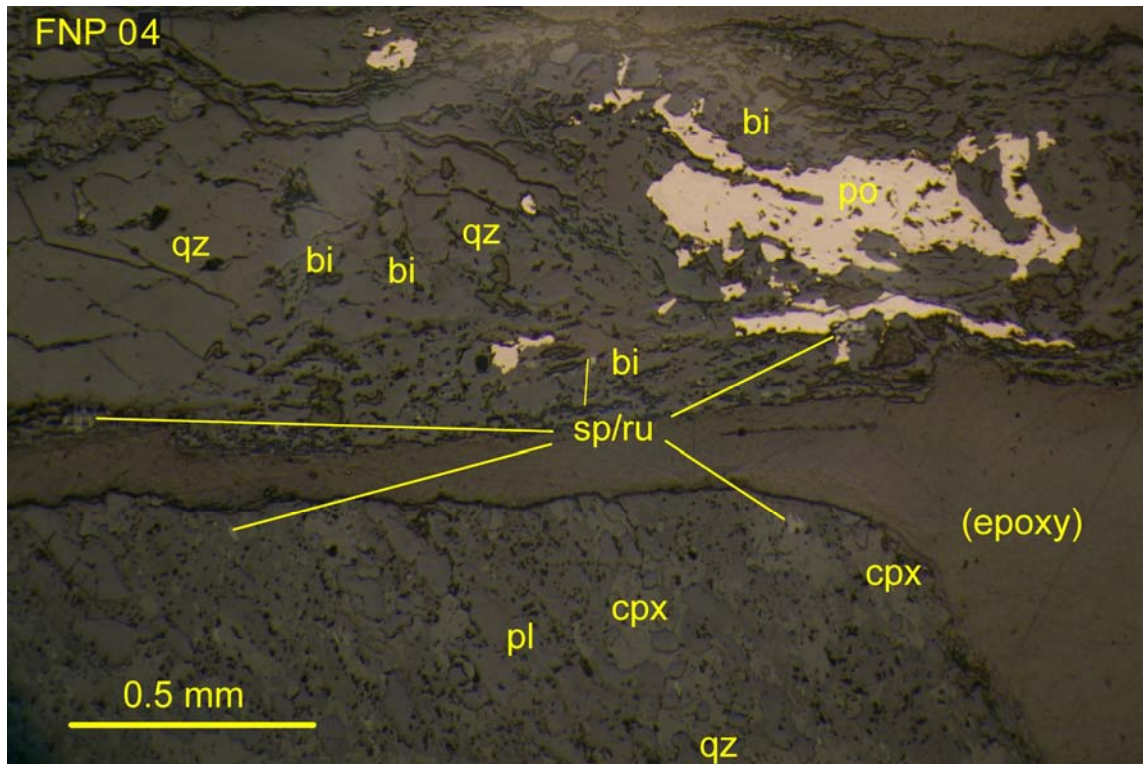


FNP 01: Well foliated schist composed of alternating ribbons of quartz (qz), biotite and sericite (bi, ser) partly altered to chlorite (ch), lesser feldspar (fs; plagioclase or Kspar, partly altered to sericite), minor epidote (ep) or amphibole, and local elongated euhedra of possible andalusite? (an?). Transmitted plane light, field of view 3.0 mm wide.

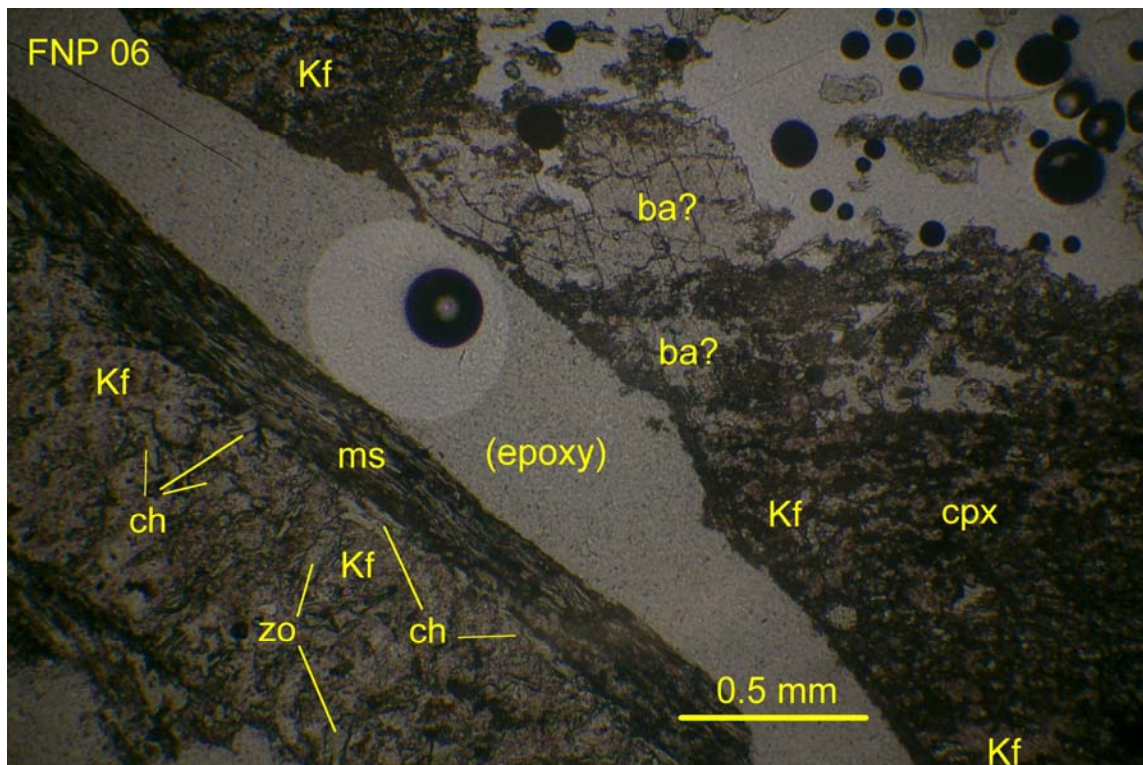


FNP 02: Gneiss or schist composed of mafic layers (clinopyroxene, cpx, partly altered to dark fibrous secondary amphibole, am?) and felsic layers (quartz, qz, and plagioclase, pl, clouded by incipient sericite alteration). Transmitted plane light, field of view 3.0 mm wide.



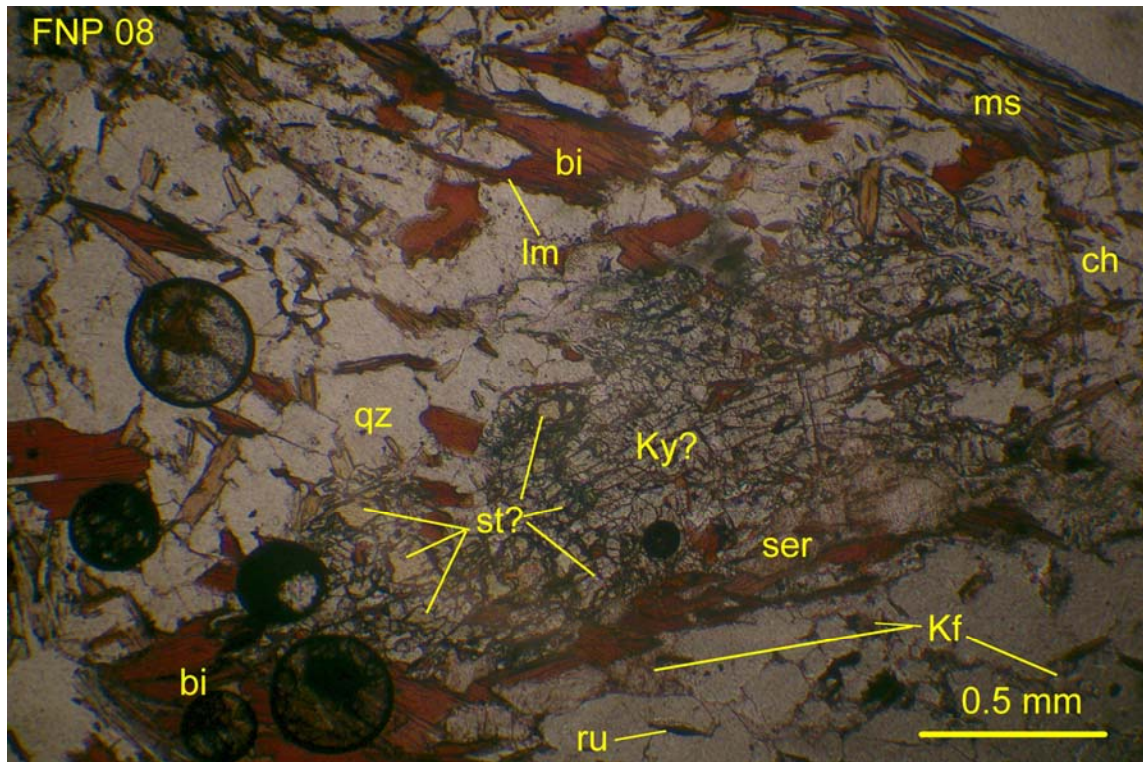


FNP 04: Two main rock types: foliated clinopyroxene (cpx)-plagioclase (pl)-quartz (qz) schist and quartz-biotite (bi) schist, the latter with accessory pyrrhotite (po) and sphene/rutile (sp). Reflected light, uncrossed polars, field of view 2.25 mm wide.

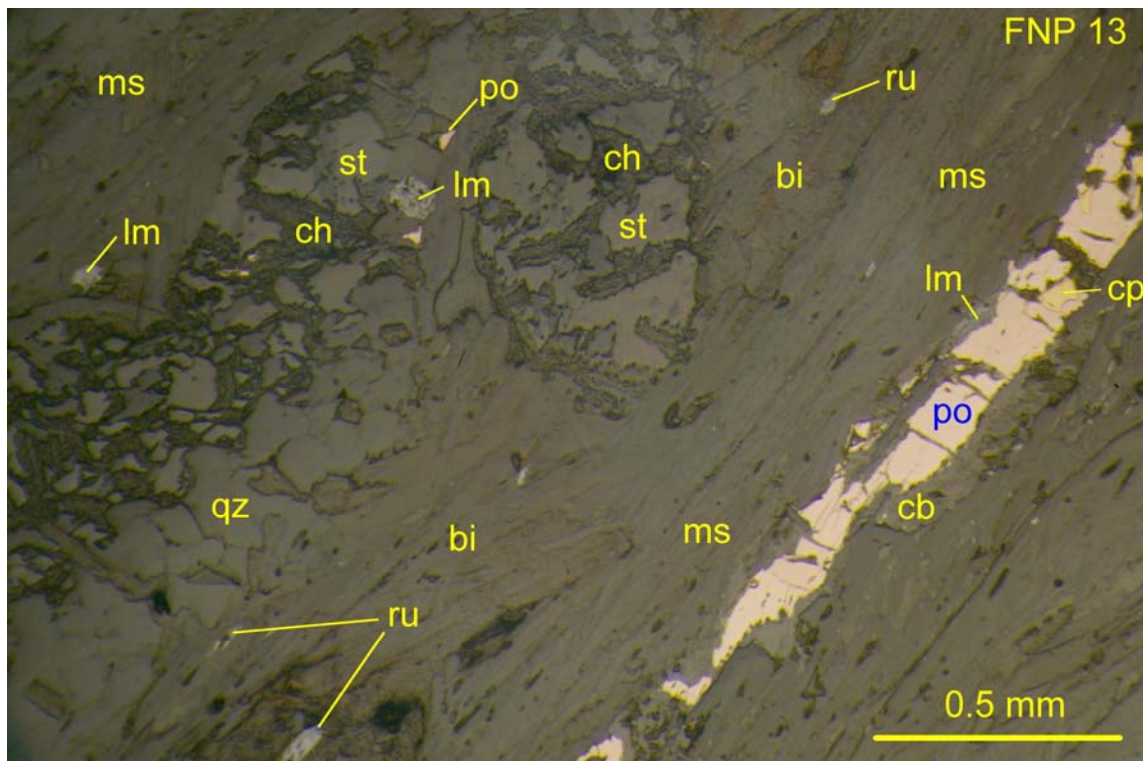


FNP 06: Chips composed of either Kspar (Kf)-clinopyroxene (cpx) with coarse barite? (ba?) that is partly plucked out, or fine-grained Kspar, chlorite (ch) and zoisite (zo) all after pyroxene (?), with layers of muscovite (ms). Note blastic growth of barite (?) over layers of pyroxene. Transmitted plane light, field of view 3.0 mm wide.



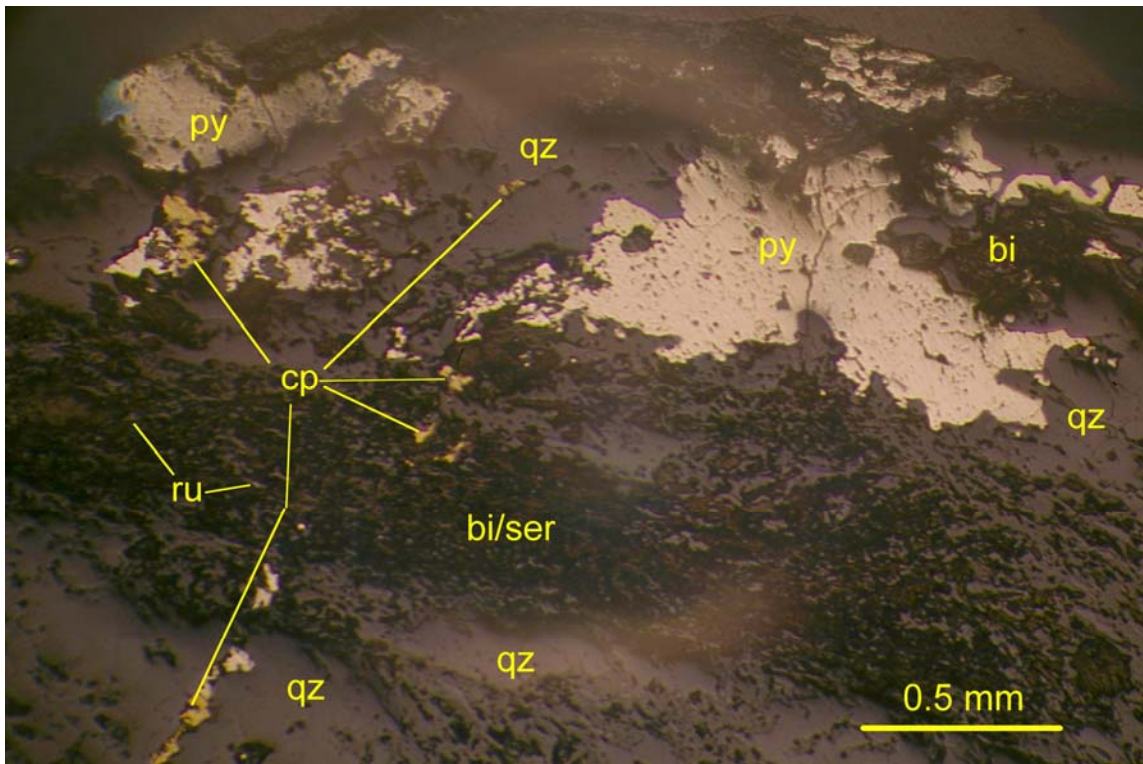


FNP 08: Porphyroblastic kyanite? (ky?) with poikilitic inclusions of pale yellow staurolite (st?), partly retrograded at one end to chlorite (ch) and sericite (ser), surrounded by quartz (qz) segregation in foliated muscovite (ms)-biotite (bi) schist locally containing needles of rutile (ru) or stained by limonite (lm). Transmitted plane light, field of view 3.0 mm wide.

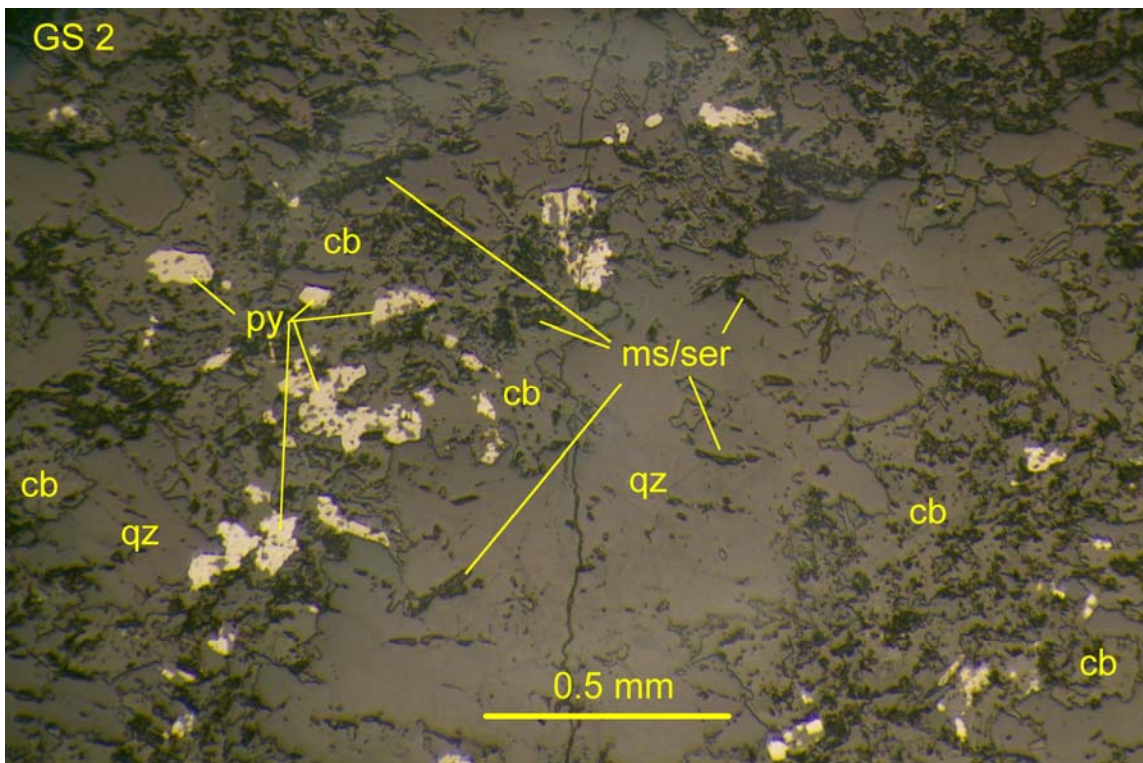


FNP 13: Porphyroblasts of staurolite (st) partly retrograded to chlorite (ch), in foliated matrix of muscovite (ms)-quartz (qz)-biotite (bi)  $\pm$  rutile/sphene (ru), with lensey layers of pyrrhotite (po)-minor chalcopyrite (cp) partly oxidized at margins (or replaced) by limonite (lm) and coated by Fe-carbonate? (cb?). Reflected light, uncrossed, 2.25 mm wide.



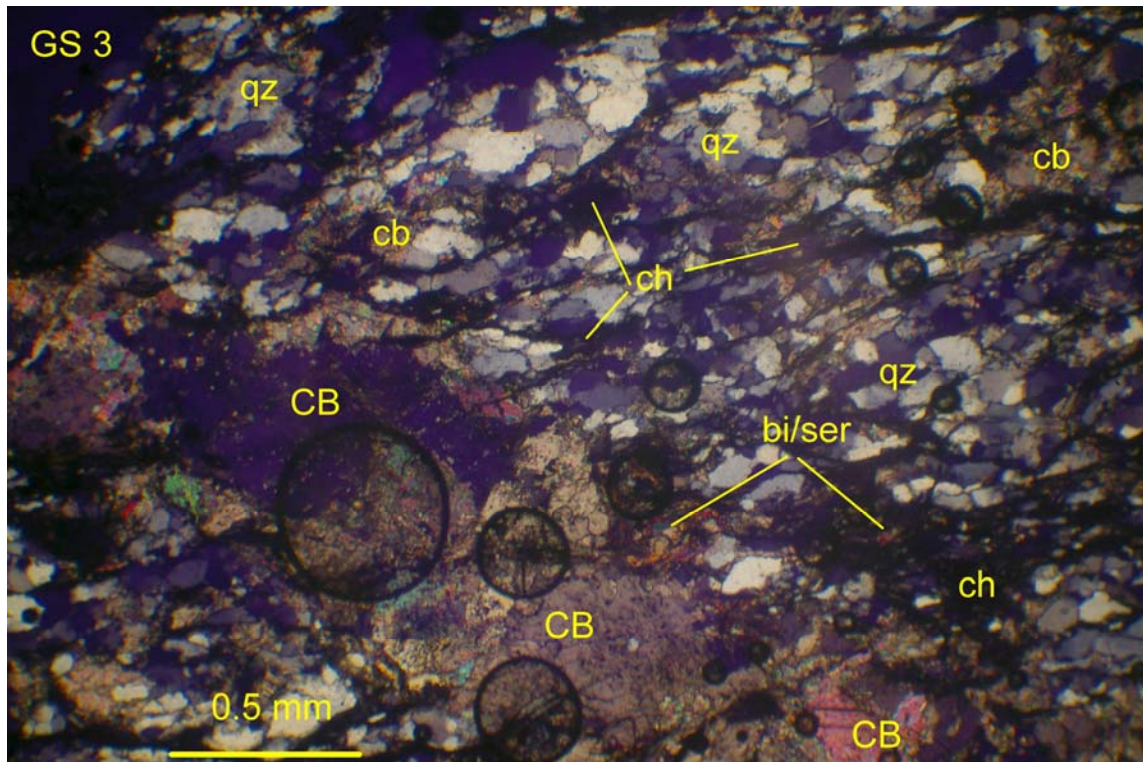


FNP 14: Sulfides, mostly pyrite (py) but likely after former pyrrhotite, as coarse irregular subhedra intergrown with quartz (qz) and biotite (bi), adjacent to foliated layer of biotite-muscovite/sericite (bi/ser), cut by narrow veinlet of pyrite (after marcasite?)-minor chalcopyrite (cp). Reflected light, uncrossed polars, field of view 2.75 mm wide.

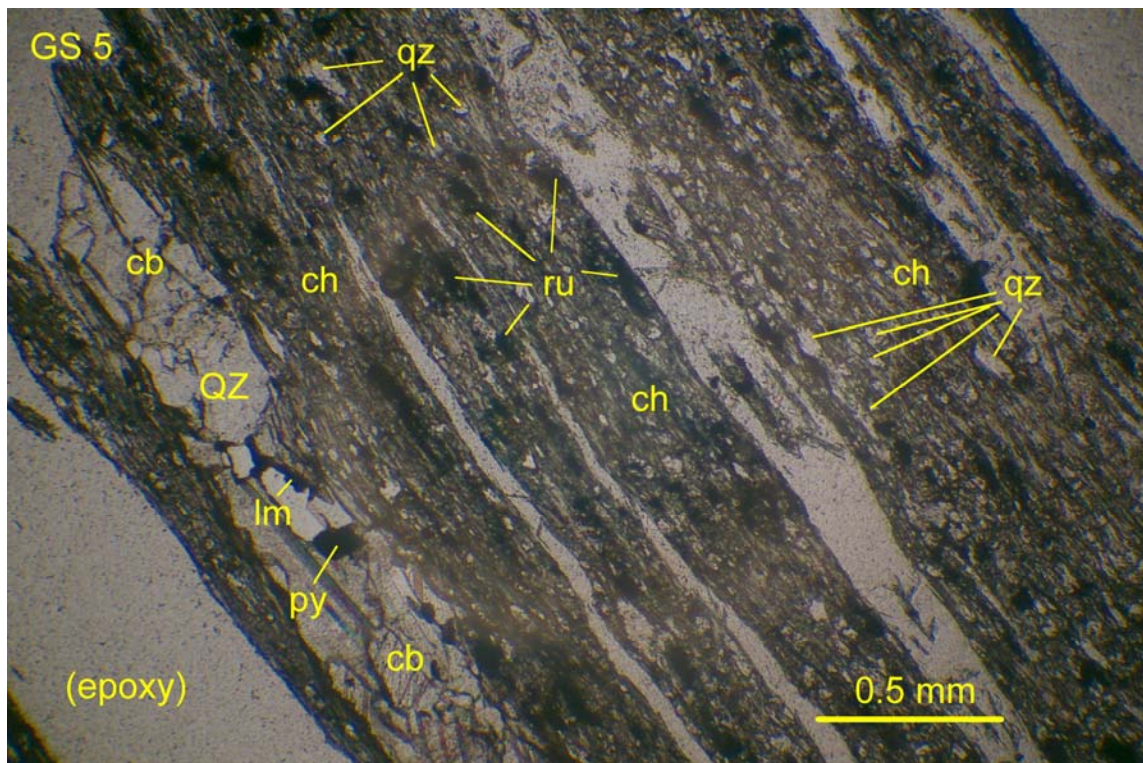


GS 2: Weakly layered rock composed of quartz (qz) rich segregations and intervening carbonate (cb)-minor muscovite rich foliae, the latter locally containing sulfides (pyrite, py) contained within or enclosed by carbonate. Reflected light, uncrossed polars, field of view 2.25 mm wide.



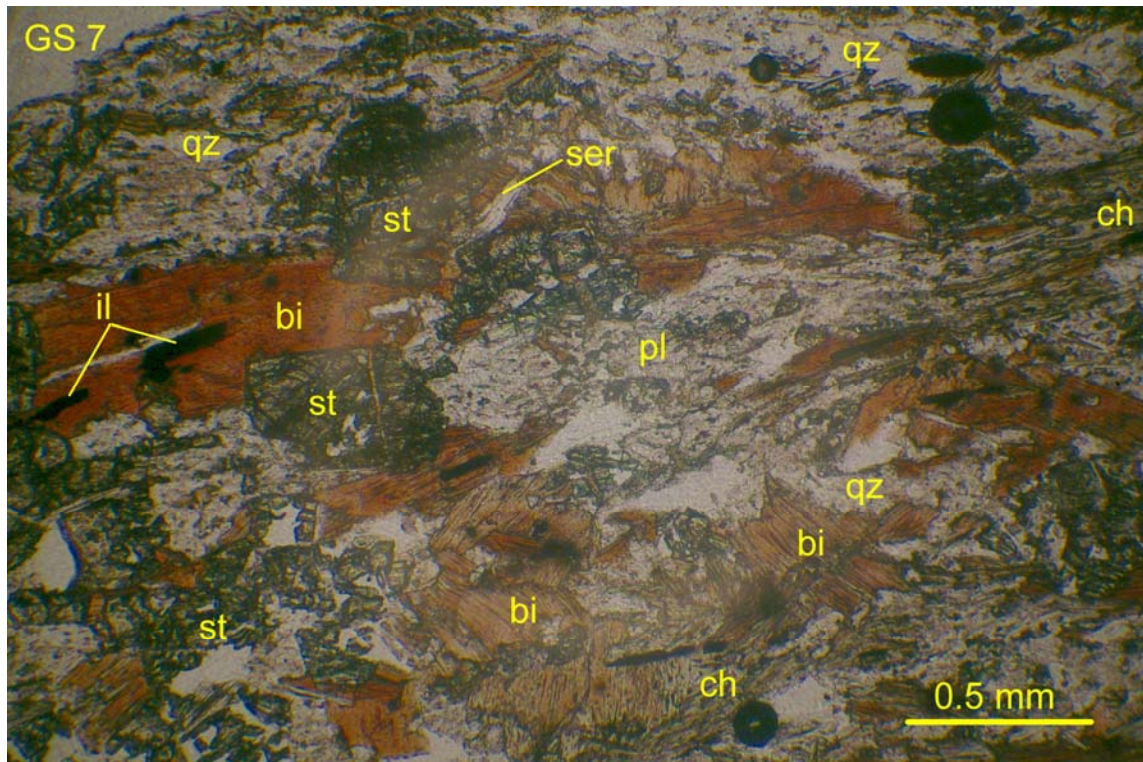


GS 3: Schist/gneiss composed of granular quartz (qz) with wispy foliae of chlorite (ch)-relict biotite (bi)-minor muscovite (ms), associated with significant carbonate (cb) that also occurs in veins (CB) oblique to the foliation. Transmitted light, crossed polars, field of view 3.0 mm wide.

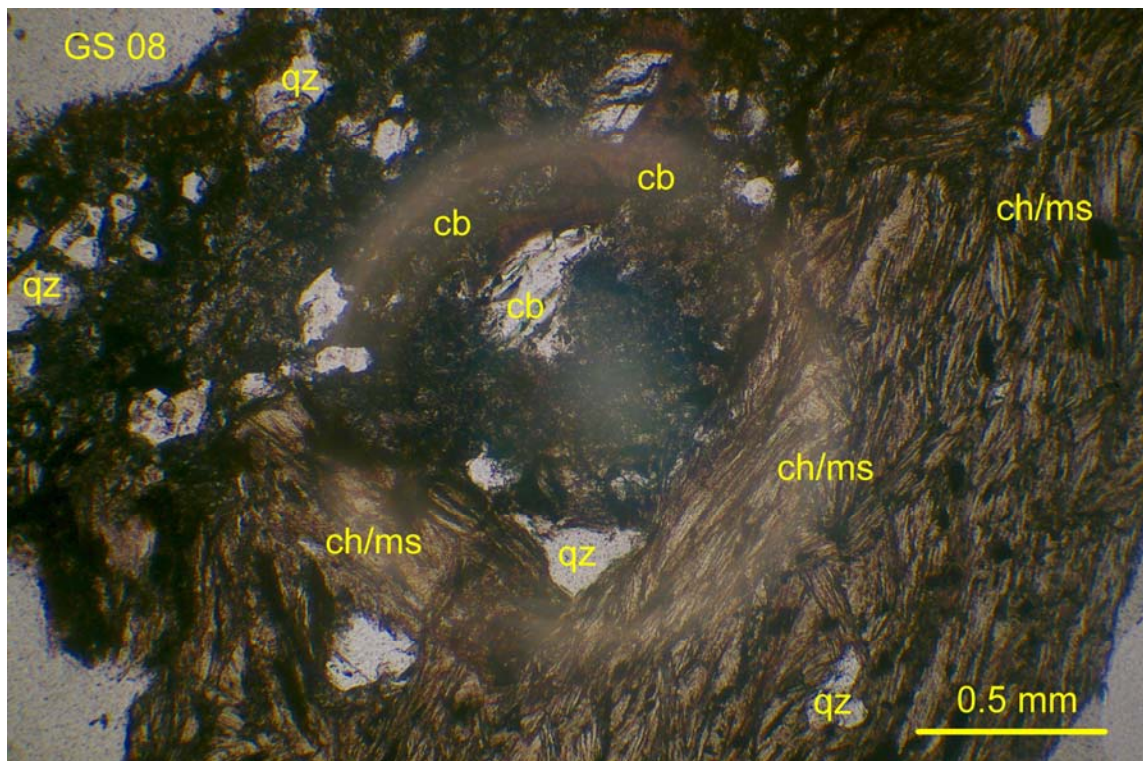


GS 5: Strongly foliated "paper schist" composed of quartz (qz), chlorite (ch) with minor muscovite, and Fe carbonate associated with aggregates of rutile (ru, opaque), cut by foliation-parallel veinlets of quartz (QZ) and carbonate (cb; could be dolomite) plus trace pyrite (py) partly oxidized to limonite (lm). Transmitted plane light, field of view 3.0 mm wide.



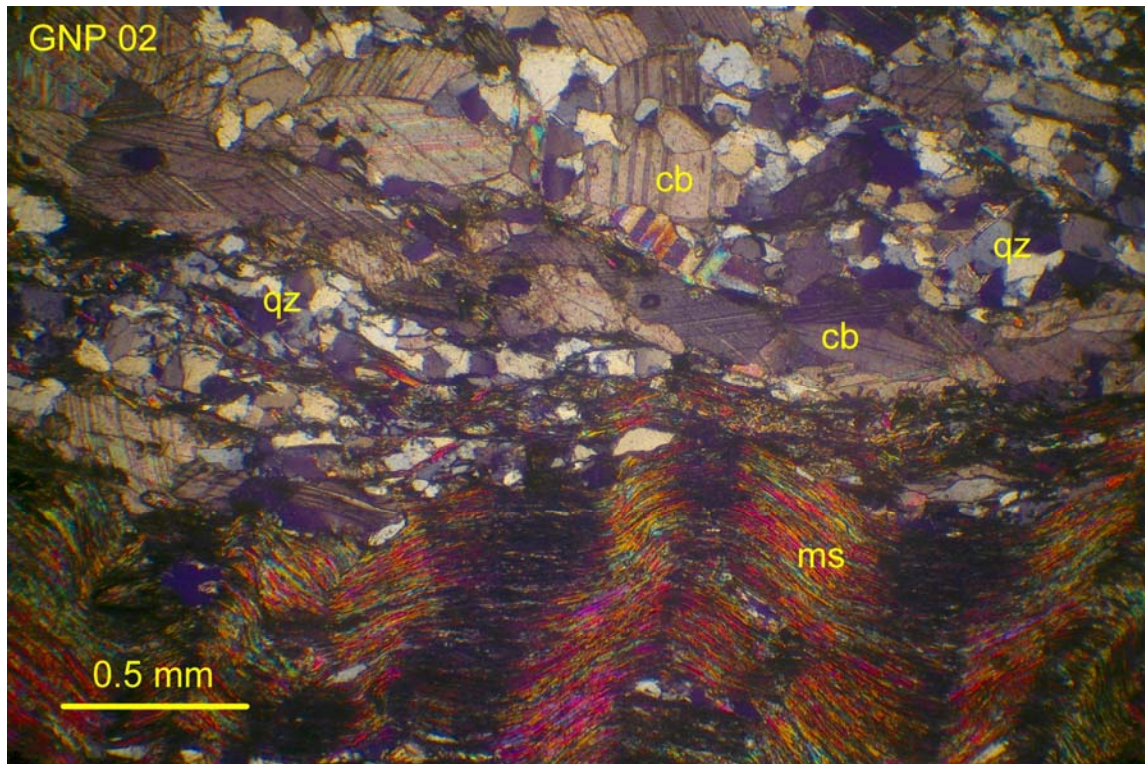


GS 7: Blastic staurolite (st) and biotite (bi, with included opaque tabular ilmenite), both partly retrograded to chlorite (ch) and sericite (ser), in matrix of fine-grained quartz (qz) and cloudy, incipiently sericitized plagioclase (pl). Transmitted plane light, field of view 3.0 mm wide.

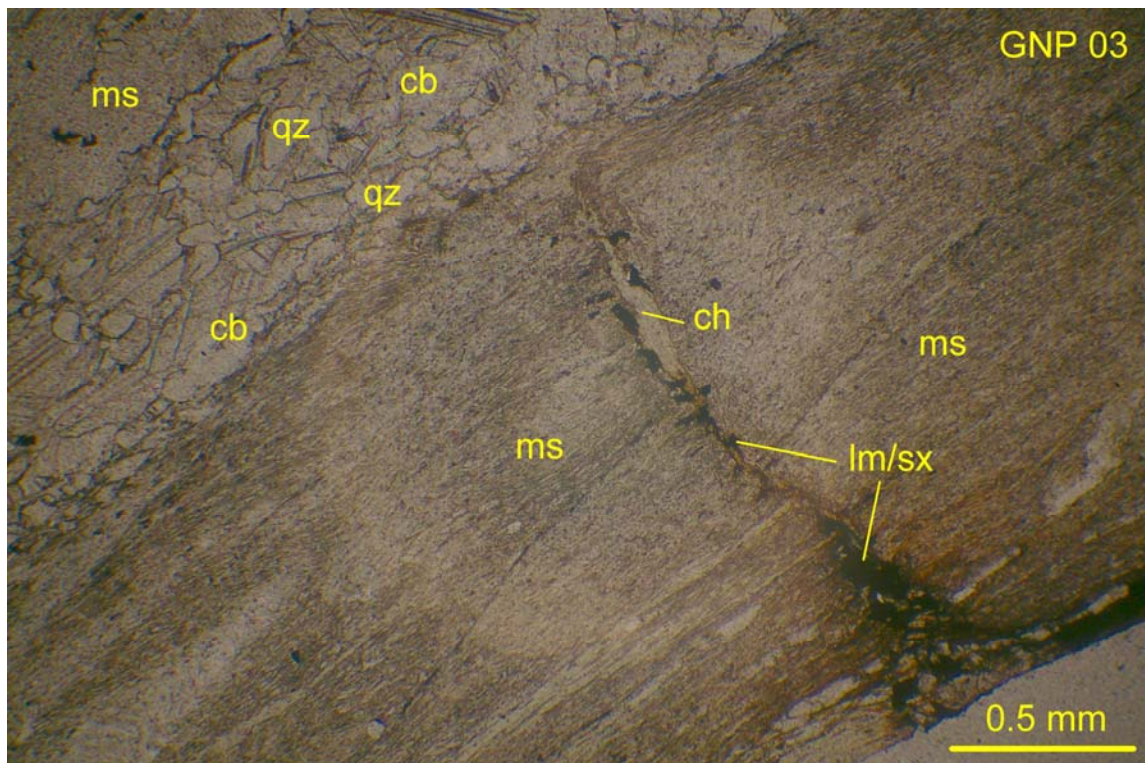


GS 8: Coarse-grained, weakly foliated schist composed of relict biotite altered to chlorite/muscovite (ch/ms) with scattered rutile (opaque, ru) partly after former tabular ilmenite (?), with local fine-grained aggregates of Fe carbonate (cb, partly stained by limonite) and interstitial quartz (qz). Transmitted plane light, field of view 3.0 mm wide.



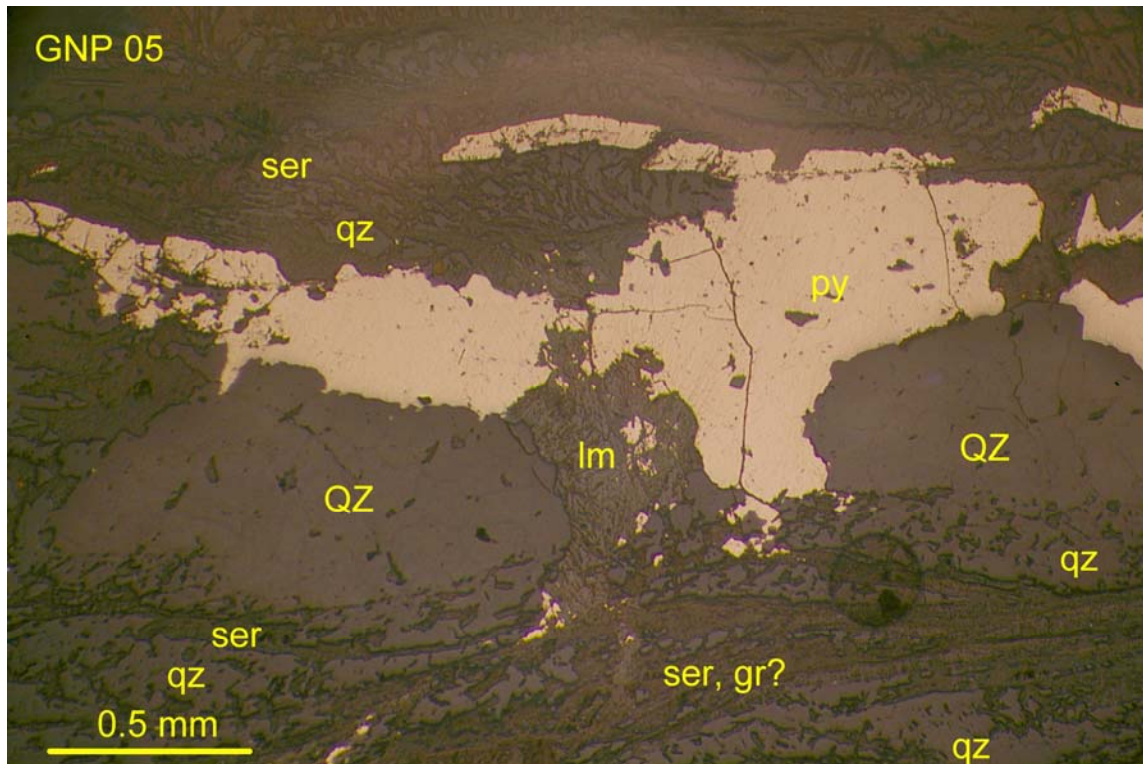


GNP 02: Schist composed of alternating layers of quartz (qz)-carbonate (cb) or strongly foliated, crenulated/kink banded muscovite (ms)-minor chlorite (not readily visible at this scale). Transmitted light, crossed polars, field of view 3.0 mm wide.

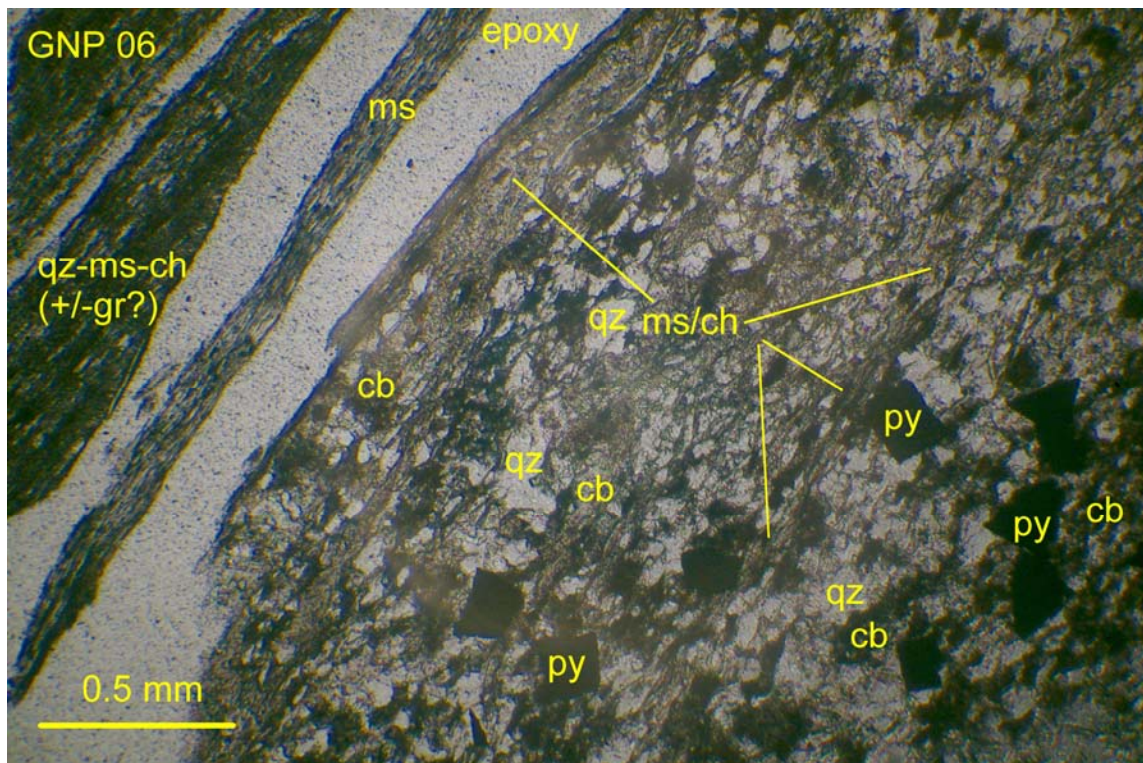


GNP 03: Strongly foliated, vaguely kink-banded muscovite (ms)-minor chlorite layer alternating with coarser-grained, carbonate (cb)-quartz (qz) rich layer. Note minor limonite around cross-cutting thin veinlet of pyrrhotite (opaque), associated with chlorite (ch). Transmitted plane light, field of view 3.0 mm wide.



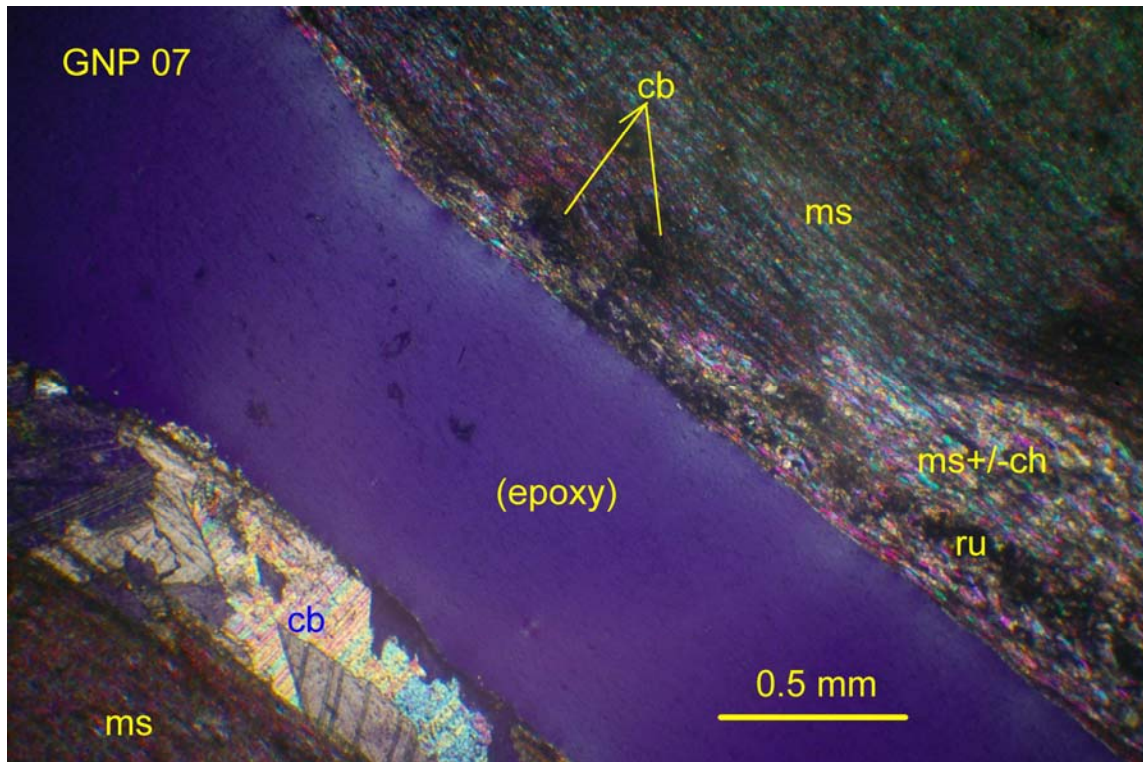


GNP 05: Pyrite (py) partly oxidized to limonite, Im) associated with coarse-grained quartz (QZ) sweat parallel to foliation in finer-grained, quartz (qz)-muscovite (ms) rich schist with wispy laminae enriched in sub-microscopic opaque matter that may be partly graphite (gr?). Reflected light, uncrossed polars, field of view 2.75 mm wide.

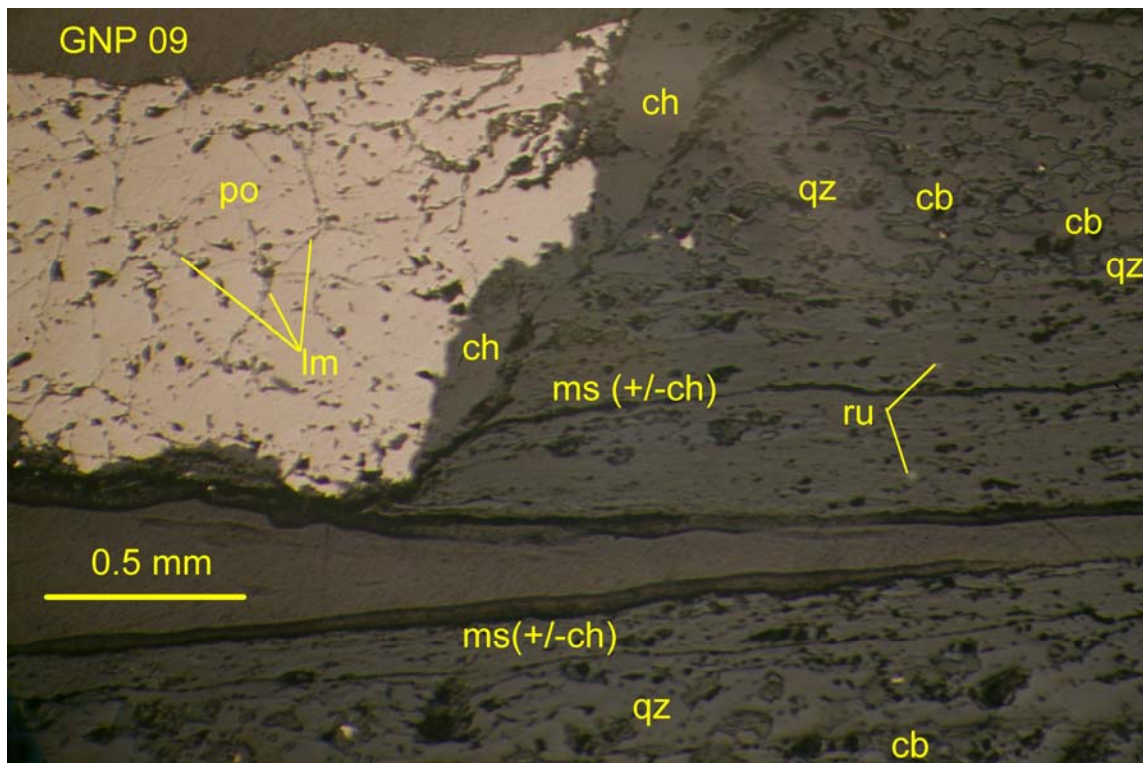


GNP 06: Well-foliated quartz-muscovite-chlorite schist with muscovite (ms)-rich partings, more quartz (qz) rich layers that contain local pyrite (py) cubes partly enclosed in limonite-stained Fe carbonate (cb) and minor muscovite, chlorite (too fine to separate at this scale). Transmitted plane light, field of view 3.0 mm wide.



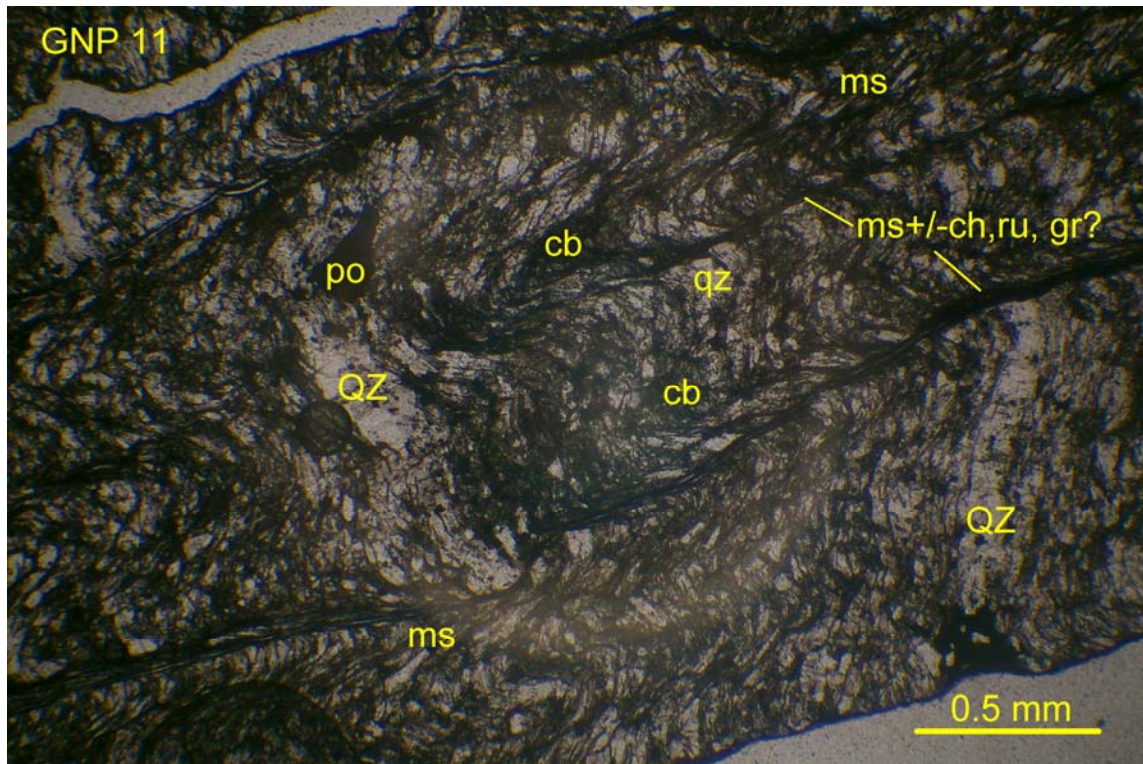


GNP 07: Extremely fine-grained, well-foliated muscovite (ms) schist, with local coarser layers in which chlorite is identifiable, along with accessory rutile (ru, opaque) and tourmaline (not identifiable at this scale), or local layer-parallel carbonate (cb) veinlets. Transmitted light, crossed polars, field of view 3.0 mm wide.

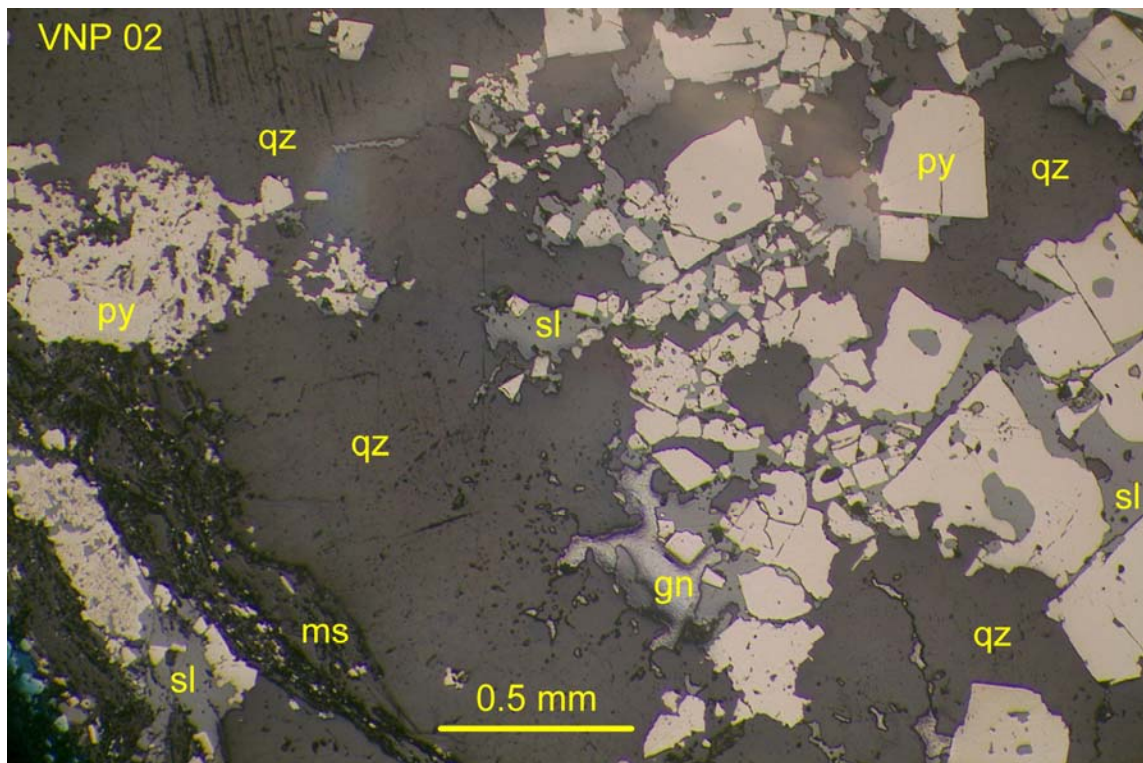


GNP 09: Pyrrhotite (po) slightly altered along microfractures to limonite (lm), and in contact with porphyroblasts of slightly magnesian chlorite (ch), in lensey segregation in schist composed of quartz (qz)-carbonate (cb) rich layers alternating with muscovite (ms)-minor chlorite-trace rutile (ru) layers. Reflected light, uncrossed polars, field of view 2.75 mm wide.





GNP 11: Strong crenulation cleavage in quartz-muscovite-carbonate schist (grains mostly too small to be identified at this scale; minor chlorite is hard to distinguish but is concentrated in cleavage with rutile, ru, possible graphite, gr). Pyrrhotite (po, opaque) is concentrated in lensey quartz (QZ) rich segregations. Transmitted plane light, field of view 3.0 mm wide.



VNP 02: Euhedral pyrite (py) associated with interstitial sphalerite (sl) and lesser galena (gn), in matrix of (mainly secondary) quartz (qz) that locally contains foliated laminae of muscovite (ms) rich rock locally containing traces of Fe carbonate and rutile too small to distinguish at this scale. Reflected light, uncrossed polars, field of view 2.75 mm wide.



Overviews of thin sections and offcuts (green semi-circles mark photomicrograph locations).





PETROGRAPHIC REPORT ON 2 SAMPLES (PROJECT SRK-Anvil Range 2-21-900)

Report for: Ivy Rajan  
CANTEST  
4606 Canada Way  
BURNABY, B.C. V5G 1K5 (604) 734-7276

Invoice 080966

Nov. 13, 2008.

SUMMARY:

Capsule descriptions are as follows:

FNP 17: slightly deuteritic (sericite-chlorite) altered, somewhat weathered biotite granodiorite (on the boundary with quartz diorite), with minor accessory pyrite and chalcopyrite (both partly oxidized to limonite), apatite and sphene. Carbonate does not appear to be present in the slide.

FNP-18: slightly deuteritic (sericite-chlorite-carbonate) altered, somewhat weathered hornblende-biotite granodiorite (near the boundary with quartz diorite), with minor accessory pyrite and chalcopyrite (both partly oxidized to limonite), ilmenite, magnetite, and apatite. Carbonate-altered hornblende is circled on the slide for future reference.

Detailed petrographic descriptions and photomicrographs are appended (by email attachment). If you have any questions regarding the petrography, please do not hesitate to contact me.

Craig H.B. Leitch, Ph.D., P. Eng. (250) 653-9158 [craig.leitch@gmail.com](mailto:craig.leitch@gmail.com)  
492 Isabella Point Road, Salt Spring Island, B.C. Canada V8K 1V4

**FNP 17: BIOTITE GRANODIORITE/QUARTZ DIORITE (ACCESSORY PYRITE, CHALCOPYRITE PARTLY OXIDIZED TO LIMONITE, TRACE APATITE, ILMENITE, SPHENE), SLIGHT ALTERATION TO SERICITE-CHLORITE**

Sample consists of mostly <1 cm diameter, angular, weathered/oxidized (limonite stained) chips of medium-grained granitic-looking rock with coarse flakes of black biotite. The rock is not magnetic, shows no reaction to cold dilute HCl, and only minor stain for K-feldspar in the etched offcut. Modal mineralogy in polished thin section is approximately:

Plagioclase (andesine, partly sericite altered)	55%
Quartz (primary)	20%
Biotite (partly chloritized)	15%
K-feldspar (primary)	5%
Sericite (mainly after plagioclase)	1-2%
Chlorite (mostly after biotite)	1-2%
Limonite	1%
Pyrite, minor chalcopyrite (both partly oxidized to limonite)	<1% each
Apatite, ilmenite, sphene	<1%

The chips in this sample mostly appear to represent a slightly weathered plutonic rock composed of interlocking, hypidiomorphic crystals of plagioclase, quartz, biotite, and minor interstitial K-feldspar plus accessory sulfides (partly oxidized to limonite), apatite and ilmenite or sphene.

Plagioclase forms mainly sub/euhedral crystals up to about 1.25 mm in diameter, with cores commonly 10-25% replaced by fine-grained sericite (subhedral flakes mostly <0.1 mm in diameter). Replacement is rarely up to 50% (where accompanied by lesser chlorite of similar size). Composition appears to be about andesine, ranging from cores of An<sub>45</sub> to rims of An<sub>27</sub> (based on extinction  $Z^{001} = -16$  to 0 degrees, and relief similar or slightly positive compared to quartz). K-feldspar occurs as small (mainly <0.35 mm) subhedral crystals found in interstices between plagioclase, or included within, quartz crystals.

Quartz forms mainly sub- to locally euhedral crystals up to almost 2 mm in diameter that are slightly fractured but generally only weakly strained (weak undulose extinction, no sub-grain development or suturing of grain boundaries). Quartz commonly poikilitically encloses plagioclase (and to a lesser degree K-feldspar).

Biotite forms mainly euhedral crystals mostly <1.5 mm, but locally up to 2.5 mm in diameter (the latter poikilitically enclose plagioclase crystals) with pale reddish to dark, blackish brown pleochroism, locally partly interleaved or replaced by chlorite, mainly around the margins. Locally, especially where associated with minor sulfides which comprise mainly pyrite (sub/euhedra <0.1 mm, aggregating to ~1 mm) and minor chalcopyrite (subhedra to 0.3 mm) both partly rimmed or locally pseudomorphed, by bright red-brown (goethitic?) limonite, the biotite is green (ferriferous?).

Chlorite forms sub/euhedral flakes mostly <50 microns in diameter with optical character (weak but distinct pale green pleochroism, length-slow greenish grey birefringence) indicative of Fe:Fe+Mg, or F:M, ratio, around 0.5 (?). Traces of apatite (minute euhedral prisms <50 microns long) and ilmenite (subhedra to 75 microns) or sphene (aggregates to 35 microns of smaller subhedra) are associated with the altered biotite sites.

In summary, this appears to represent slightly deuteric (sericite-chlorite) altered, somewhat weathered biotite granodiorite (on the boundary with quartz diorite), with minor accessory pyrite and chalcopyrite (both partly oxidized to limonite), apatite and sphene. Carbonate does not appear to be present in the slide.

FNP-18:HORNBLende BIOTITE GRANODIORITE/QUARTZ DIORITE (ACCESSORY PYRITE, CHALCOPYRITE PARTLY OXIDIZED TO LIMONITE, ILMENITE, MAGNETITE, TRACE APATITE), SLIGHT ALTERATION TO SERICITE-CHLORITE-CARBONATE

Sample consists of angular chips mostly <2 cm in diameter of grey (relatively unweathered) medium-grained felsic/intermediate plutonic rock with common flakes of black biotite, and interstitial orange-pink K-feldspar. The rock is locally slightly magnetic, shows trace reaction to cold dilute HCl, and minor stain for K-feldspar in the etched offcut. Modal mineralogy in polished thin section is approximately:

Plagioclase (andesine, partly sericite altered)	55%
Quartz (primary)	20%
Biotite (partly chloritized)	10%
K-feldspar (primary)	7%
Amphibole (hornblende?)	3-5%
Sericite (mainly after plagioclase)	1%
Chlorite (mostly after biotite)	1%
Carbonate (mainly calcite?)	<1%
Limonite	<1%
Pyrite, minor chalcopyrite (both partly oxidized to limonite)	<1%
Apatite, ilmenite, sphene	<1%

The chips in this sample mostly appear to represent a relatively unweathered plutonic rock composed of interlocking, hypidiomorphic crystals of plagioclase, quartz, biotite, amphibole, minor interstitial K-feldspar plus accessory sulfides (partly oxidized to limonite), ilmenite, magnetite, and trace apatite.

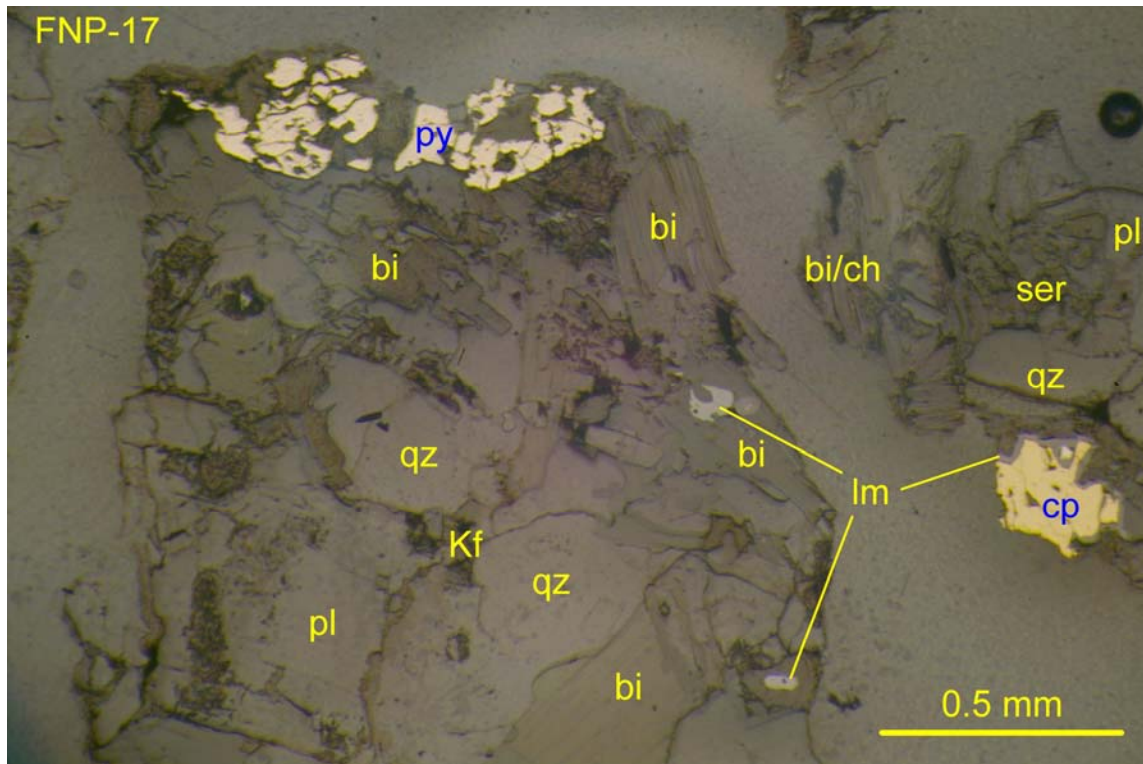
Plagioclase forms mainly sub/euhedral crystals up to about 1.5 mm in diameter, with cores commonly 5-15% replaced by fine-grained sericite (subhedral flakes mostly <0.1 mm in diameter). Replacement is rarely up to 30% (where accompanied by lesser chlorite of similar size). Composition appears to be about andesine, ranging from innermost cores of An<sub>55</sub> (labradorite) through intermediate zones of An<sub>45</sub> to rims of An<sub>24</sub> (based on extinction  $Z^{001} = -30$  to  $-16$  to  $+2$  degrees, and relief similar or slightly positive compared to quartz). K-feldspar occurs as small (mainly <0.5 mm) subhedral crystals found in interstices between plagioclase, or included within, quartz crystals.

Quartz forms mainly sub- to locally euhedral crystals up to about 2.5 mm in diameter that are slightly fractured but generally only weakly strained (weak undulose extinction, no sub-grain development or suturing of grain boundaries). Quartz commonly poikilitically encloses plagioclase (and to a lesser degree K-feldspar).

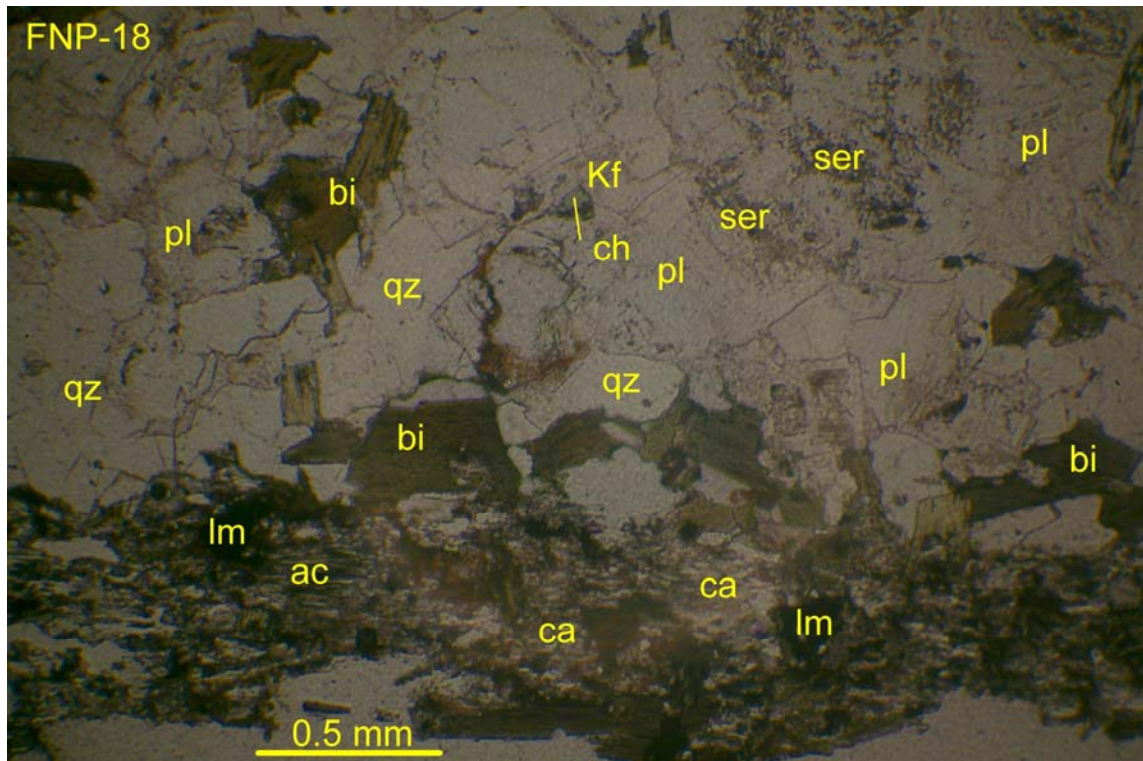
Biotite forms mainly euhedral crystals mostly <1.5 mm, but locally up to 2.5 mm in diameter (the latter poikilitically enclose plagioclase crystals) with pale reddish to dark brown pleochroism, locally partly interleaved or replaced by chlorite, mainly around the margins. Amphibole forms ragged to irregular, locally subhedral crystals up to 4 mm long with olive-green pleochroism (possibly hornblende?) that are locally partly replaced or pseudomorphed by fibrous actinolite up to 0.3 mm long, and minor carbonate (likely calcite, forming ragged subhedra mostly <0.2 mm). Traces of ilmenite (subhedra to 0.15 mm) or magnetite (aggregates to 0.15 mm of smaller subhedra) are associated with or contained within the biotite crystals, locally with traces of apatite (minute euhedral prisms <50 microns long). Locally, minor sulfides comprising mainly pyrite (sub/euhedra <0.1 mm, aggregating to ~1 mm) and minor chalcopyrite (subhedra to 0.3 mm), both partly rimmed or locally pseudomorphed, by bright red-brown (goethitic?) limonite, are associated with biotite or amphibole, and locally the biotite adjacent to sulfides is green (ferriferous?). Chlorite forms sub/euhedral flakes mostly <50 microns in diameter with optical character (weak but distinct pale green pleochroism, length-slow greenish grey birefringence) indicative of Fe:Fe+Mg, or F:M, ratio, around 0.5 (?).

In summary, this appears to represent slightly deuteric (sericite-chlorite-carbonate) altered, somewhat weathered hornblende-biotite granodiorite (near the boundary with quartz diorite), with minor accessory pyrite and chalcopyrite (both partly oxidized to limonite), ilmenite, magnetite, and apatite. Carbonate-altered hornblende is circled on the slide for future reference.

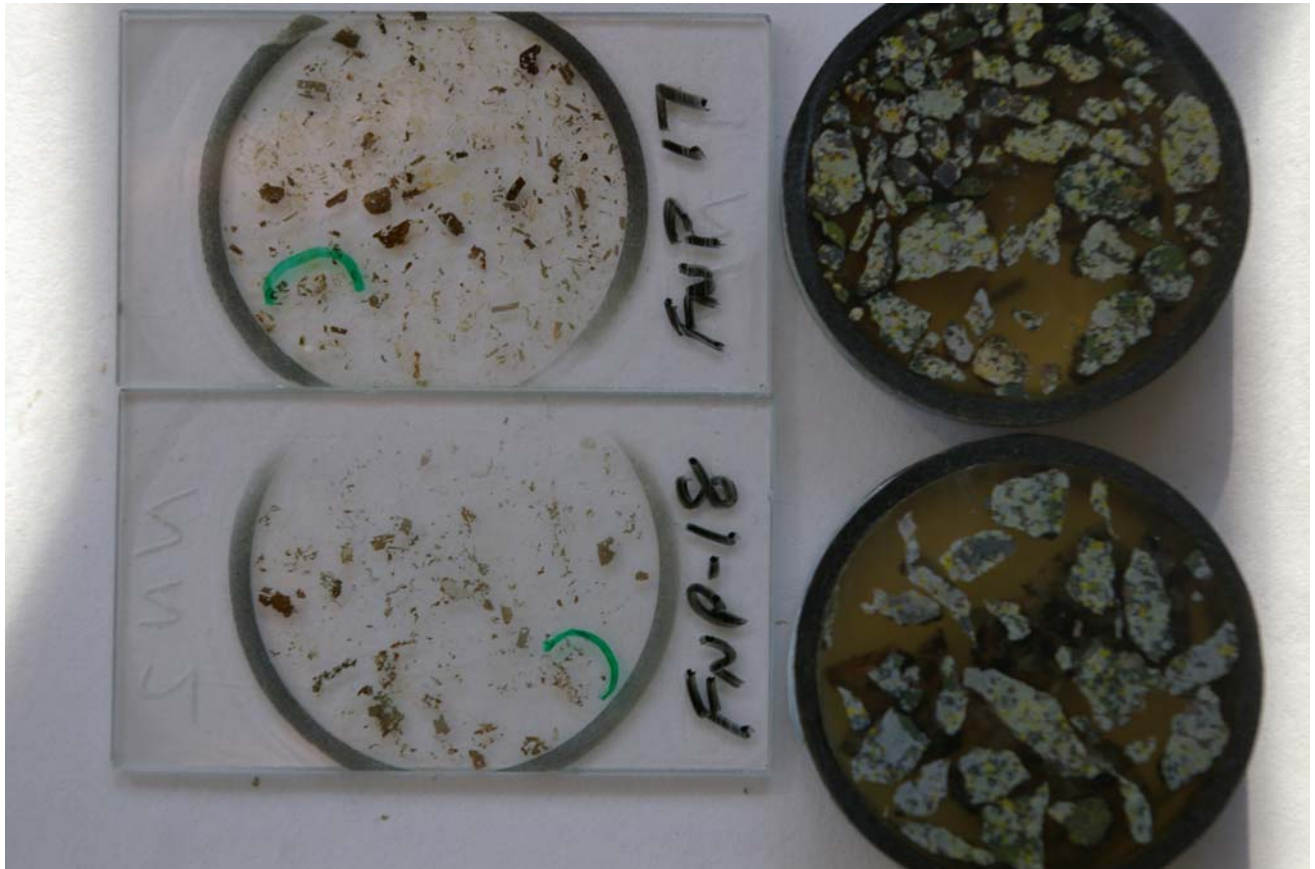




FNP-17: Minor sulfides (pyrite, py and chalcopyrite, cp) partly rimmed or locally pseudomorphed by limonite (lm), in granodiorite composed of plagioclase (pl) partly altered to sericite (ser), quartz (qz), biotite (bi) partly altered to chlorite (ch) and minor interstitial Kspar (Kf). Reflected light, uncrossed polars, field of view 2.25 mm wide.



FNP-18: Elongated relict hornblende site altered to actinolite (ac), carbonate (likely calcite, ca), and mantled by biotite (bi) and containing minor limonite (lm) after sulfides, in granodiorite composed of plagioclase (pl) partly altered to sericite (ser), quartz (qz), biotite (bi) partly altered to chlorite (ch) and minor interstitial Kspar (Kf). Transmitted plane light, field of view 3.0 mm wide.



Overview of thin sections and offcuts (green semi-circles mark photomicrograph locations).

## **Appendix D**

### **X-ray Diffraction Results**

**QUANTITATIVE PHASE ANALYSIS OF 20 POWDER SAMPLES USING THE  
RIETVELD METHOD AND X-RAY POWDER DIFFRACTION DATA.**

**Project: SRK – Anvil Range  
Cantest Project No: 2-21-900  
Internal Requisition No: R 72288**

---

**Ivy Rajan  
CanTest Ltd.  
3650 Wesbrook Mall  
Vancouver, BC V6S 2L2**

---

---

**Mati Raudsepp, Ph.D.  
Elisabetta Pani, Ph.D.  
Dept. of Earth & Ocean Sciences  
6339 Stores Road  
The University of British Columbia  
Vancouver, BC V6T 1Z4**

**August 27, 2008**

## EXPERIMENTAL METHODS

The twenty samples of Project SRK – Anvil Range were reduced to the optimum grain-size range for quantitative X-ray analysis ( $<10\ \mu\text{m}$ ) by grinding under ethanol in a vibratory McCrone Micronising Mill for 7 minutes. Fine grain-size is an important factor in reducing micro-absorption contrast between phases.

Step-scan X-ray powder-diffraction data were collected over a range  $3\text{--}80^\circ 2\theta$  with  $\text{CoK}\alpha$  radiation on a standard Siemens (Bruker) D5000 Bragg-Brentano diffractometer equipped with an Fe monochromator foil,  $0.6\ \text{mm}$  ( $0.3^\circ$ ) divergence slit, incident- and diffracted-beam Soller slits and a Vantec-1 strip detector. The long fine-focus Co X-ray tube was operated at 35 kV and 40 mA, using a take-off angle of  $6^\circ$ .

## RESULTS

The X-ray diffractograms were analyzed using the International Centre for Diffraction Database PDF-4 using Search-Match software by Siemens (Bruker). X-ray powder-diffraction data of the samples were refined with Rietveld program Topas 3 (Bruker AXS). The results of quantitative phase analysis by Rietveld refinements are given in Table 1 (separate file, *CanTest Results Proj SRK-Anvil Range.xls*). These amounts represent the relative amounts of crystalline phases normalized to 100%. The Rietveld refinement plots are shown in Figures 1-20. The ideal mineral formulae are given in Table 2.

The pattern of sample **FNP 06** (Figure 4) shows a hump between  $5\text{--}9^\circ 2\theta$  that likely corresponds to a disordered/nanoscale smectite group mineral or mixed chlorite-smectite; an empirical montmorillonite structure model has been fitted as an approximation.

**Table 1. Results of quantitative phase analysis (wt.%) - XRD-Rietveld**  
**CanTest Proj. SRK - Anvil Range**

[illegible]

**Table 2.**

<b>Mineral</b>	<b>Ideal Formula</b>
Actinolite	$\text{Ca}_2(\text{Mg}, \text{Fe}^{2+})_5\text{Si}_8\text{O}_{22}(\text{OH})_2$
Anatase	$\text{TiO}_2$
Andalusite	$\text{Al}_2\text{SiO}_5$
Ankerite	$\text{Ca}(\text{Fe}^{2+}, \text{Mg}, \text{Mn})(\text{CO}_3)_2$
Biotite	$\text{K}(\text{Mg}, \text{Fe}^{2+})_3\text{AlSi}_3\text{O}_{10}(\text{OH})_2$
Calcite	$\text{K}(\text{Mg}, \text{Fe}^{2+})_3\text{AlSi}_3\text{O}_{10}(\text{OH})_2$
Cerussite	$\text{PbCO}_3$
Clinochlore	$(\text{Mg}, \text{Fe}^{2+})_5\text{Al}(\text{Si}_3\text{Al})\text{O}_{10}(\text{OH})_8$
Clinozoisite	$\text{Ca}_2\text{Al}_3(\text{SiO}_4)_3(\text{OH})$
Cummingtonite	$\text{Mg}_7\text{Si}_8\text{O}_{22}(\text{OH})_2$
Diopside	$\text{CaMgSi}_2\text{O}_6$
Dolomite	$\text{CaMg}(\text{CO}_3)_2$
Galena	$\text{PbS}$
Kaolinite	$\text{Al}_2\text{Si}_2\text{O}_5(\text{OH})_4$
K-feldspar	$\text{KAlSi}_3\text{O}_8$
Montmorillonite Model	$(\text{Na}, \text{Ca})_{0.3}(\text{Al}, \text{Mg})_2\text{Si}_4\text{O}_{10}(\text{OH})_2 \cdot n\text{H}_2\text{O}$
Muscovite	$\text{KAl}_2\text{AlSi}_3\text{O}_{10}(\text{OH})_2$
Paragonite	$\text{NaAl}_2\text{AlSi}_3\text{O}_{10}(\text{OH})_2$
Plagioclase	$\text{NaAlSi}_3\text{O}_8 - \text{CaAl}_2\text{Si}_2\text{O}_8$
Prehnite	$\text{Ca}_2\text{Al}_2\text{Si}_3\text{O}_{10}(\text{OH})_2$
Pyrite	$\text{FeS}_2$
Pyrrhotite	$\text{Fe}_{1-x}\text{S}$
Rutile	$\text{TiO}_2$
Quartz	$\text{SiO}_2$
Siderite	$\text{Fe}^{2+}\text{CO}_3$
Sphalerite	$(\text{Zn}, \text{Fe})\text{S}$

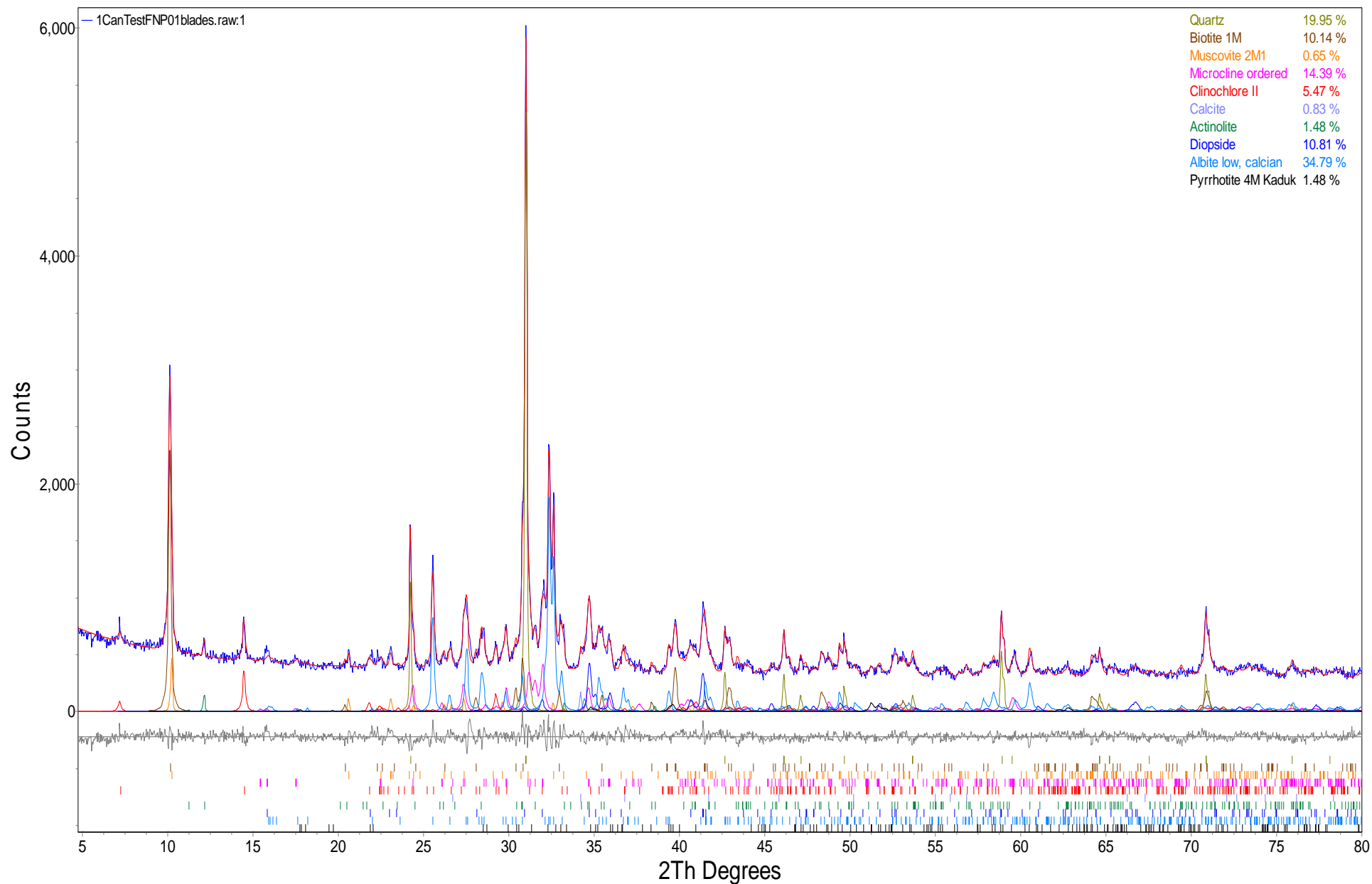


Figure 1. Rietveld refinement plot of sample **FNP-01** (blue line - observed intensity at each step; red line - calculated pattern; solid grey line below – difference between observed and calculated intensities; vertical bars, positions of all Bragg reflections). Coloured lines are individual diffraction patterns of all phases.



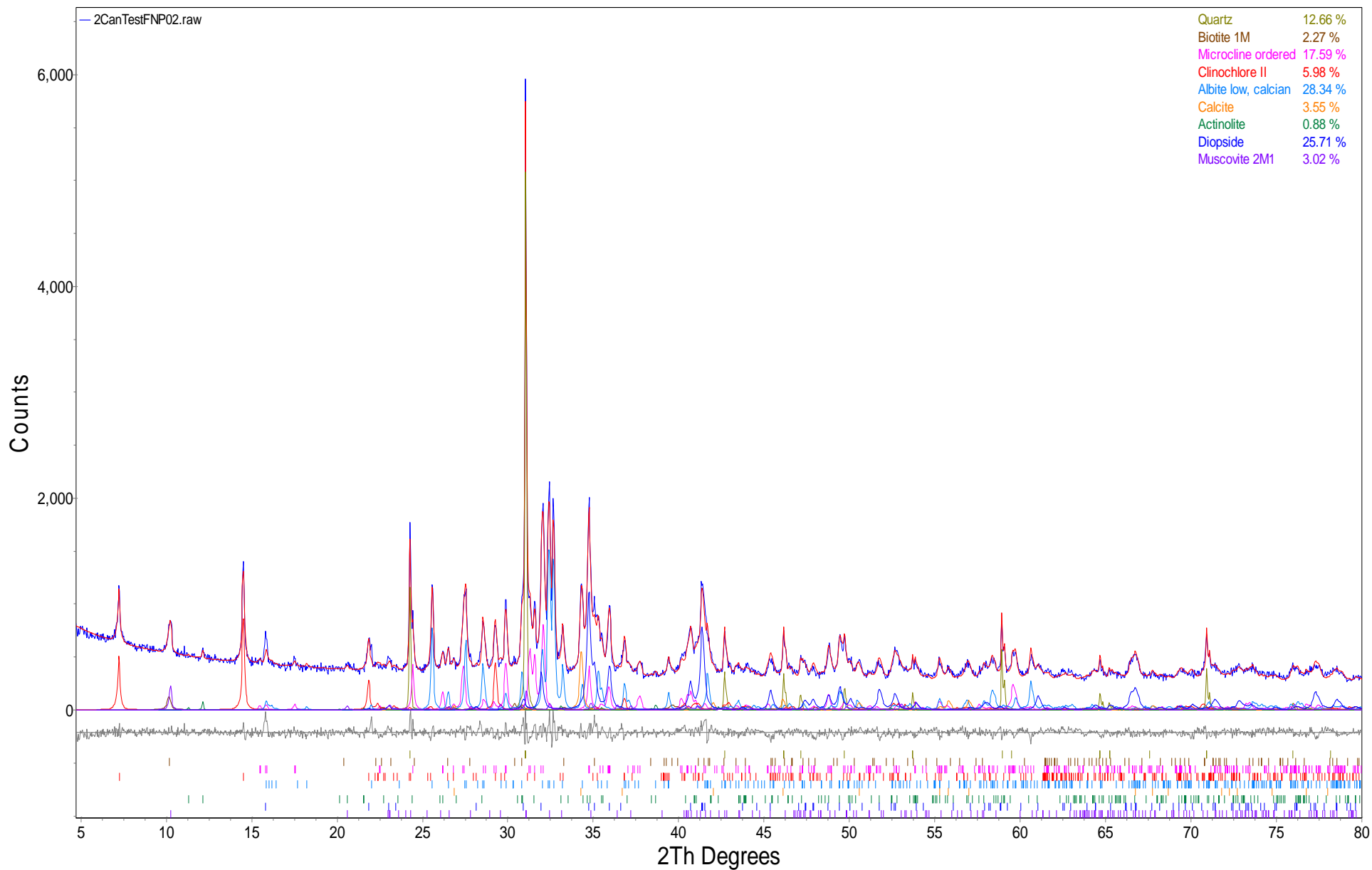


Figure 2. Rietveld refinement plot of sample **FNP-02** (blue line - observed intensity at each step; red line - calculated pattern; solid grey line below – difference between observed and calculated intensities; vertical bars, positions of all Bragg reflections). Coloured lines are individual diffraction patterns of all phases.

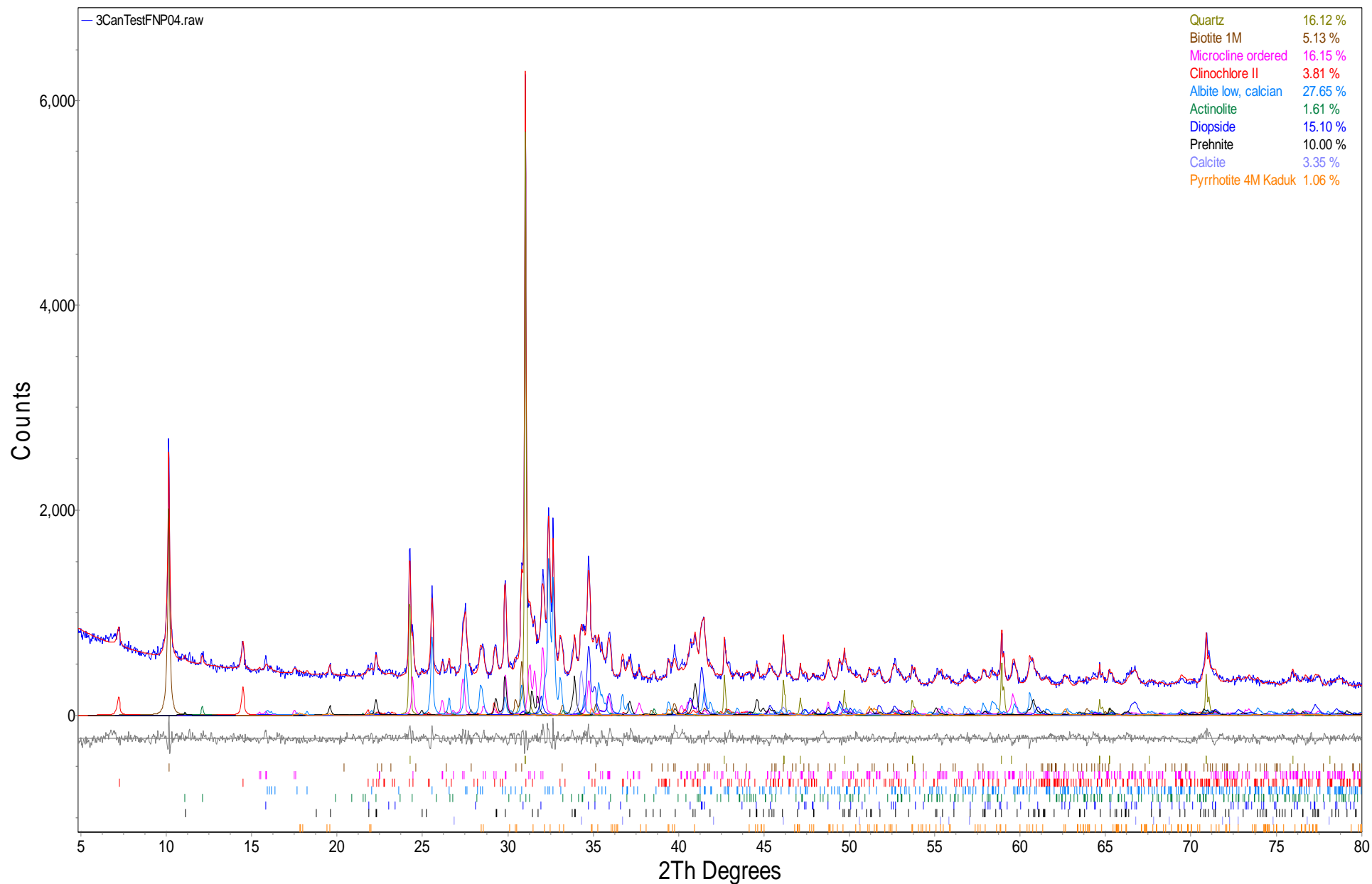


Figure 3. Rietveld refinement plot of sample **FNP-04** (blue line - observed intensity at each step; red line - calculated pattern; solid grey line below – difference between observed and calculated intensities; vertical bars, positions of all Bragg reflections). Coloured lines are individual diffraction patterns of all phases.

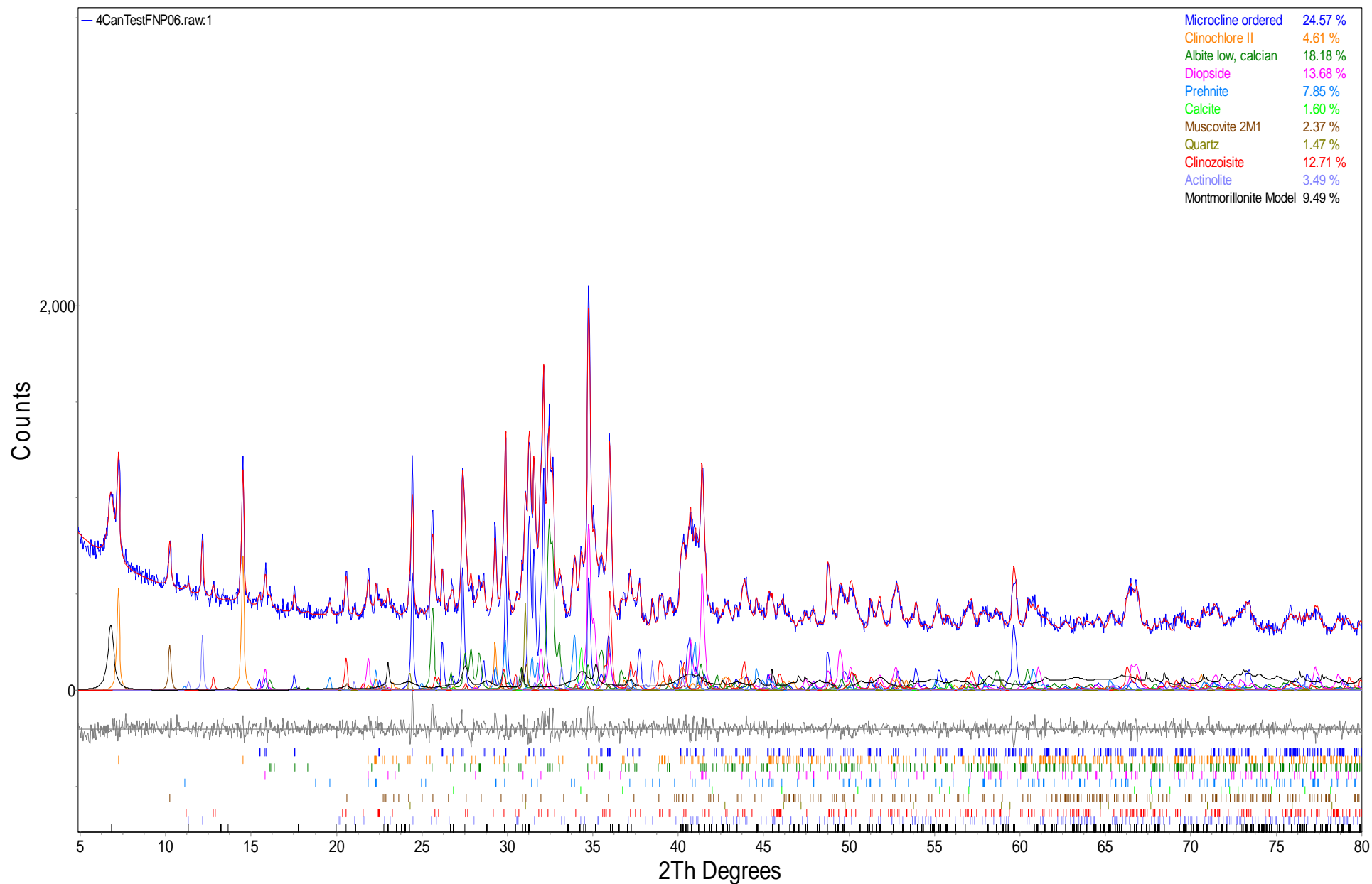


Figure 4. Rietveld refinement plot of sample **FNP-06** (blue line - observed intensity at each step; red line - calculated pattern; solid grey line below – difference between observed and calculated intensities; vertical bars, positions of all Bragg reflections). Coloured lines are individual diffraction patterns of all phases.

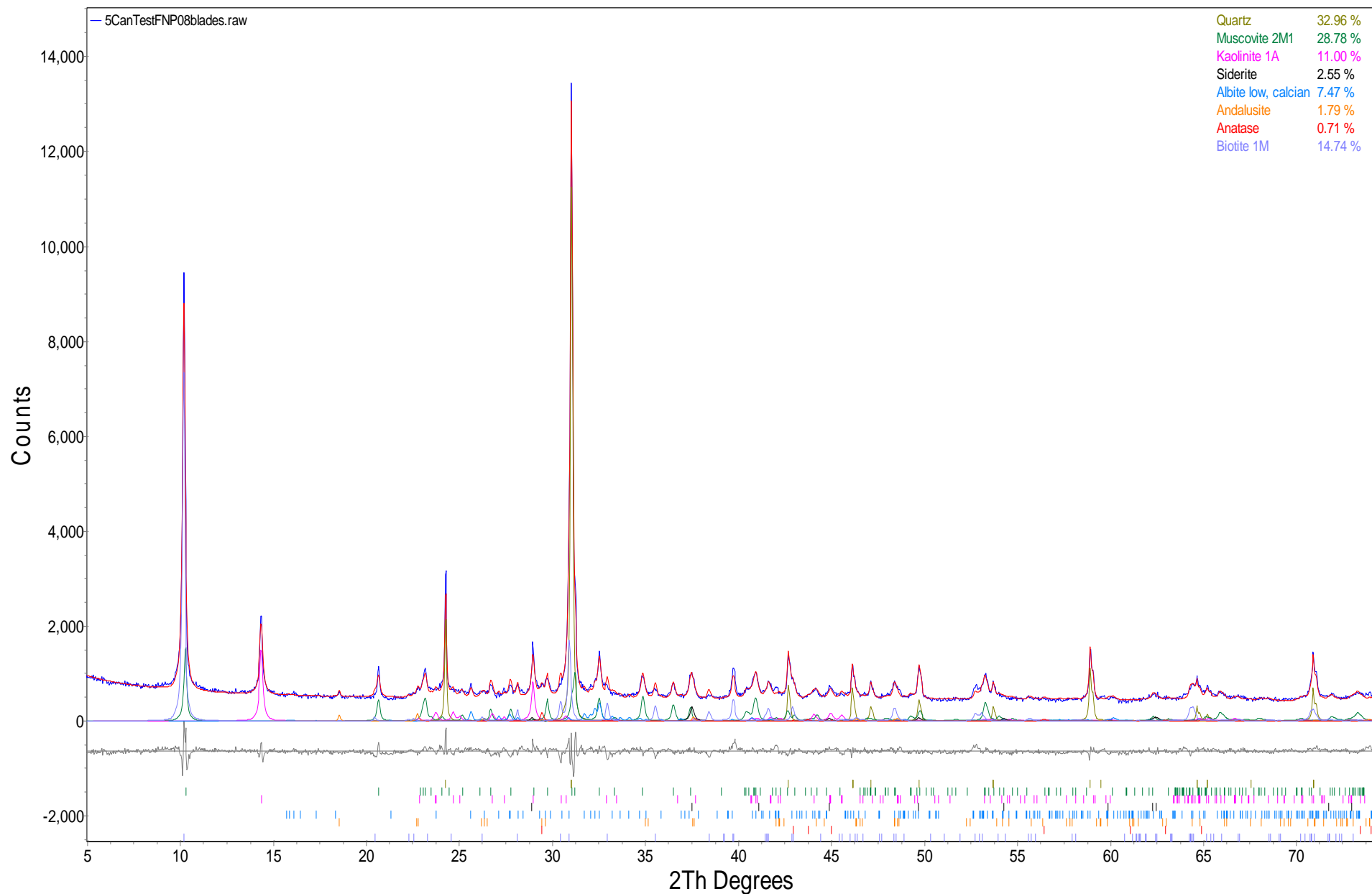


Figure 5. Rietveld refinement plot of sample **FNP-08** (blue line - observed intensity at each step; red line - calculated pattern; solid grey line below – difference between observed and calculated intensities; vertical bars, positions of all Bragg reflections). Coloured lines are individual diffraction patterns of all phases.

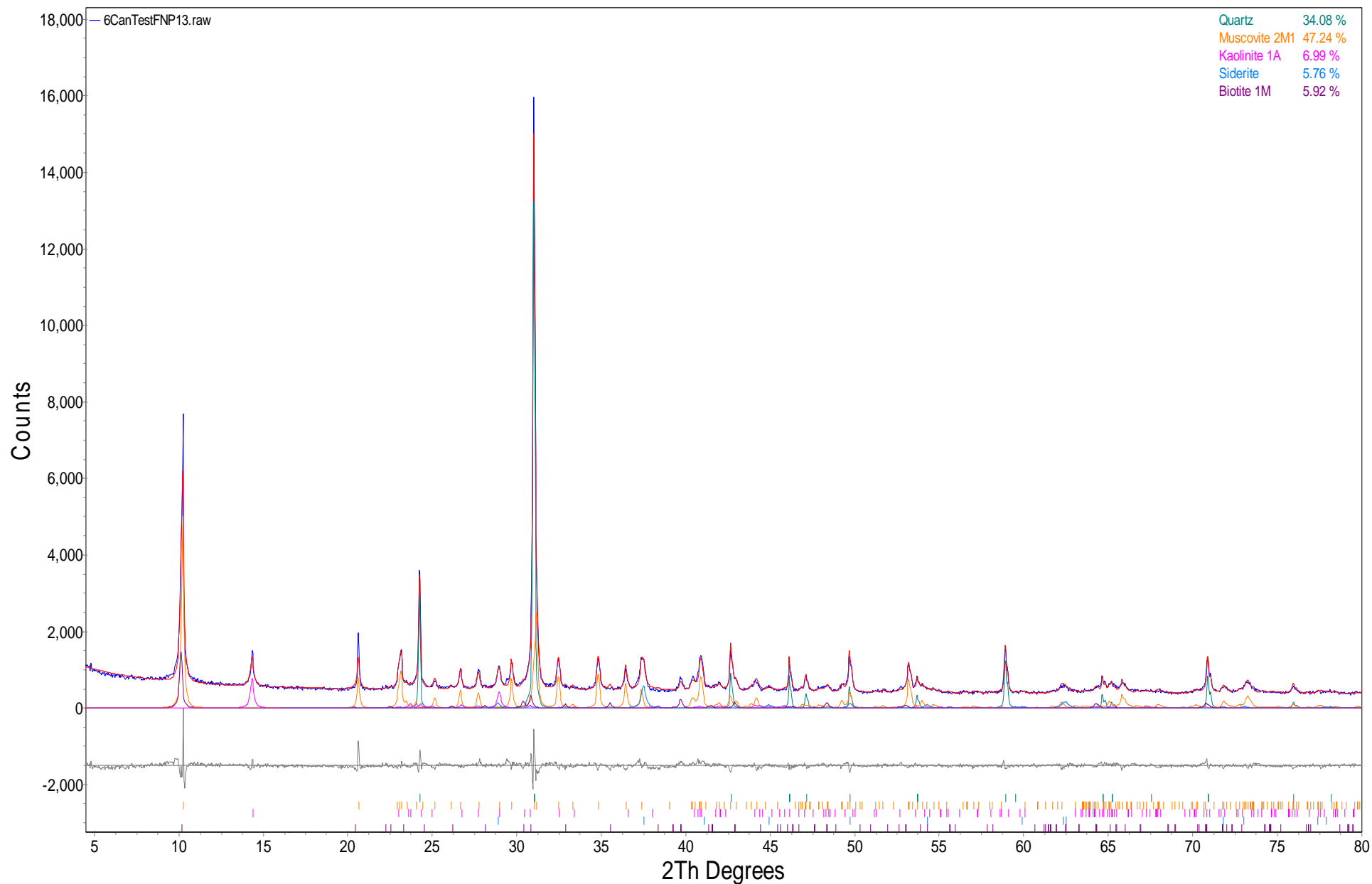


Figure 6. Rietveld refinement plot of sample **FNP-13** (blue line - observed intensity at each step; red line - calculated pattern; solid grey line below – difference between observed and calculated intensities; vertical bars, positions of all Bragg reflections). Coloured lines are individual diffraction patterns of all phases.

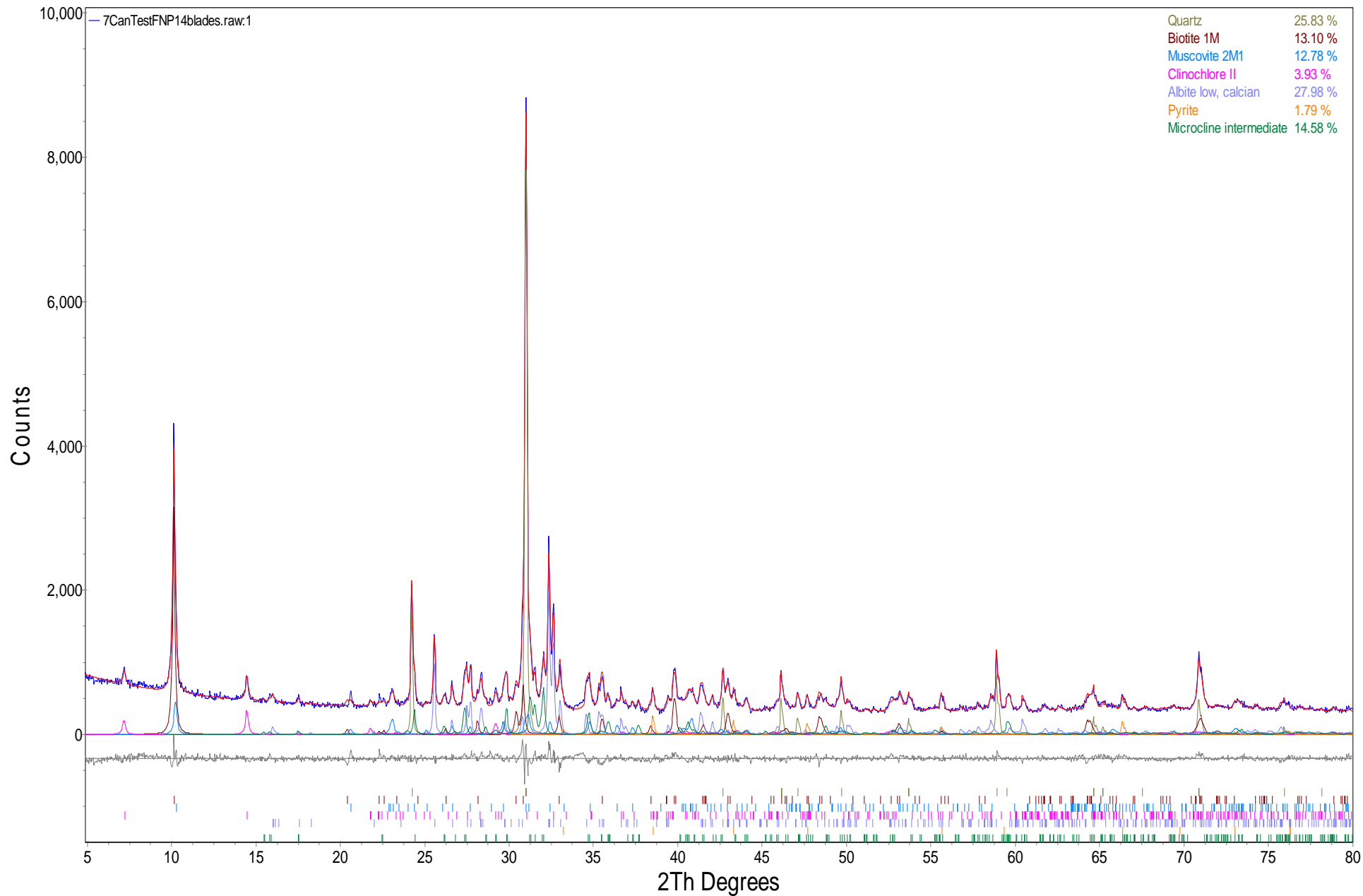


Figure 7. Rietveld refinement plot of sample **FNP-14** (blue line - observed intensity at each step; red line - calculated pattern; solid grey line below — difference between observed and calculated intensities; vertical bars, positions of all Bragg reflections). Coloured lines are individual diffraction patterns of all phases.

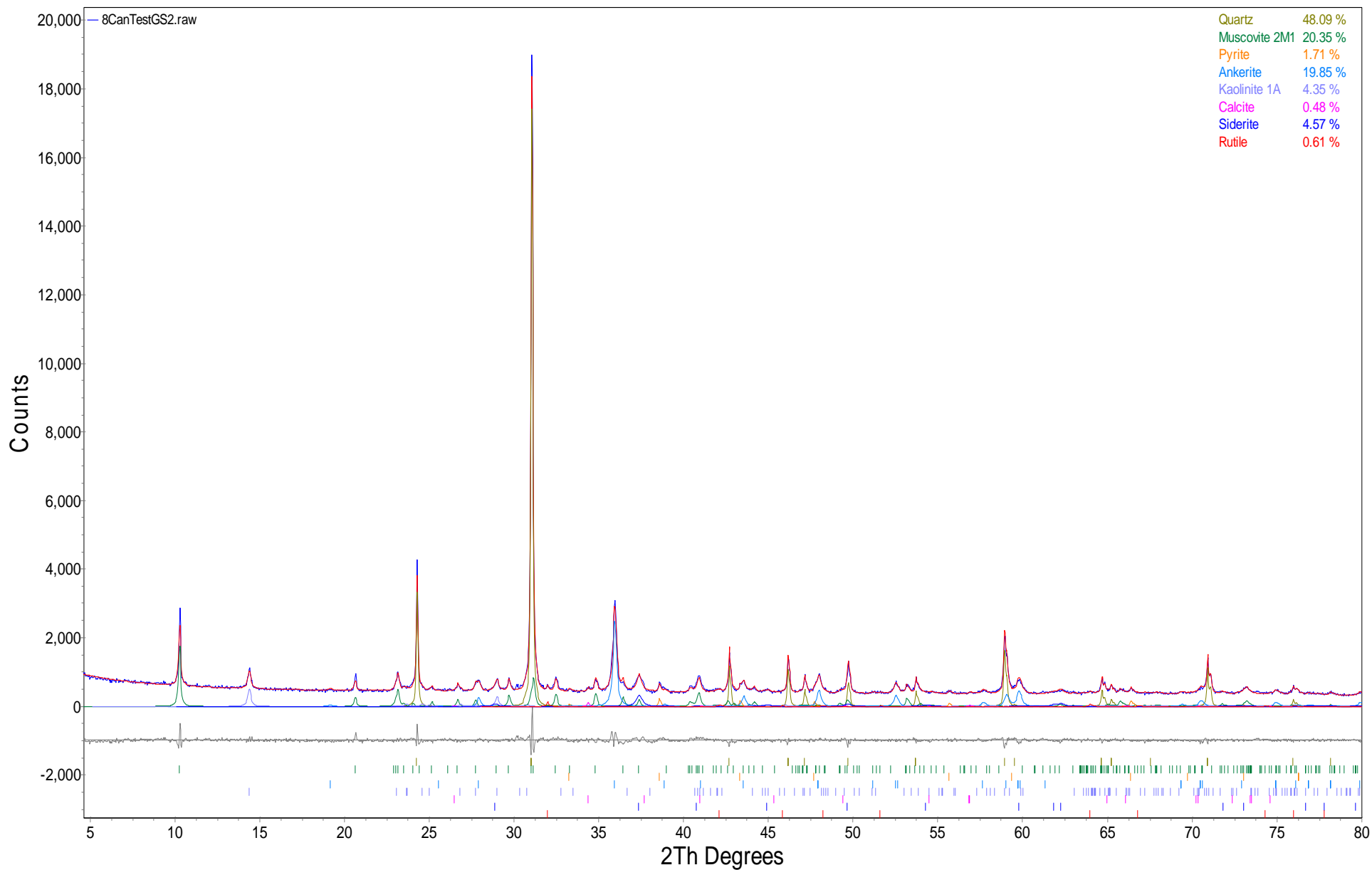


Figure 8. Rietveld refinement plot of sample **GS2** (blue line - observed intensity at each step; red line - calculated pattern; solid grey line below – difference between observed and calculated intensities; vertical bars, positions of all Bragg reflections). Coloured lines are individual diffraction patterns of all phases.

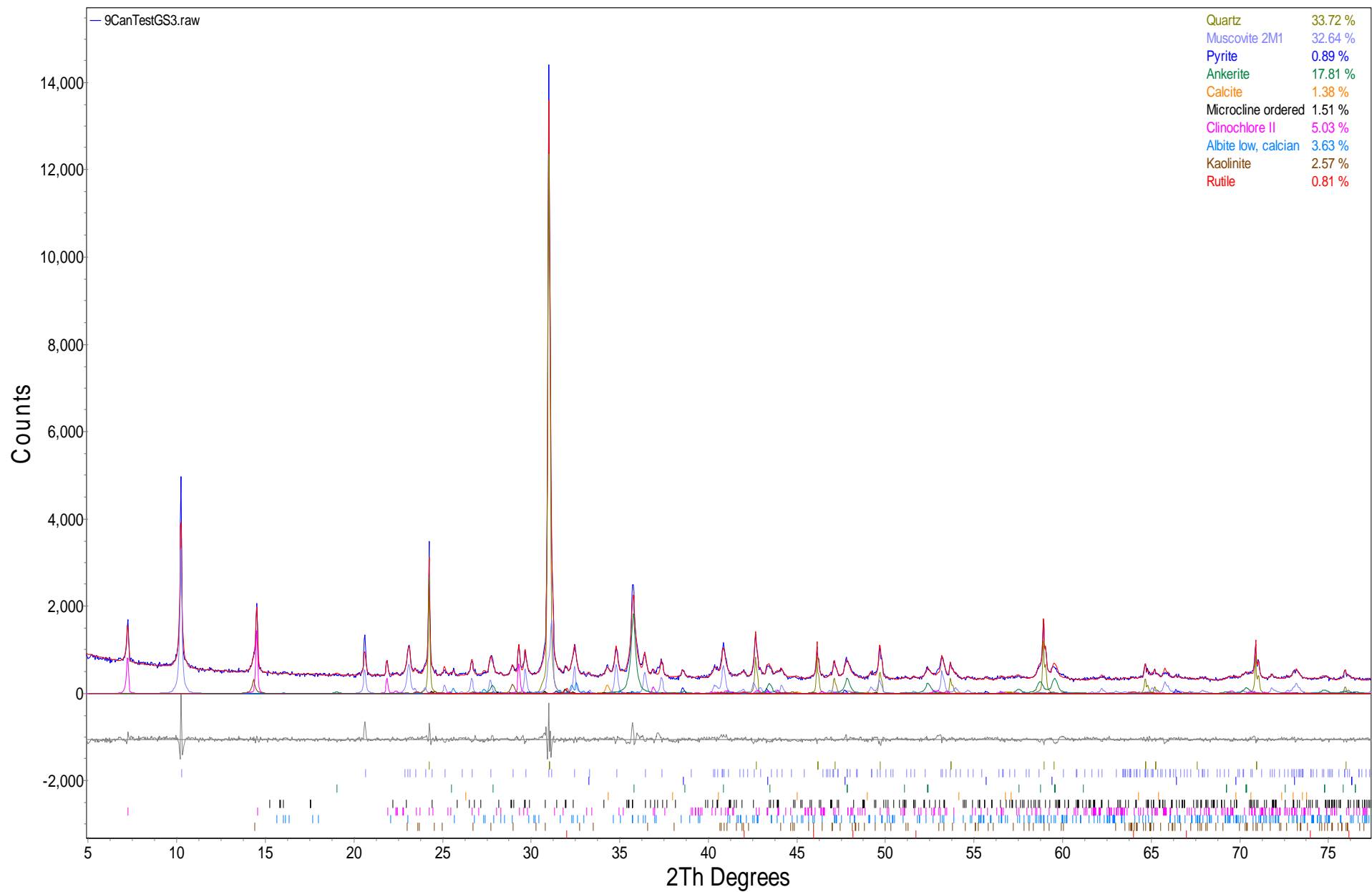


Figure 9. Rietveld refinement plot of sample **GS3** (blue line - observed intensity at each step; red line - calculated pattern; solid grey line below – difference between observed and calculated intensities; vertical bars, positions of all Bragg reflections). Coloured lines are individual diffraction patterns of all phases.



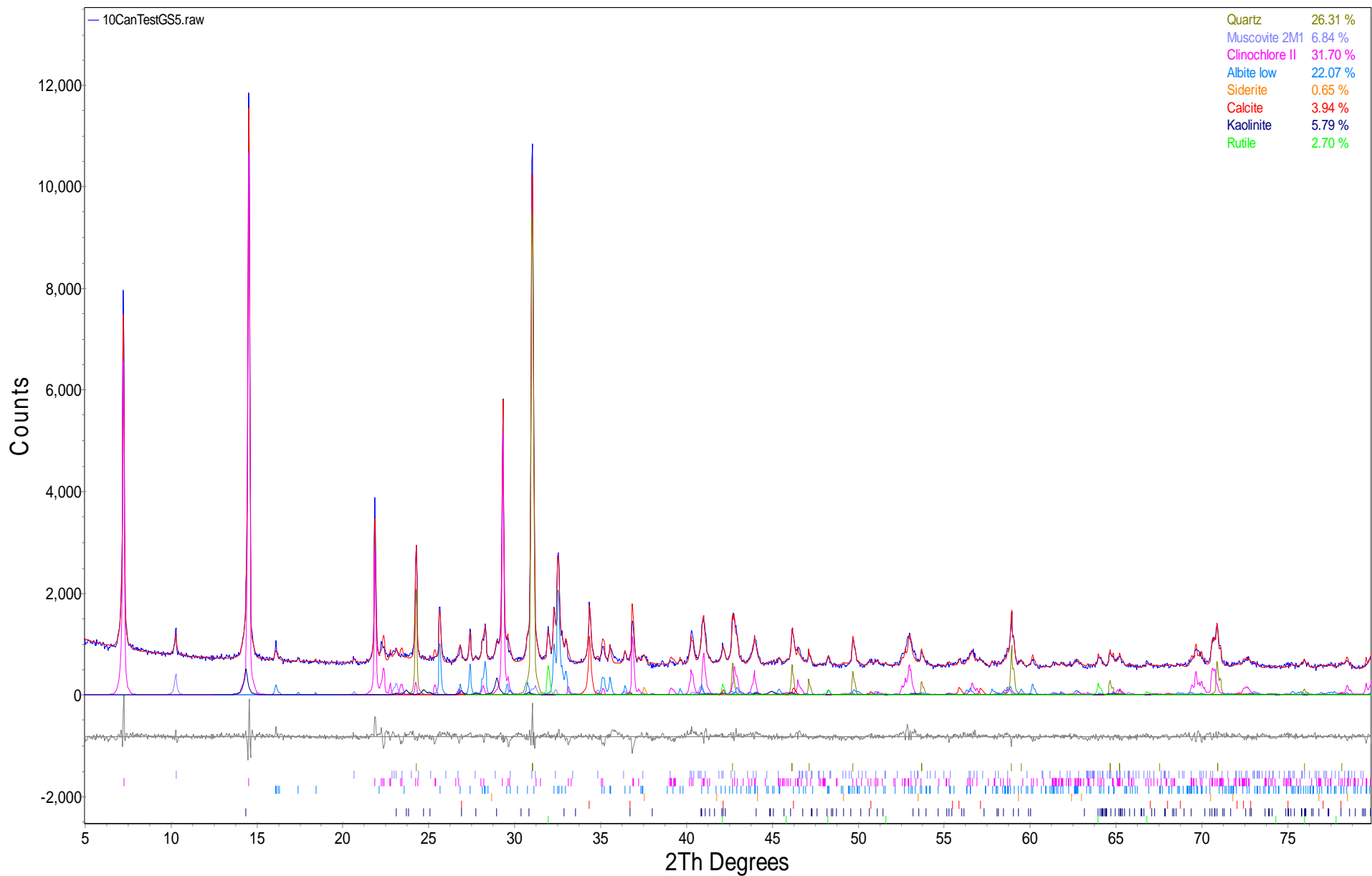


Figure 10. Rietveld refinement plot of sample **GS5** (blue line - observed intensity at each step; red line - calculated pattern; solid grey line below – difference between observed and calculated intensities; vertical bars, positions of all Bragg reflections). Coloured lines are individual diffraction patterns of all phases.

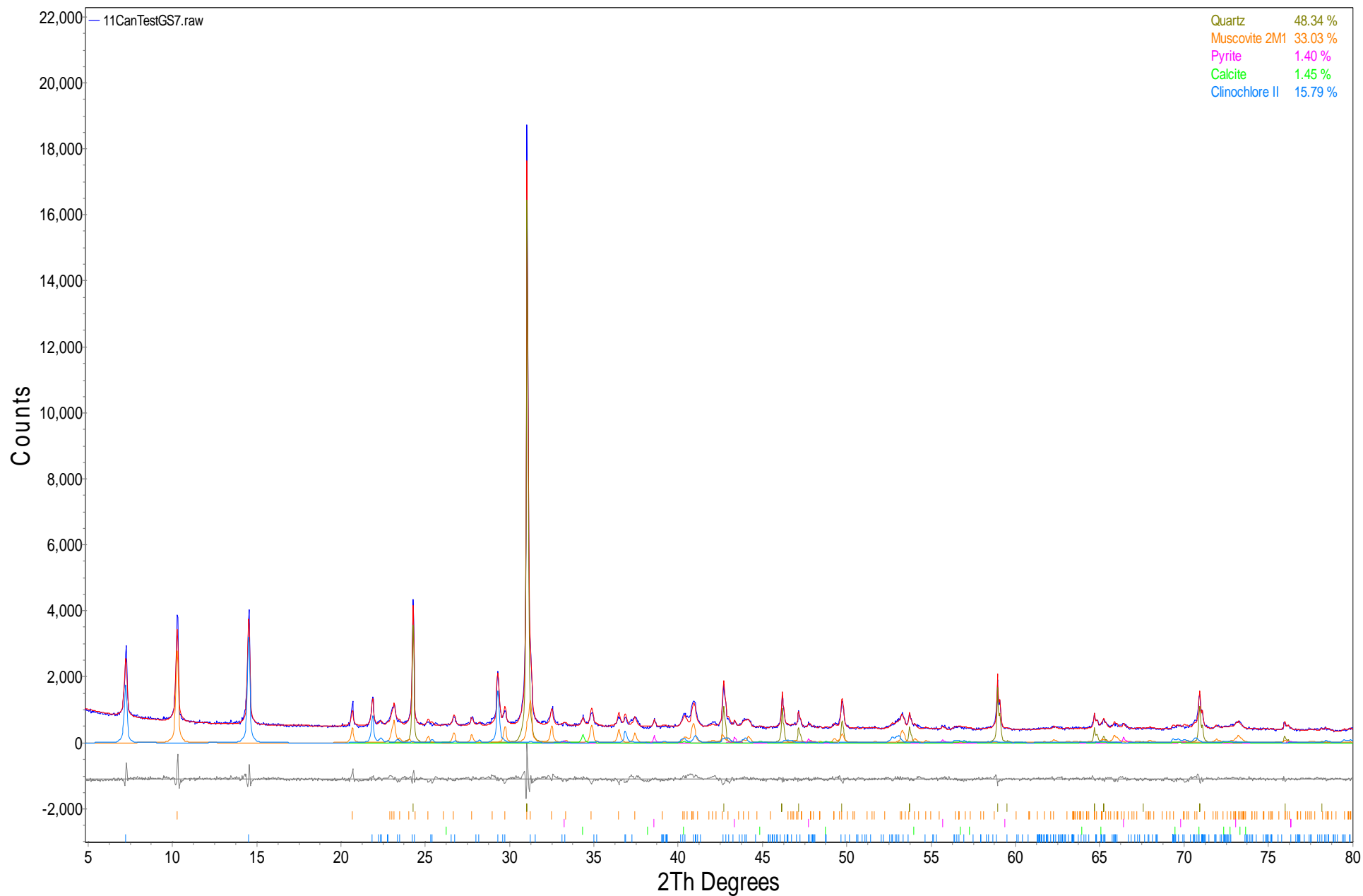


Figure 11. Rietveld refinement plot of sample **GS7** (blue line - observed intensity at each step; red line - calculated pattern; solid grey line below - difference between observed and calculated intensities; vertical bars, positions of all Bragg reflections). Coloured lines are individual diffraction patterns of all phases.

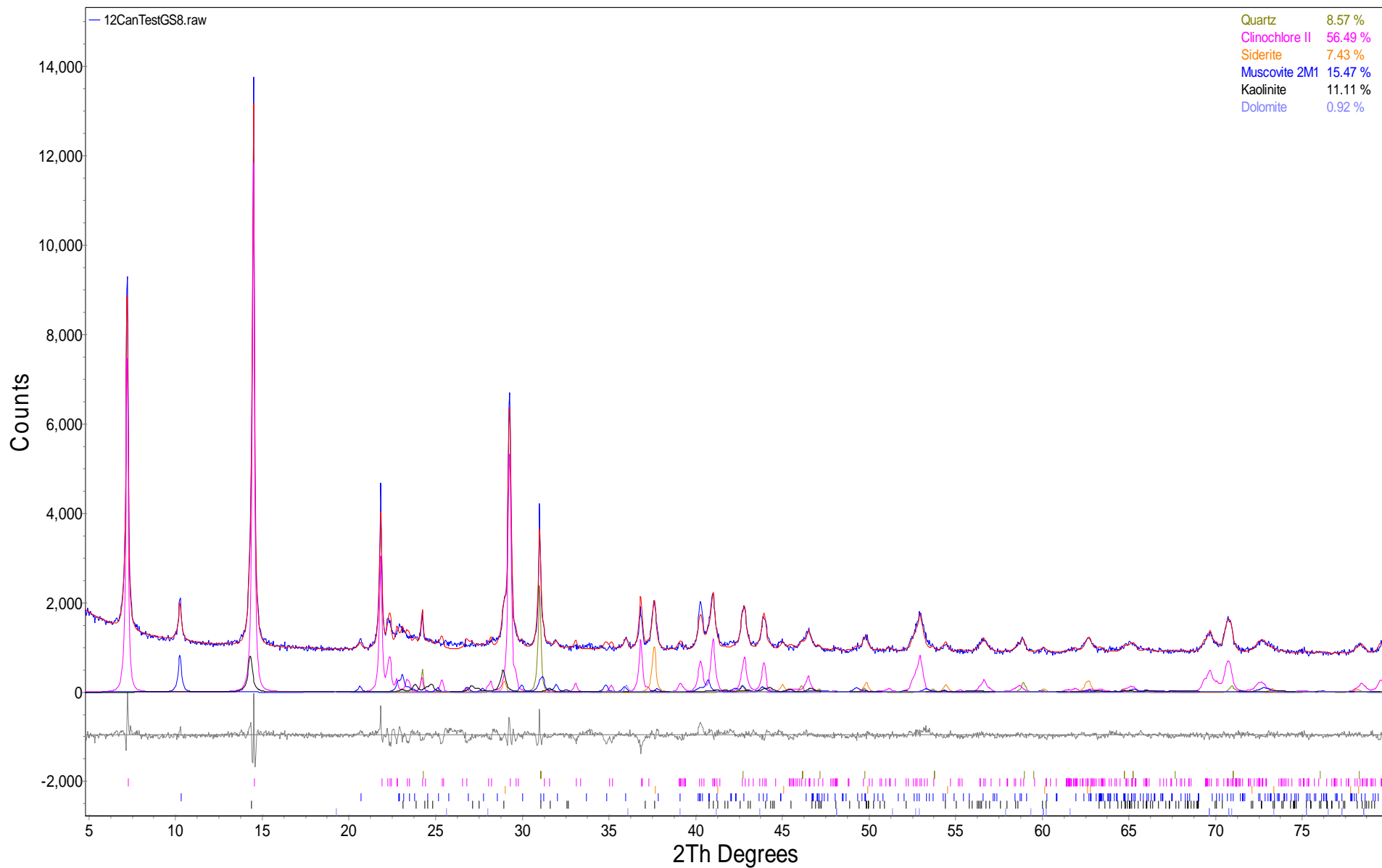


Figure 12. Rietveld refinement plot of sample **GS8** (blue line - observed intensity at each step; red line - calculated pattern; solid grey line below – difference between observed and calculated intensities; vertical bars, positions of all Bragg reflections). Coloured lines are individual diffraction patterns of all phases.

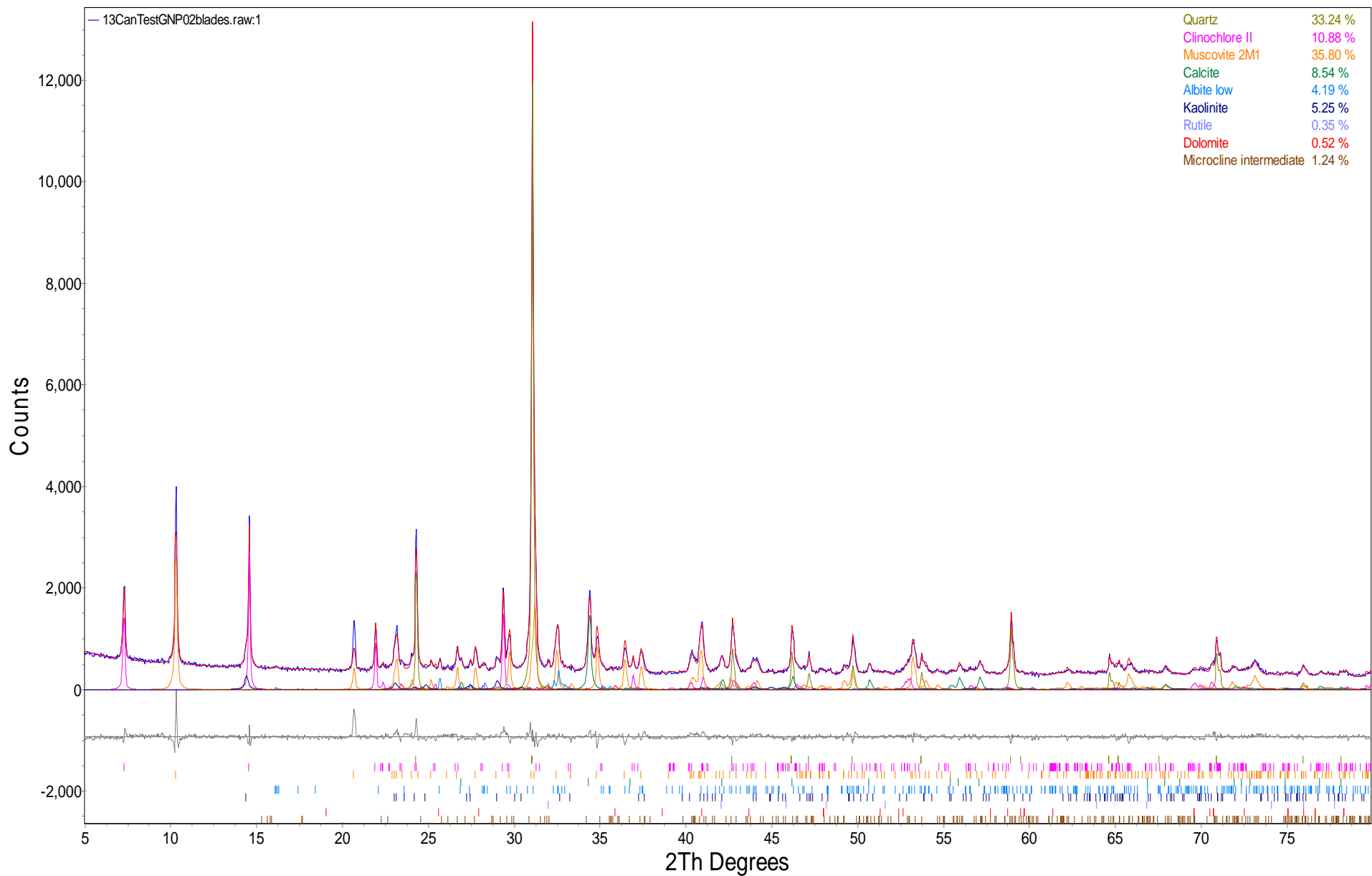


Figure 13. Rietveld refinement plot of sample **GNP02** (blue line - observed intensity at each step; red line - calculated pattern; solid grey line below — difference between observed and calculated intensities; vertical bars, positions of all Bragg reflections). Coloured lines are individual diffraction patterns of all phases.

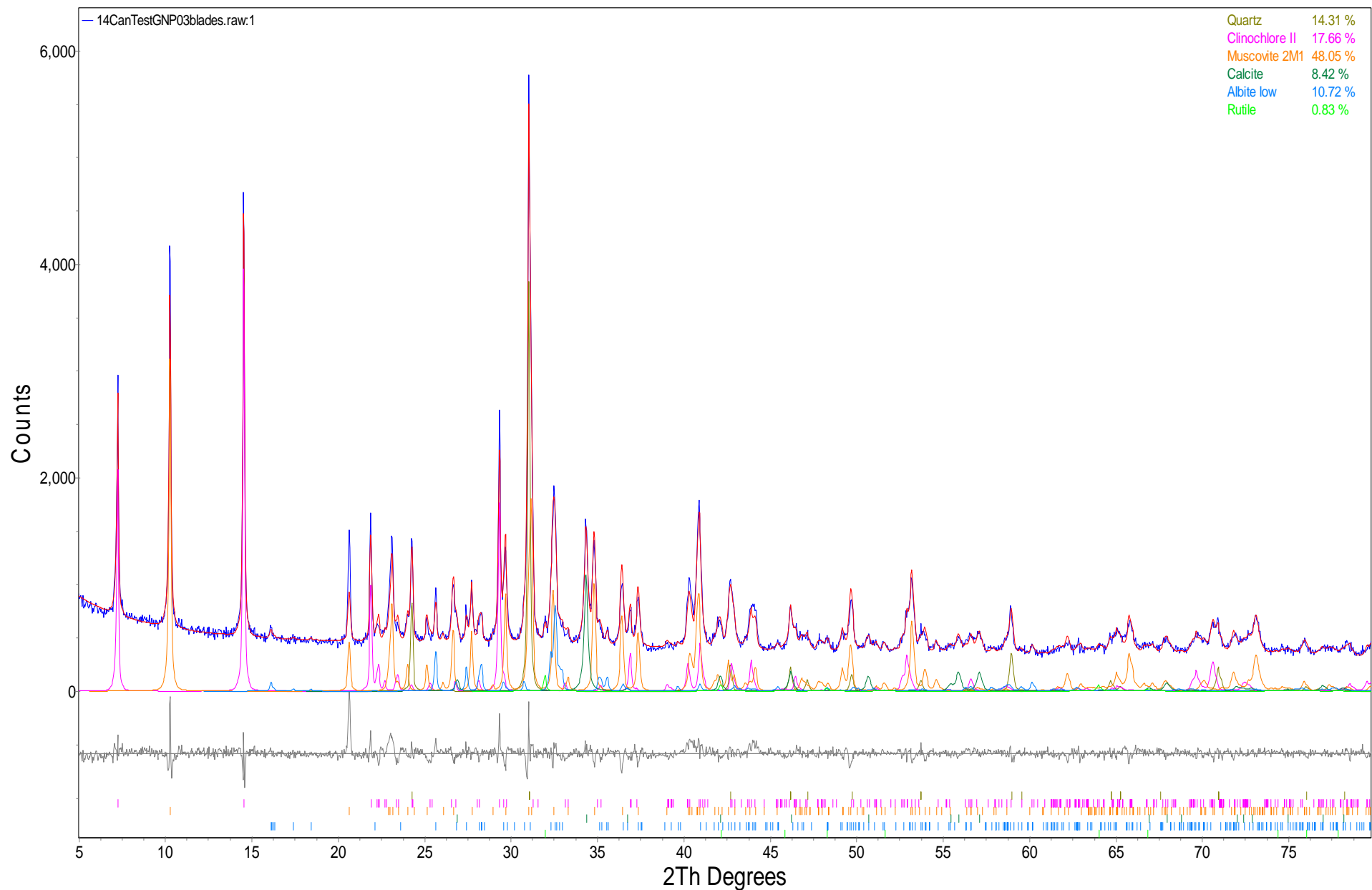


Figure 14. Rietveld refinement plot of sample **GNP03** (blue line - observed intensity at each step; red line - calculated pattern; solid grey line below – difference between observed and calculated intensities; vertical bars, positions of all Bragg reflections). Coloured lines are individual diffraction patterns of all phases.

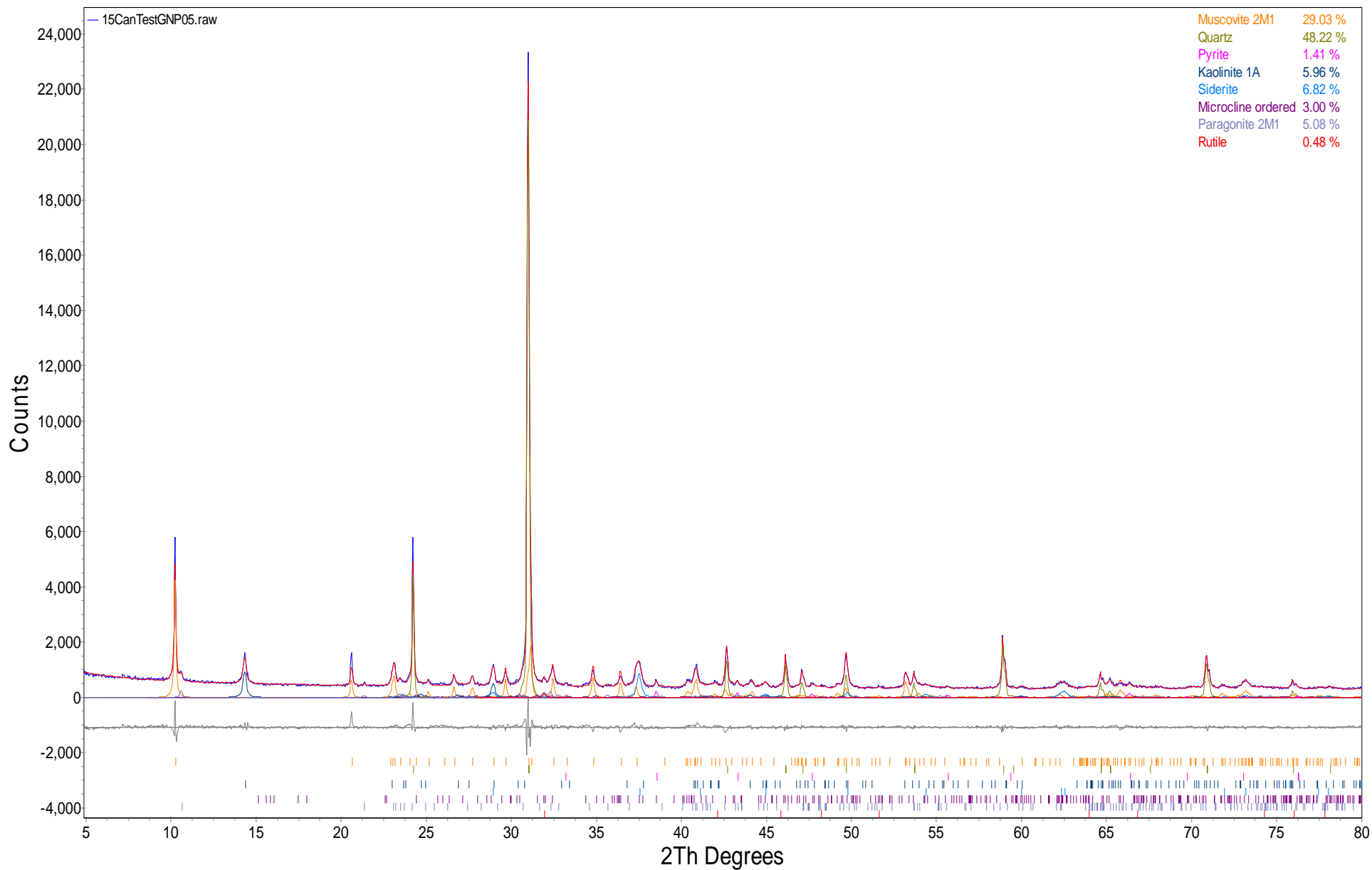


Figure 15. Rietveld refinement plot of sample **GNP05** (blue line - observed intensity at each step; red line - calculated pattern; solid grey line below – difference between observed and calculated intensities; vertical bars, positions of all Bragg reflections). Coloured lines are individual diffraction patterns of all phases.

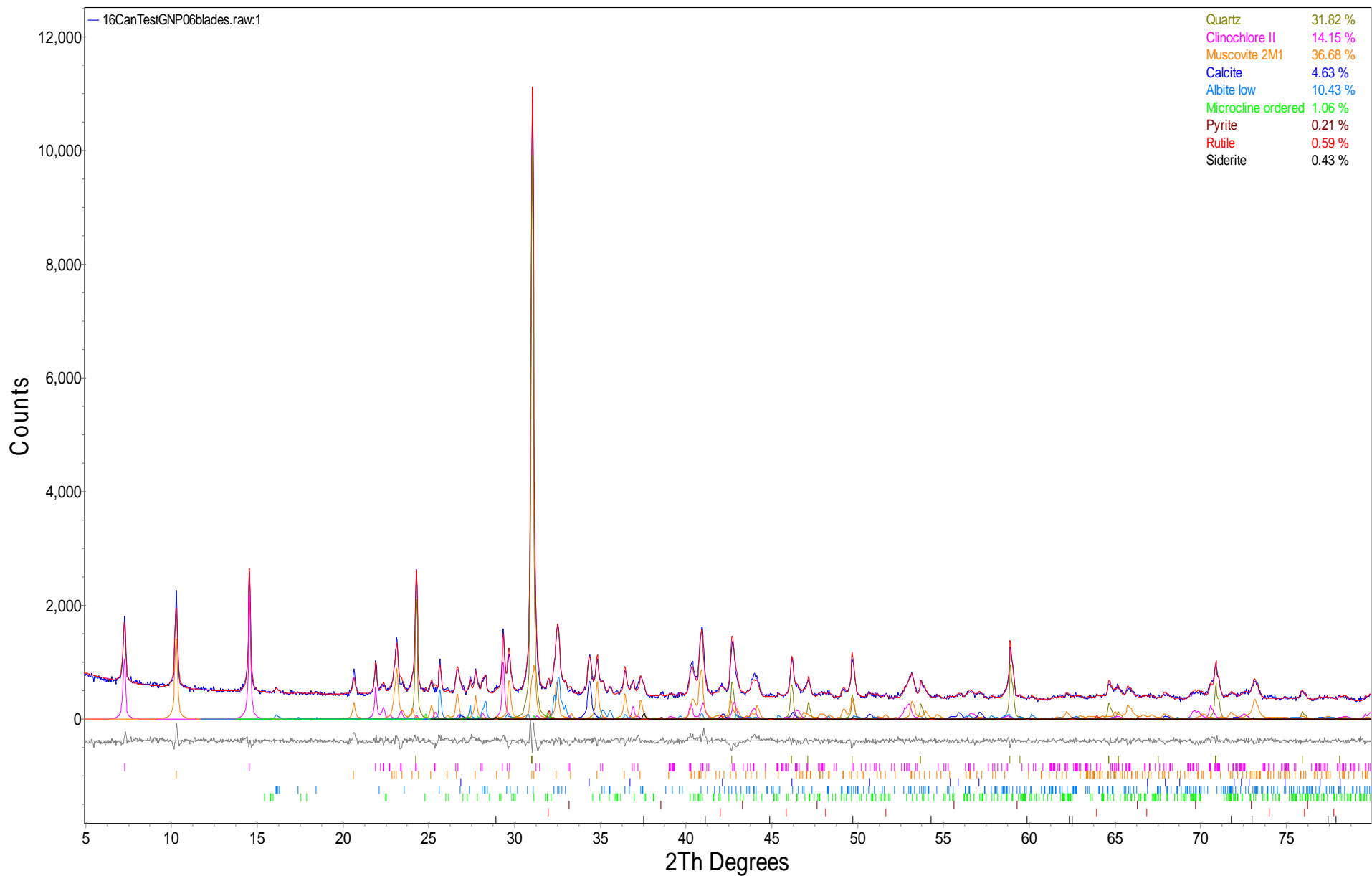


Figure 16. Rietveld refinement plot of sample **GNP06** (blue line - observed intensity at each step; red line - calculated pattern; solid grey line below – difference between observed and calculated intensities; vertical bars, positions of all Bragg reflections). Coloured lines are individual diffraction patterns of all phases.



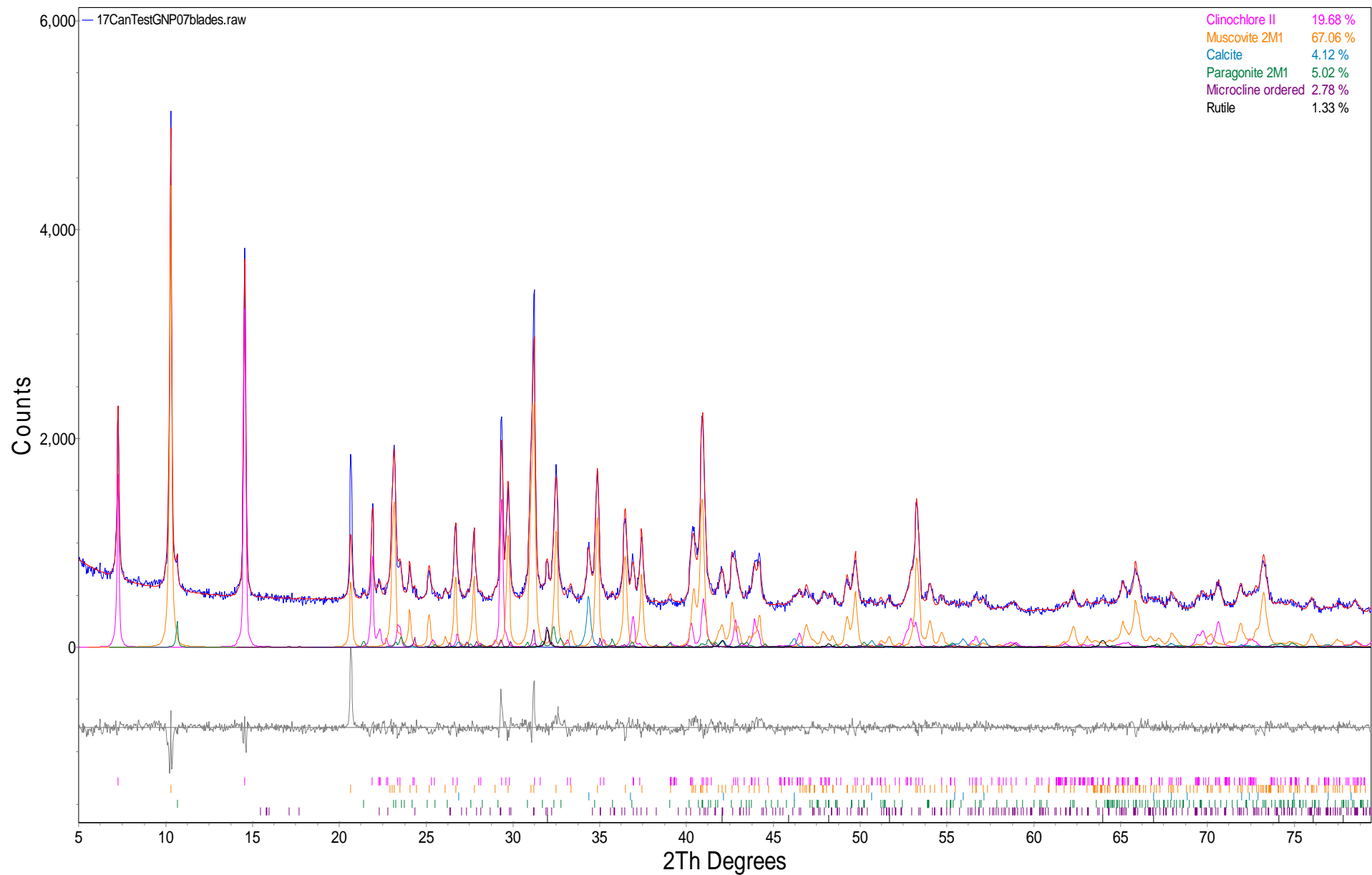


Figure 17. Rietveld refinement plot of sample **GNP07** (blue line - observed intensity at each step; red line - calculated pattern; solid grey line below — difference between observed and calculated intensities; vertical bars, positions of all Bragg reflections). Coloured lines are individual diffraction patterns of all phases.

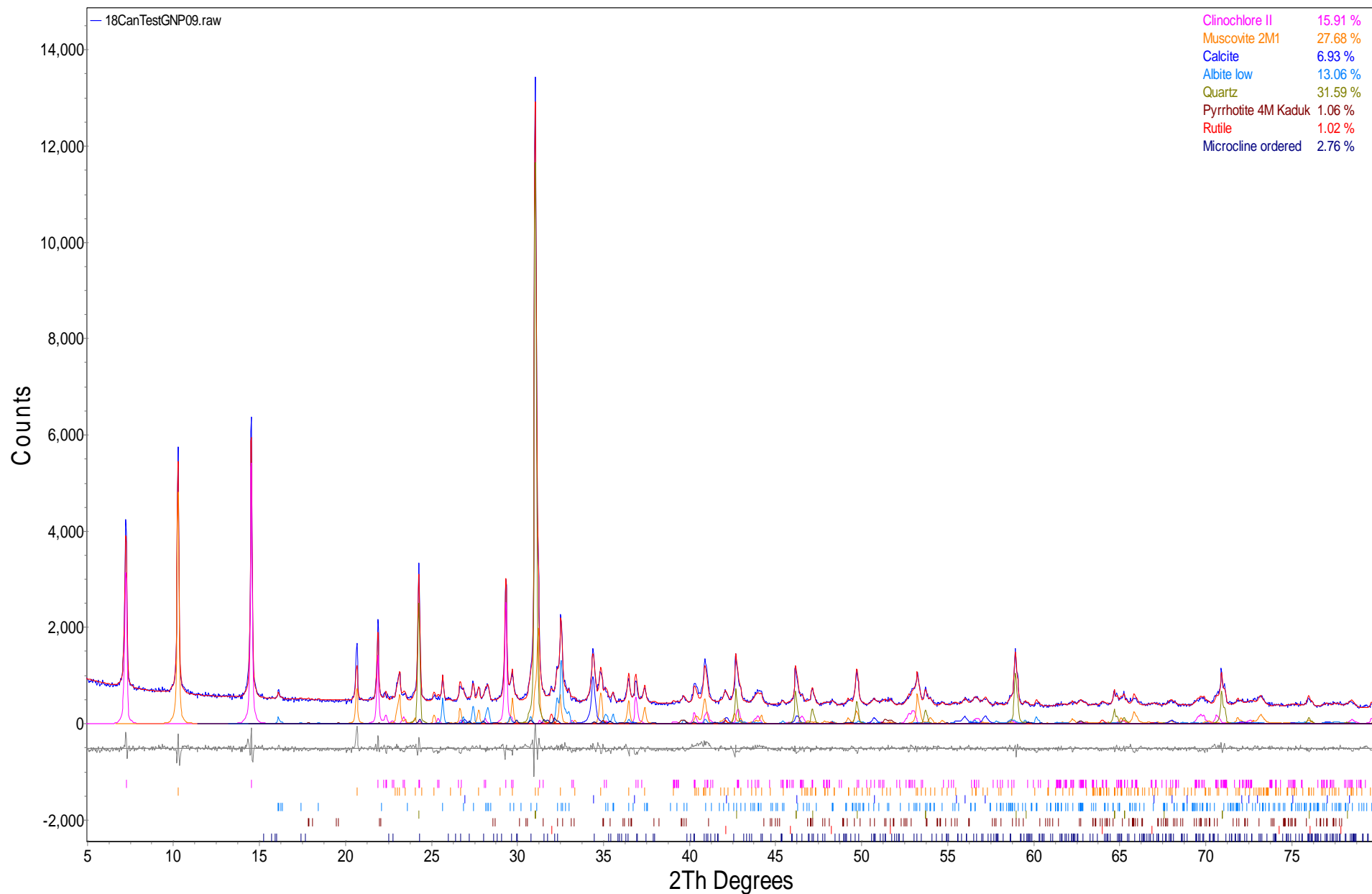


Figure 18. Rietveld refinement plot of sample **GNP09** (blue line - observed intensity at each step; red line - calculated pattern; solid grey line below – difference between observed and calculated intensities; vertical bars, positions of all Bragg reflections). Coloured lines are individual diffraction patterns of all phases.

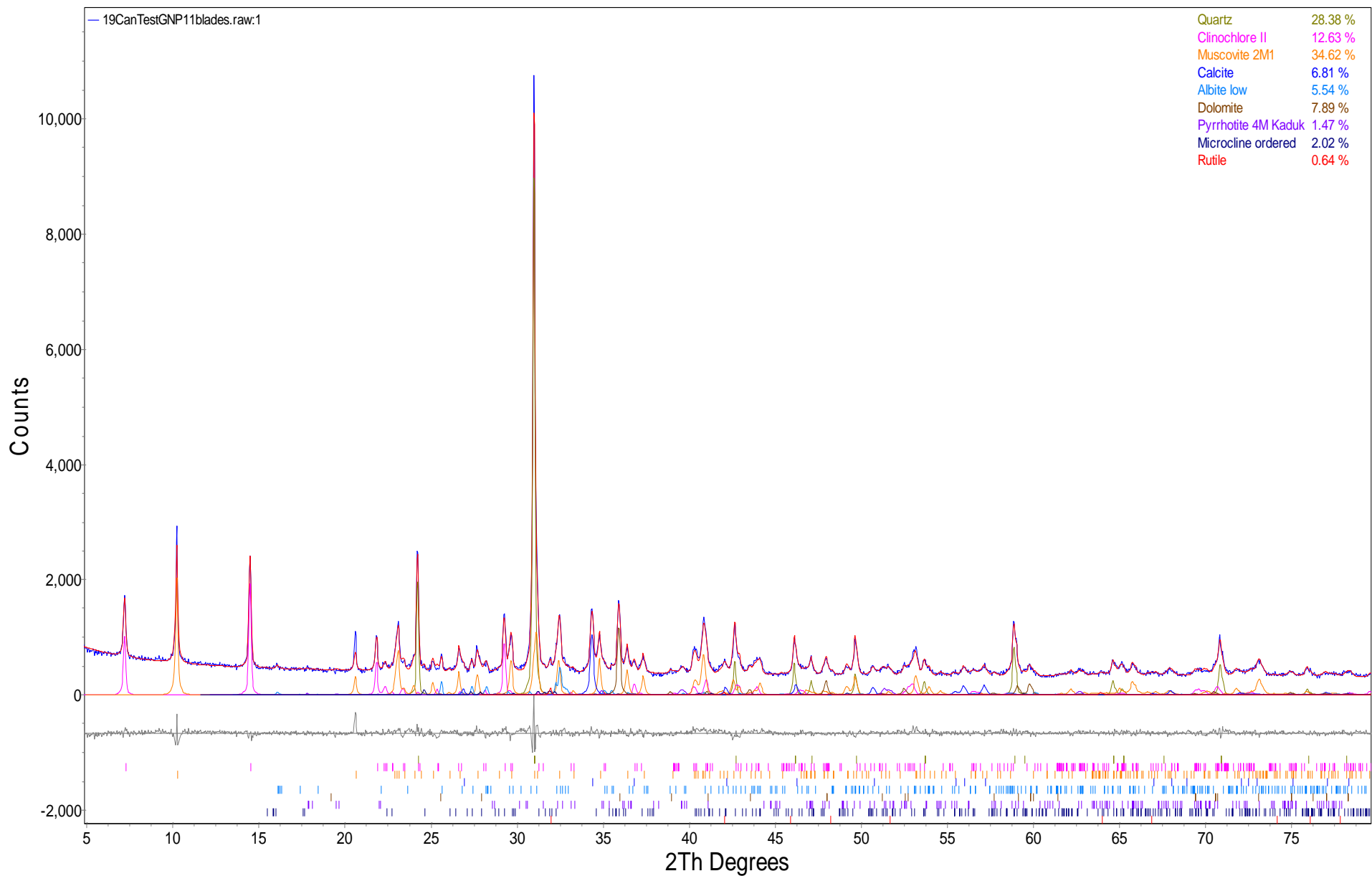


Figure 19. Rietveld refinement plot of sample **GNP11** (blue line - observed intensity at each step; red line - calculated pattern; solid grey line below – difference between observed and calculated intensities; vertical bars, positions of all Bragg reflections). Coloured lines are individual diffraction patterns of all phases.

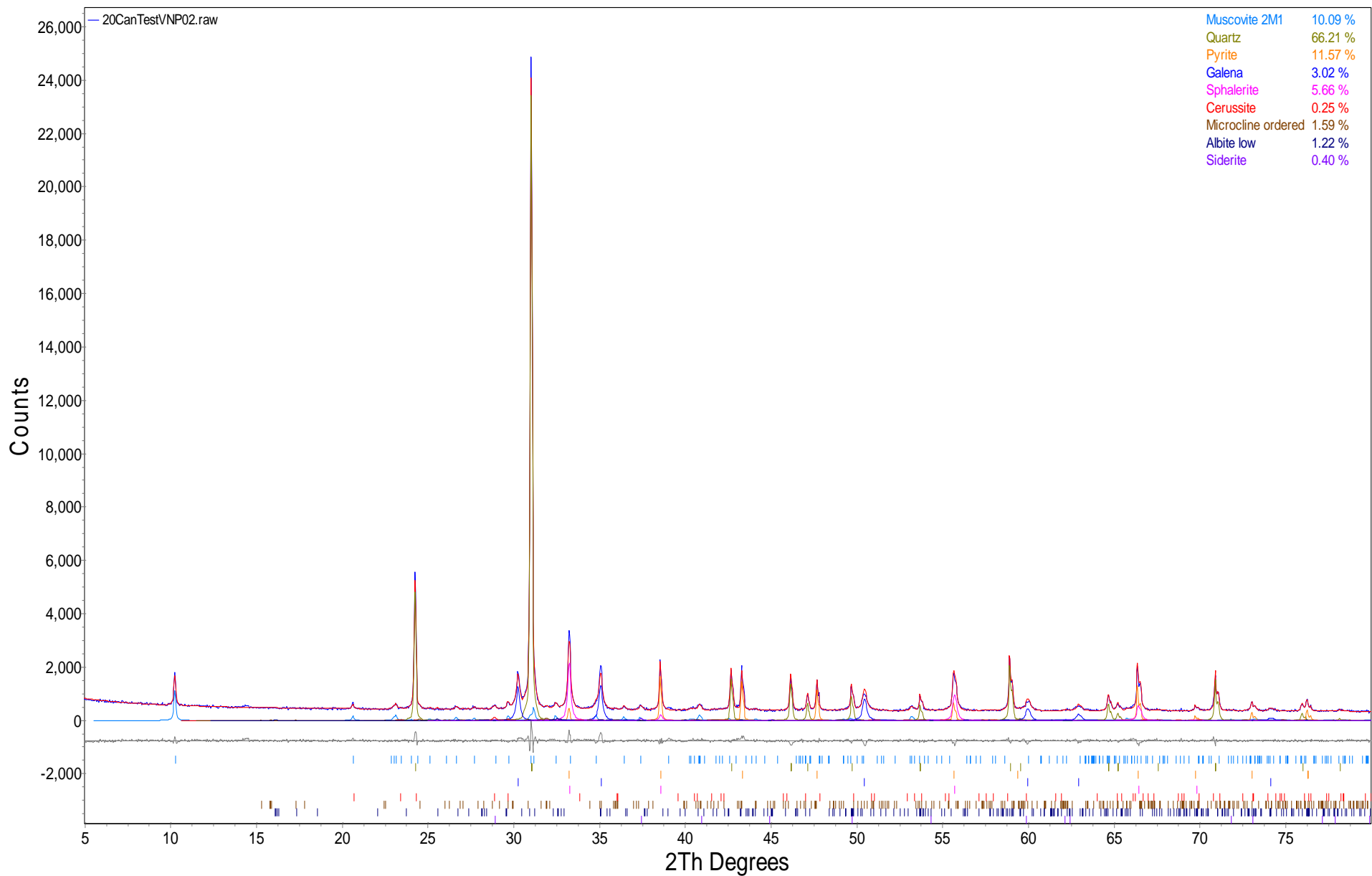


Figure 20. Rietveld refinement plot of sample **VNP02** (blue line - observed intensity at each step; red line - calculated pattern; solid grey line below – difference between observed and calculated intensities; vertical bars, positions of all Bragg reflections). Coloured lines are individual diffraction patterns of all phases.

**QUANTITATIVE PHASE ANALYSIS OF 2 POWDER SAMPLES USING THE  
RIETVELD METHOD AND X-RAY POWDER DIFFRACTION DATA.**

**Project: SRK – Anvil Range  
Cantest Project No: 2-21-900  
Internal Requisition No: R 72288**

---

**Ivy Rajan  
CANTEST Ltd.  
4606 Canada Way  
Burnaby, BC V5G 1K5**

---

---

**Mati Raudsepp, Ph.D.  
Elisabetta Pani, Ph.D.  
Dept. of Earth & Ocean Sciences  
6339 Stores Road  
The University of British Columbia  
Vancouver, BC V6T 1Z4**

**October 29, 2008**

## EXPERIMENTAL METHODS

The two samples **FNP 17** and **FNP 18** of Project SRK – Anvil Range were reduced to the optimum grain-size range for quantitative X-ray analysis ( $<10\ \mu\text{m}$ ) by grinding under ethanol in a vibratory McCrone Micronising Mill for 7 minutes. Fine grain-size is an important factor in reducing micro-absorption contrast between phases.

Step-scan X-ray powder-diffraction data were collected over a range  $3\text{--}80^\circ 2\theta$  with  $\text{CoK}\alpha$  radiation on a standard Siemens (Bruker) D5000 Bragg-Brentano diffractometer equipped with an Fe monochromator foil,  $0.6\ \text{mm}$  ( $0.3^\circ$ ) divergence slit, incident- and diffracted-beam Soller slits and a Vantec-1 strip detector. The long fine-focus Co X-ray tube was operated at 35 kV and 40 mA, using a take-off angle of  $6^\circ$ .

## RESULTS

The X-ray diffractograms were analyzed using the International Centre for Diffraction Database PDF-4 using Search-Match software by Bruker. X-ray powder-diffraction data of the samples were refined with Rietveld program Topas 3 (Bruker AXS). The results of quantitative phase analysis by Rietveld refinements are given in Table 1. These amounts represent the relative amounts of crystalline phases normalized to 100%. The Rietveld refinement plots are shown in Figures 1-2.

Table 1. Results of quantitative phase analysis (wt.%) – CanTest Project SRK – Anvil Range

Mineral	Ideal Formula	FNP 17	FNP 18
Quartz	SiO <sub>2</sub>	35.9	33.7
Clinochlore	(Mg,Fe <sup>2+</sup> ) <sub>5</sub> Al(Si <sub>3</sub> Al)O <sub>10</sub> (OH) <sub>8</sub>	3.4	4.6
Muscovite	KAl <sub>2</sub> AlSi <sub>3</sub> O <sub>10</sub> (OH) <sub>2</sub>	4.0	
Biotite	K(Mg,Fe <sup>2+</sup> ) <sub>3</sub> AlSi <sub>3</sub> O <sub>10</sub> (OH) <sub>2</sub>	9.4	8.6
K-feldspar	KAlSi <sub>3</sub> O <sub>8</sub>	7.3	11.5
Plagioclase	NaAlSi <sub>3</sub> O <sub>8</sub> – CaAl <sub>2</sub> Si <sub>2</sub> O <sub>8</sub>	39.5	40.4
Calcite	CaCO <sub>3</sub>	0.4 ?	1.1
Total		100.0	100.0



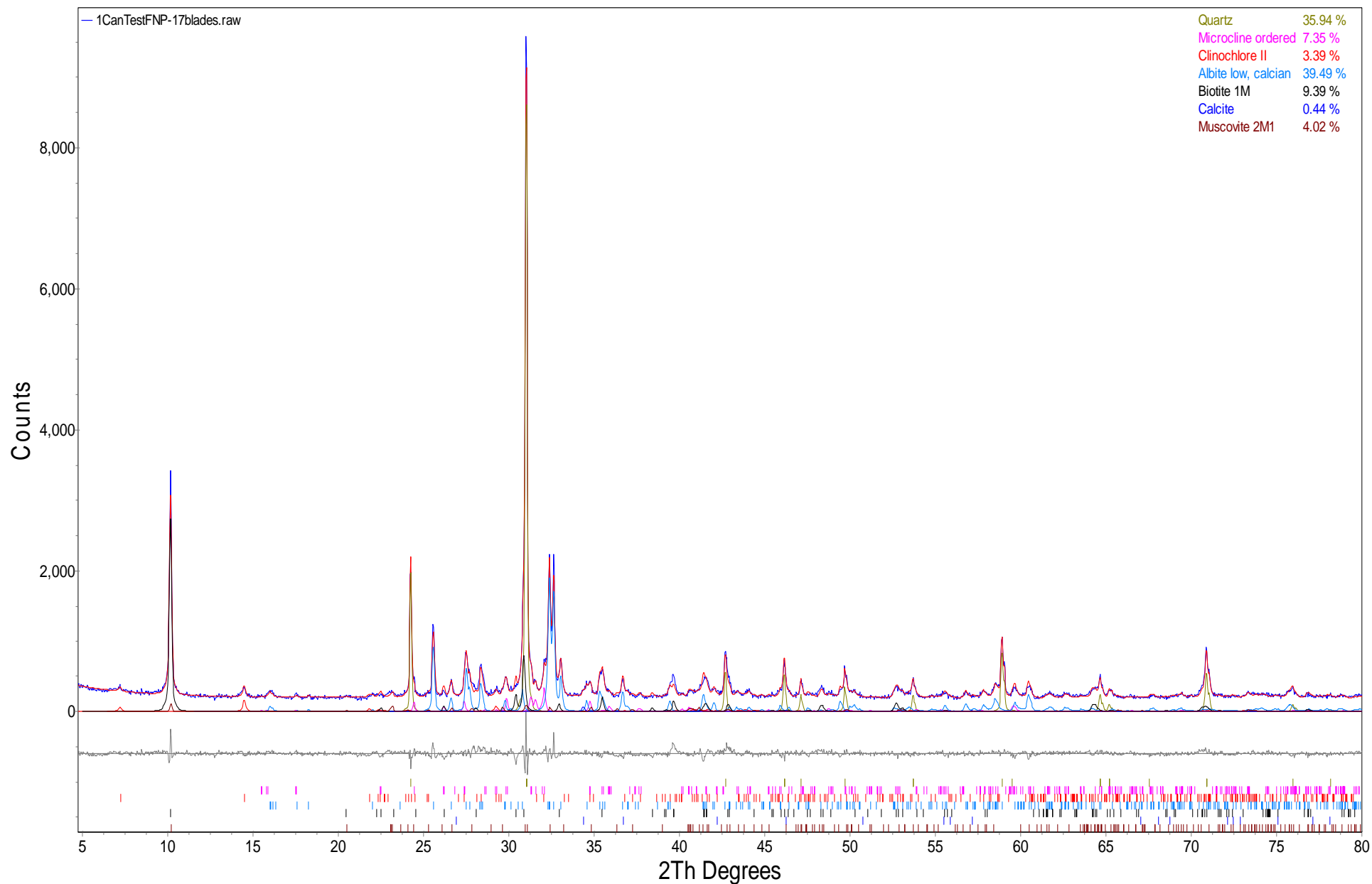


Figure 1. Rietveld refinement plot of sample **FNP-17** (blue line - observed intensity at each step; red line - calculated pattern; solid grey line below – difference between observed and calculated intensities; vertical bars, positions of all Bragg reflections). Coloured lines are individual diffraction patterns of all phases.

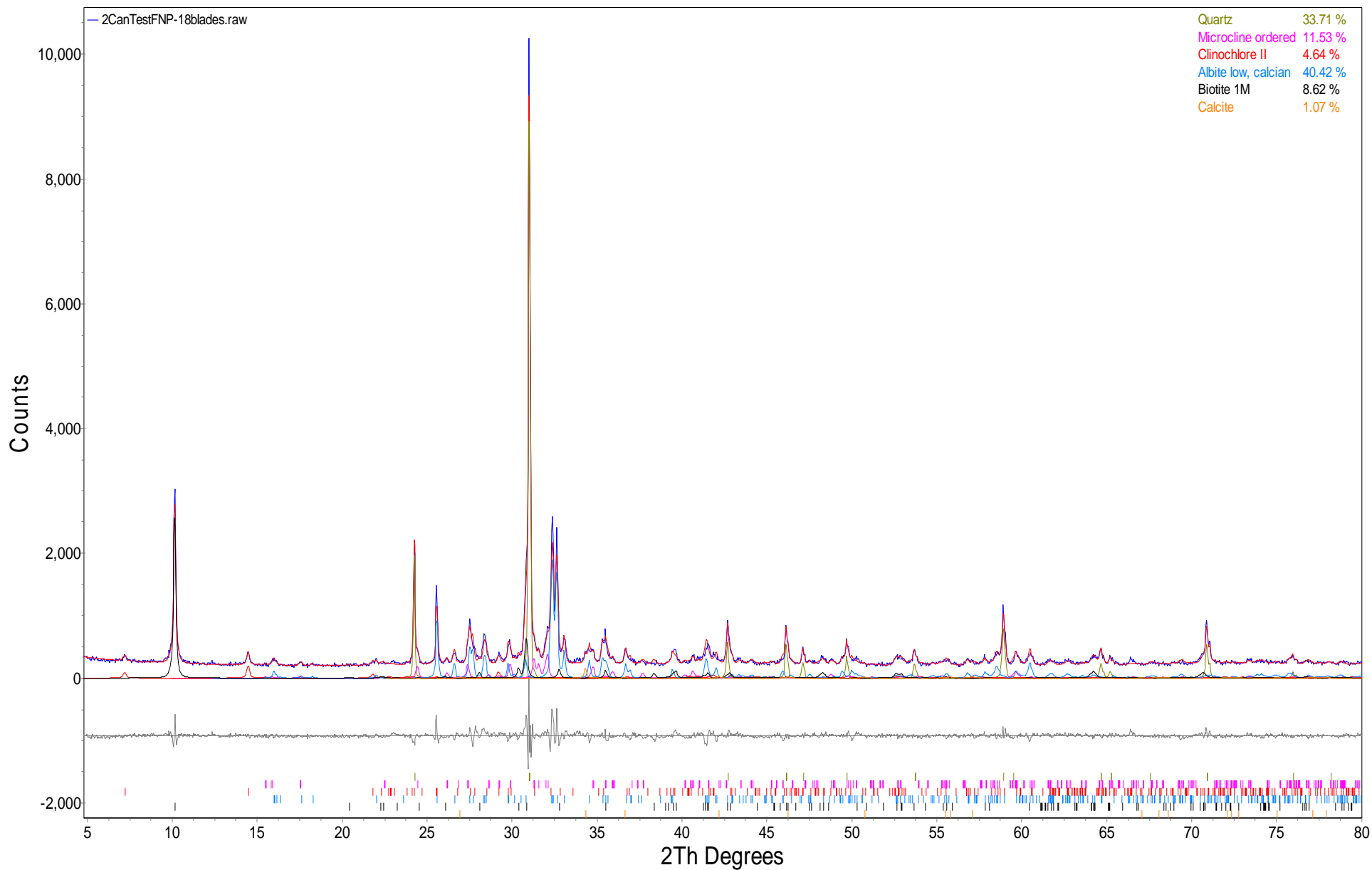


Figure 2. Rietveld refinement plot of sample **FNP-18** (blue line - observed intensity at each step; red line - calculated pattern; solid grey line below – difference between observed and calculated intensities; vertical bars, positions of all Bragg reflections). Coloured lines are individual diffraction patterns of all phases.

## **Appendix E**

### **Electron Microprobe Analyses**

## **REPORT NO. MSC08/066R**

---

**CHARACTERIZATION OF CARBONATE COMPOSITION  
IN SEVENTEEN SAMPLES FROM ANVIL RANGE'S FARO PROJECT  
BY ELECTRON MICROPROBE ANALYSIS**

---

Report prepared for

**CanTest Ltd.**  
4606 Canada Way  
Burnaby, BC  
V5G 1K5  
Canada

**SRK Consulting**  
Oceanic Plaza - 22nd Floor  
1066 West Hastings Street  
Vancouver, BC  
V6E 3X2 Canada

By

**Mineral Services Canada Inc.**  
205-930 Harbourside Drive  
North Vancouver, B.C.  
V7P 3S7  
Canada

December 2, 2008

## TABLE OF CONTENTS

<b>CONDITIONS AND DISCLAIMER.....</b>	<b>III</b>
<b>1. INTRODUCTION.....</b>	<b>1</b>
<b>2. METHODS.....</b>	<b>1</b>
<b>3. SUMMARY OF RESULTS.....</b>	<b>1</b>
APPENDIX: RESULTS OF MICROPROBE ANALYSIS	

## CONDITIONS AND DISCLAIMER

This report is issued subject to the following conditions:

This report has been prepared on the basis of information as described in section 1 below. Other than as specifically noted in this report, Mineral Services Canada (MSC) has not conducted any work to verify the source, accuracy or completeness of information provided, and is not responsible for any shortcomings in these regards.

Discussions, conclusions and / or summaries are presented to assist the reader in highlighting key points; however they cannot be interpreted in isolation and must be considered with reference to and in the context of the body of the report.

Any reports, maps, graphs, logs or other information of a geological nature or otherwise, generated by MSC and contained in this report or submitted separately (“the information”), may be used for general information purposes only by the Client to whom the information is addressed. For other uses of the information, such as public disclosure, press releases, regulatory requirements, share exchange, financing and so forth, permission must first be obtained in writing from MSC.

Any quotations, excerpts and references from the report must be made in such a manner that their meaning and intent are not materially changed from the meaning and intent as contained in the report.

MSC will not be held liable for loss or damages resulting from work undertaken or reported in terms of this assignment, or decisions taken on the basis of such work and / or reporting.

---

**CHARACTERIZATION OF CARBONATE COMPOSITION  
IN SEVENTEEN SAMPLES FROM ANVIL RANGE'S FARO PROJECT  
BY ELECTRON MICROPROBE ANALYSIS**

---

## **1. INTRODUCTION**

The results of microprobe analysis of seventeen samples from the zinc-lead Faro Mine (Yukon) are presented in this report. The samples were received October 22, 2008 from Ivy Rajan of CanTest Ltd.

The purpose of the study was to characterize the composition of carbonates using electron microprobe analysis of 15 to 20 target carbonate grains per sample. The polished thin sections prepared previously for petrographic analysis of the samples were made available for this study.

## **2. METHODS**

### **1) Target grain definition**

Polished thin sections of the samples were examined by the author in the office of Mineral Services Canada Inc. using a Nikon eclipse E400 microscope equipped with transmitted and reflected light. Representative carbonate grains were selected for analysis and maps to facilitate recognition of these target grains under the microprobe were also prepared.

### **2) Microprobe analyses**

Electron microprobe analysis was carried out by Mati Raudsepp at the University of British Columbia, on a fully-automated Cameca SX-50 Electron Microprobe with four vertical wavelength-dispersion X-ray spectrometers and a fully-integrated SAMx energy-dispersion X-ray spectrometer. One of the spectrometers has two layered dispersion elements (W/Si, Ni/C), which allow for quantitative analysis of the light elements (F, O, N, C, B). The detection limit for Pb is about 0.3 wt%.

## **3. SUMMARY OF RESULTS**

The results of microprobe analysis are presented in the Appendix and summarized in Table 1 below. Measurements with total oxides between 98.00 and 102.00 wt% are considered reliable.



**Table 1:** Summary of electron microprobe results for carbonate grains analysed in this study. Twenty carbonate grains were analysed in each sample except in sample VNP-02 in which only nine measurements were performed due to the rarity and fineness of the carbonates present.

	% of reliable measurements	Calcite	Dolomite - ankerite	Siderite	Cerussite
<b>FNP 01</b>	Not analysed				
<b>FNP 02</b>	65	Only carbonate recognized; very low MgO, MnO and FeO concentrations ( $\leq 0.21$ wt% FeO)	-	-	-
<b>FNP 04</b>	95	Only carbonate recognized; locally Fe-rich ( $\leq 5.11$ wt% FeO)	-	-	-
<b>FNP 06</b>	25	Only carbonate recognized; reliable measurements have very low MgO, MnO and FeO concentrations ( $< 0.44$ wt% FeO)	-	-	-
<b>FNP 08</b>	Not analysed				
<b>FNP 13</b>	75	-	Three grains recognized; MgO : FeO ratios close to 1	Main carbonate; present as magnesian siderite (7.5 to 16.5 wt% MgO)	-
<b>FNP 14</b>	Not analysed				
<b>GS 2</b>	100	Reported from Rietveld XRD, but not encountered during microprobe analysis	Dominant carbonate; contains variable amounts of MgO (9 - 15 wt%) and FeO (8 - 19 wt%); MnO content is well below 1 wt%	Magnesian siderite with MgO content between 10 and 14 wt%	-
<b>GS 3</b>	100	Three grains recognized; locally Fe-rich ( $\leq 2.5$ wt% FeO)	Dominant carbonate; MgO : FeO ratios roughly close to 1	Characterized by lower MgO contents than siderite in most other samples ( $< 5$ wt% MgO)	-

**Table 1 (continued):** Summary of electron microprobe results for carbonate grains analysed in this study. Twenty carbonate grains were analysed in each sample except in VNP-02 in which only nine measurements were performed due to the rarity and fineness of the carbonates present.

<b>GS 5</b>	45	Dominant carbonate; reliable measurements have generally low MgO, MnO and FeO concentrations (<1 wt%)	One grain, composition close to ankerite end-member	One grain of reliable composition with low CaO and MgO contents	-
<b>GS 7</b>	30	Only carbonate recognized; characterized by variable FeO concentration (0.1 to 2.4 wt%)	-	-	-
<b>GS 8</b>	45	-	Three reliable analyses; high MgO (15.5 to 17 wt%) and low FeO (6.5 to 9 wt%) concentrations	Magnesian siderite (13 to 22 wt% MgO) with typically minor CaO concentration (<1.5 wt%)	-
<b>GNP 02</b>	95	Dominant carbonate; FeO concentration up to 1.3 wt%	Two grains with variable MgO and FeO contents; MnO concentration well below 1 wt%	One magnesian siderite (reliable analysis) with 6.8 wt% MgO	-
<b>GNP 03</b>	40	Only carbonate recognized; contains variable FeO content (1.2 to 1.4 wt%)	-	-	-
<b>GNP 05</b>	100	-	-	Only carbonate recognized; contains variable MgO (2 to 17 wt%) and CaO (1 to 4.5 wt%) contents	-
<b>GNP 06</b>	100	Near end-member composition with MgO, MnO and FeO concentrations below 1 wt%)	-	Characterized by lower MgO (4 to 11 wt%) and higher CaO (6 to 8 wt%) contents than most samples	-
<b>GNP 07</b>	100	Only carbonate recognized; characterized by low MgO and FeO contents (typically below 0.75 wt%)	-	-	-

**Table 1 (continued):** Summary of electron microprobe results for carbonate grains analysed in this study. Twenty carbonate grains were analysed in each sample except in sample VNP-02 in which only nine measurements were performed due to the rarity and fineness of the carbonates present.

<b>GNP 09</b>	100	Only carbonate recognized; characterized by variable FeO content (0.2 to 1.9 wt%)	-	-	-
<b>GNP 11</b>	65	Dominant carbonate; has low FeO and MgO concentrations	Three grains, each with similar FeO and MgO contents	-	-
<b>VNP 02</b>	89	-	One grain with high concentration of FeO and MgO	Dominant carbonate with variable MgO, CaO, MnO and PbO contents (up to 4.43 wt% PbO)	Reported from Rietveld XRD but not encountered during microprobe analysis

The results indicate the following:

- The proportion of reliable analyses obtained for each sample (total 20 analyses per sample in all but one of the samples) varies from 25 to 100%. Carbonates in samples with fewer reliable measurements are typically finer-grained and more internally strained.
- The samples contain a wide range of carbonates including calcite, siderite and members of the dolomite-ankerite solid-solution series.
- The carbonates identified by microprobe analyses generally correlate with those identified by Rietveld XRD, although the number of carbonate types detected by microprobe analyses is commonly greater (likely because some carbonates are present in amounts below the detection limit of Rietveld XRD).
- In two cases, the presence of carbonates suggested by XRD was not confirmed by microprobe analyses, likely because they are present in very low amounts. Rietveld XRD suggests the presence of cerussite (0.2 wt%) in sample VNP 02 and the presence of calcite (0.5 wt%) in sample GS 2. Additionally, the very fine-grained texture of the carbonates in sample VNP 02 prevented reliable analyses.
- Calcite grains typically have low MgO and MnO contents (<1 wt%). The FeO content of the calcite varies from less than 1 wt% to more than 5 wt% (sample FNP 04).
- Siderite is magnesian in most samples, with MgO contents varying from approximately 6 to 22 wt%. Only three samples are characterized by MgO contents below 5 wt% (samples GS 02, GS 03 and GNP 06).
- Members of the dolomite-ankerite solid-solution series contain approximately 23 to 34 wt% CaO, 5 to 17 wt% MgO and 6 to 28.5 wt% FeO. Minor (<< 1 wt%) MnO occurs in the grains present in most samples, on rare occasions reaching up to 4 wt%.

Results reported by:

Alexandra Mauler-Steinmann,  
Ph. D., P. Geo.

Report reviewed by:

Tom Nowicki, P. Geo.

**APPENDIX: RESULTS OF MICROPROBE ANALYSIS**

(Analyses with total oxide contents of less than 98% or greater than 102% are highlighted in grey.)

**A1: FNP 02**

	<b>Oxide wt.% (*CO2 from stoichiometry)</b>						
	MGO	CAO	MNO	FEO	PBO	CO2 *	TOTAL
FNP02-1	0.03	56.73	0.00	0.05	n.a.	44.59	101.40
FNP02-2	0.06	56.57	0.09	0.08	n.a.	44.57	101.37
FNP02-3	0.03	57.48	0.01	0.07	n.a.	45.19	102.78
FNP02-4	0.06	56.76	0.11	0.08	n.a.	44.73	101.74
FNP02-5	0.04	56.51	0.01	0.12	n.a.	44.47	101.15
FNP02-6	0.04	56.90	0.04	0.15	n.a.	44.82	101.95
FNP02-7	0.06	57.14	0.05	0.10	n.a.	45.00	102.35
FNP02-8	0.00	57.07	0.08	0.04	n.a.	44.86	102.05
FNP02-9	0.01	56.61	0.07	0.21	n.a.	44.61	101.51
FNP02-10	0.05	57.15	0.05	0.05	n.a.	44.97	102.27
FNP02-11	0.00	56.94	0.06	0.21	n.a.	44.85	102.06
FNP02-12	0.02	56.69	0.12	0.18	n.a.	44.70	101.71
FNP02-13	0.02	56.56	0.00	0.11	n.a.	44.48	101.17
FNP02-14	0.06	56.84	0.08	0.08	n.a.	44.77	101.83
FNP02-15	0.03	57.13	0.08	0.11	n.a.	44.99	102.34
FNP02-16	0.05	56.78	0.13	0.10	n.a.	44.76	101.82
FNP02-17	0.02	56.90	0.03	0.08	n.a.	44.74	101.77
FNP02-18	0.01	56.97	0.04	0.11	n.a.	44.81	101.94
FNP02-19	0.06	57.02	0.05	0.08	n.a.	44.90	102.11
FNP02-20	0.03	56.88	0.03	0.12	n.a.	44.76	101.82

n.a. = not analyzed

**A2: FNP 04**

	<b>Oxide wt.% (*CO2 from stoichiometry)</b>						
	MGO	CAO	MNO	FEO	PBO	CO2 *	TOTAL
FNP04-1	0.92	51.32	0.26	4.87	n.a.	44.43	101.80
FNP04-2	1.09	49.48	0.35	5.11	n.a.	43.37	99.40
FNP04-3	0.94	50.63	0.27	5.07	n.a.	44.03	100.94
FNP04-4	0.88	49.23	0.39	5.05	n.a.	42.93	98.48
FNP04-5	1.14	50.91	0.31	2.75	n.a.	43.08	98.19
FNP04-6	0.76	54.18	0.39	1.04	n.a.	44.23	100.60
FNP04-7	0.10	52.84	0.09	0.11	n.a.	41.70	94.84
FNP04-8	0.07	56.13	0.06	0.15	n.a.	44.26	100.67
FNP04-9	0.06	54.81	0.04	0.13	n.a.	43.19	98.23
FNP04-10	0.18	56.01	0.02	0.18	n.a.	44.28	100.67
FNP04-11	0.81	53.54	0.11	0.55	n.a.	43.31	98.32
FNP04-12	0.02	55.05	0.05	0.05	n.a.	43.29	98.46
FNP04-13	0.05	56.47	0.01	0.05	n.a.	44.41	100.99
FNP04-14	0.04	56.82	0.05	0.07	n.a.	44.71	101.69
FNP04-15	0.17	55.82	0.07	0.23	n.a.	44.18	100.47
FNP04-16	0.04	56.15	0.05	0.10	n.a.	44.20	100.54
FNP04-17	0.06	55.81	0.02	0.09	n.a.	43.93	99.91
FNP04-18	0.13	55.95	0.09	0.24	n.a.	44.25	100.66
FNP04-19	0.10	54.44	0.10	0.18	n.a.	43.01	97.83
FNP04-20	0.14	55.24	0.09	0.20	n.a.	43.68	99.35

n.a. = not analyzed

**A3: FNP 06**

	<b>Oxide wt.% (*CO2 from stoichiometry)</b>						
	MGO	CAO	MNO	FEO	PBO	CO2 *	TOTAL
FNP06-1	0.02	57.79	0.24	0.18	n.a.	45.63	103.86
FNP06-2	0.06	57.86	0.16	0.16	n.a.	45.67	103.91
FNP06-3	0.06	55.99	0.09	0.18	n.a.	44.17	100.49
FNP06-4	0.02	56.88	0.06	0.15	n.a.	44.79	101.90
FNP06-5	0.03	58.52	0.05	0.13	n.a.	46.07	104.80
FNP06-6	0.34	56.06	0.00	0.44	n.a.	44.64	101.48
FNP06-7	0.06	54.95	0.13	0.12	n.a.	43.34	98.60
FNP06-8	0.02	57.71	0.03	0.10	n.a.	45.39	103.25
FNP06-9	0.03	54.86	0.11	0.16	n.a.	43.25	98.41
FNP06-10	0.06	58.02	0.10	0.15	n.a.	45.75	104.08
FNP06-11	0.05	57.73	0.20	0.05	n.a.	45.52	103.55
FNP06-12	0.06	58.04	0.20	0.09	n.a.	45.79	104.18
FNP06-13	0.06	57.67	0.18	0.23	n.a.	45.58	103.72
FNP06-14	0.16	57.25	0.12	0.22	n.a.	45.31	103.06
FNP06-15	1.67	49.10	0.49	3.57	n.a.	42.85	97.68
FNP06-16	2.21	47.05	0.63	4.70	n.a.	42.61	97.20
FNP06-17	1.45	48.20	0.45	4.49	n.a.	42.44	97.03
FNP06-18	0.03	57.89	0.14	0.19	n.a.	45.67	103.92
FNP06-19	0.00	57.77	0.15	0.18	n.a.	45.54	103.64
FNP06-20	0.08	57.90	0.16	0.27	n.a.	45.79	104.20

n.a. = not analyzed

**A4: FNP 13**

	<b>Oxide wt.% (*CO2 from stoichiometry)</b>						
	MGO	CAO	MNO	FEO	PBO	CO2 *	TOTAL
FNP13-1	11.21	1.54	0.57	45.94	n.a.	41.94	101.20
FNP13-2	9.64	1.97	0.32	46.24	n.a.	40.60	98.77
FNP13-3	12.00	4.86	0.40	40.39	n.a.	41.91	99.56
FNP13-4	7.52	2.09	0.90	50.26	n.a.	41.20	101.97
FNP13-5	14.19	29.10	0.67	11.68	n.a.	45.90	101.54
FNP13-6	13.65	25.15	0.48	16.29	n.a.	44.92	100.49
FNP13-7	16.54	23.46	0.67	14.13	n.a.	45.54	100.34
FNP13-8	11.92	2.45	0.65	43.89	n.a.	42.23	101.14
FNP13-9	8.83	4.05	0.53	46.13	n.a.	41.41	100.95
FNP13-10	7.83	1.82	1.23	48.98	n.a.	40.74	100.60
FNP13-11	7.90	3.87	0.75	47.08	n.a.	40.97	100.57
FNP13-12	10.79	3.62	0.95	43.92	n.a.	42.12	101.40
FNP13-13	13.45	1.87	0.53	43.43	n.a.	43.09	102.37
FNP13-14	9.94	1.91	0.55	46.38	n.a.	41.10	99.88
FNP13-15	9.79	3.98	0.72	45.55	n.a.	42.16	102.20
FNP13-16	4.64	2.48	0.65	54.15	n.a.	40.59	102.51
FNP13-17	10.56	1.48	0.82	46.67	n.a.	41.79	101.32
FNP13-18	8.85	2.92	0.60	47.99	n.a.	41.72	102.08
FNP13-19	9.25	2.05	0.62	48.52	n.a.	41.82	102.26
FNP13-20	13.52	3.38	0.63	41.21	n.a.	43.05	101.79

n.a. = not analyzed



**A5: GS 2**

	<b>Oxide wt.% (*CO2 from stoichiometry)</b>						
	MGO	CAO	MNO	FEO	PBO	CO2 *	TOTAL
GS2-1	11.26	28.95	0.51	15.29	n.a.	44.70	100.71
GS2-2	9.22	28.59	0.27	19.17	n.a.	44.42	101.67
GS2-3	11.13	28.83	0.38	15.75	n.a.	44.66	100.75
GS2-4	11.50	28.95	0.40	15.62	n.a.	45.09	101.56
GS2-5	11.66	28.85	0.40	14.69	n.a.	44.62	100.22
GS2-6	11.07	28.85	0.52	16.21	n.a.	44.98	101.63
GS2-7	10.71	2.83	0.38	45.35	n.a.	41.93	101.20
GS2-8	13.56	4.24	0.21	40.50	n.a.	43.07	101.58
GS2-9	11.69	28.53	0.28	15.80	n.a.	45.01	101.31
GS2-10	11.92	3.08	0.25	43.09	n.a.	41.98	100.32
GS2-11	12.65	31.44	0.56	9.70	n.a.	44.78	99.13
GS2-12	10.12	3.64	0.14	44.76	n.a.	41.41	100.07
GS2-13	9.83	7.74	0.19	41.42	n.a.	42.30	101.48
GS2-14	14.46	31.44	0.69	8.39	n.a.	46.03	101.01
GS2-15	11.67	29.25	0.31	15.04	n.a.	45.10	101.37
GS2-16	11.82	28.77	0.29	15.62	n.a.	45.23	101.73
GS2-17	10.99	28.88	0.37	16.43	n.a.	44.96	101.63
GS2-18	9.86	27.59	0.45	17.75	n.a.	43.57	99.22
GS2-19	11.08	29.48	0.42	15.17	n.a.	44.79	100.94
GS2-20	13.27	29.16	0.48	13.18	n.a.	45.75	101.84

n.a. = not analyzed

**A6: GS 3**

	<b>Oxide wt.% (*CO2 from stoichiometry)</b>						
	MGO	CAO	MNO	FEO	PBO	CO2 *	TOTAL
GS3-1	11.07	32.13	0.52	11.88	n.a.	44.90	100.50
GS3-2	11.26	32.71	0.45	10.69	n.a.	44.79	99.90
GS3-3	5.44	4.96	0.47	49.41	n.a.	40.39	100.67
GS3-4	12.03	32.16	0.42	10.21	n.a.	44.89	99.71
GS3-5	5.63	6.91	0.49	46.40	n.a.	40.30	99.73
GS3-6	4.87	6.65	0.29	48.17	n.a.	40.22	100.20
GS3-7	3.20	49.55	0.42	2.36	n.a.	44.09	99.62
GS3-8	12.36	33.02	0.53	8.59	n.a.	45.00	99.50
GS3-9	12.66	34.00	0.49	7.32	n.a.	45.30	99.77
GS3-10	0.46	52.68	0.52	1.72	n.a.	43.22	98.60
GS3-11	0.54	52.53	0.43	1.71	n.a.	43.13	98.34
GS3-12	5.30	7.89	0.39	46.64	n.a.	40.79	101.01
GS3-13	10.54	32.88	0.42	11.06	n.a.	44.35	99.25
GS3-14	4.74	6.30	0.54	49.10	n.a.	40.53	101.21
GS3-15	4.81	6.73	0.30	48.00	n.a.	40.12	99.96
GS3-16	13.03	32.46	0.45	8.39	n.a.	45.12	99.45
GS3-17	12.35	32.69	0.40	9.64	n.a.	45.29	100.37
GS3-18	11.48	32.46	0.60	10.87	n.a.	45.04	100.45
GS3-19	13.30	32.60	0.45	8.08	n.a.	45.34	99.77
GS3-20	5.25	5.84	0.49	48.70	n.a.	40.45	100.73

n.a. = not analyzed

**A7: GS 5**

	<b>Oxide wt.% (*CO2 from stoichiometry)</b>						
	MGO	CAO	MNO	FEO	PBO	CO2 *	TOTAL
GS5-1	0.55	55.20	0.58	1.05	n.a.	44.92	102.30
GS5-2	0.43	55.37	0.46	0.76	n.a.	44.68	101.70
GS5-3	7.59	5.81	0.34	46.74	n.a.	41.69	102.17
GS5-4	5.42	24.61	0.42	28.52	n.a.	42.96	101.93
GS5-5	0.33	56.01	0.45	0.58	n.a.	44.95	102.32
GS5-6	0.35	55.99	0.39	0.72	n.a.	45.01	102.46
GS5-7	0.35	55.99	0.50	0.79	n.a.	45.12	102.75
GS5-8	0.34	55.86	0.46	0.76	n.a.	44.96	102.38
GS5-9	0.46	55.53	0.41	0.76	n.a.	44.80	101.96
GS5-10	4.46	1.00	0.47	56.34	n.a.	40.46	102.73
GS5-11	4.77	2.05	0.37	55.02	n.a.	40.75	102.96
GS5-12	4.15	3.01	0.58	53.31	n.a.	39.91	100.96
GS5-13	3.55	48.75	0.43	4.13	n.a.	44.93	101.79
GS5-14	0.34	55.56	0.44	0.71	n.a.	44.68	101.73
GS5-15	0.40	55.28	0.50	0.71	n.a.	44.57	101.46
GS5-16	0.33	55.10	0.39	0.76	n.a.	44.31	100.89
GS5-17	0.34	56.02	0.53	0.69	n.a.	45.09	102.67
GS5-18	0.80	54.28	0.46	1.43	n.a.	44.63	101.60
GS5-19	0.76	54.83	0.32	1.39	n.a.	44.91	102.21
GS5-20	0.51	55.05	0.44	1.49	n.a.	44.95	102.44

n.a. = not analyzed

**A8: GS 7**

	<b>Oxide wt.% (*CO2 from stoichiometry)</b>						
	MGO	CAO	MNO	FEO	PBO	CO2 *	TOTAL
GS7-1	0.36	53.80	0.62	2.43	n.a.	44.49	101.70
GS7-2	0.31	54.89	0.75	1.54	n.a.	44.83	102.32
GS7-3	0.21	55.28	0.56	0.96	n.a.	44.55	101.56
GS7-4	0.24	55.40	0.27	1.25	n.a.	44.67	101.83
GS7-5	0.32	54.17	0.62	1.36	n.a.	44.08	100.55
GS7-6	0.36	54.70	0.59	1.83	n.a.	44.81	102.29
GS7-7	0.07	56.55	0.67	0.24	n.a.	45.02	102.55
GS7-8	0.08	56.60	0.61	0.09	n.a.	44.94	102.32
GS7-9	0.02	56.64	0.51	0.20	n.a.	44.91	102.28
GS7-10	0.06	57.00	0.55	0.10	n.a.	45.20	102.91
GS7-11	0.02	56.28	0.82	0.39	n.a.	44.94	102.45
GS7-12	0.06	56.85	0.46	0.12	n.a.	45.04	102.53
GS7-13	0.22	55.78	0.68	0.65	n.a.	44.84	102.17
GS7-14	0.08	56.55	0.71	0.37	n.a.	45.14	102.85
GS7-15	0.16	56.09	0.60	0.46	n.a.	44.85	102.16
GS7-16	0.13	56.70	0.19	0.39	n.a.	45.00	102.41
<b>GS7-17</b>	<b>0.87</b>	<b>54.63</b>	<b>0.40</b>	<b>1.05</b>	<b>n.a.</b>	<b>44.72</b>	<b>101.67</b>
GS7-18	0.20	56.32	0.30	0.56	n.a.	44.95	102.33
GS7-19	0.03	56.74	0.44	0.01	n.a.	44.84	102.06
GS7-20	0.12	55.89	0.68	0.42	n.a.	44.67	101.78

n.a. = not analyzed

**A9: GS 8**

	<b>Oxide wt.% (*CO2 from stoichiometry)</b>						
	MGO	CAO	MNO	FEO	PBO	CO2 *	TOTAL
GS8-1	15.74	1.23	0.31	38.81	n.d.	42.12	98.21
GS8-2	13.50	8.73	0.24	35.23	n.d.	43.32	101.02
GS8-3	16.28	1.42	0.28	38.25	n.d.	42.50	98.73
GS8-4	17.33	1.31	0.25	39.03	n.d.	44.01	101.93
GS8-5	15.33	29.24	0.84	10.20	n.d.	46.46	102.07
GS8-6	15.69	30.02	0.73	8.92	n.d.	46.61	101.97
GS8-7	15.52	30.02	0.62	9.68	n.d.	46.82	102.66
GS8-8	15.49	27.04	0.42	13.14	n.d.	46.44	102.53
GS8-9	14.80	30.77	0.57	10.43	n.d.	47.05	103.62
GS8-10	16.31	30.71	0.74	8.44	n.d.	47.54	103.74
GS8-11	13.05	1.29	0.25	42.88	n.d.	41.68	99.15
GS8-12	22.01	0.62	0.33	32.91	n.d.	44.88	100.75
GS8-13	22.08	0.71	0.26	33.91	n.d.	45.60	102.56
GS8-14	16.44	30.18	0.85	7.98	n.d.	47.05	102.50
GS8-15	16.47	30.61	0.74	7.99	n.d.	47.36	103.17
GS8-16	16.81	30.99	0.91	6.99	n.d.	47.52	103.22
GS8-17	16.45	30.84	0.04	6.86	n.d.	46.39	100.58
GS8-18	15.29	31.15	0.70	9.10	n.d.	47.15	103.39
GS8-19	15.17	30.67	0.67	9.92	n.d.	47.13	103.56
GS8-20	16.84	30.67	0.82	6.64	n.d.	47.03	102.00

n.d. = not detected

**A10: GNP 02**

	<b>Oxide wt.% (*CO2 from stoichiometry)</b>						
	MGO	CAO	MNO	FEO	PBO	CO2 *	TOTAL
GNP02-1	0.39	54.80	0.35	1.00	n.a.	44.26	100.80
GNP02-2	0.30	54.68	0.38	0.91	n.a.	44.03	100.30
GNP02-3	0.41	54.98	0.38	0.72	n.a.	44.27	100.76
GNP02-4	0.36	55.28	0.45	0.77	n.a.	44.53	101.39
GNP02-5	0.52	54.36	0.48	1.29	n.a.	44.32	100.97
GNP02-6	0.48	54.71	0.40	1.01	n.a.	44.33	100.93
GNP02-7	0.48	54.33	0.52	0.92	n.a.	44.05	100.30
GNP02-8	0.45	54.40	0.49	0.90	n.a.	44.04	100.28
GNP02-9	13.12	34.14	0.32	7.16	n.a.	45.70	100.44
GNP02-10	0.47	54.55	0.45	1.13	n.a.	44.30	100.90
GNP02-11	0.37	55.18	0.37	1.02	n.a.	44.56	101.50
GNP02-12	0.45	54.72	0.40	1.09	n.a.	44.35	101.01
GNP02-13	0.36	54.91	0.36	1.18	n.a.	44.43	101.24
GNP02-14	0.43	54.89	0.34	1.06	n.a.	44.41	101.13
GNP02-15	0.48	54.49	0.36	1.16	n.a.	44.22	100.71
GNP02-16	11.58	33.14	0.35	10.88	n.a.	45.53	101.48
GNP02-17	6.77	2.94	0.30	49.32	n.a.	40.10	99.43
GNP02-18	10.03	1.42	0.56	48.26	n.a.	41.98	102.25
GNP02-19	0.24	55.79	0.27	0.55	n.a.	44.55	101.40
GNP02-20	0.16	56.24	0.32	0.43	n.a.	44.77	101.92

n.a. = not analyzed

**A11: GNP 03**

	<b>Oxide wt.% (*CO2 from stoichiometry)</b>						
	MGO	CAO	MNO	FEO	PBO	CO2 *	TOTAL
GNP03-1	0.51	57.36	0.48	1.12	n.a.	46.56	106.03
GNP03-2	0.56	56.08	0.48	1.49	n.a.	45.83	104.44
GNP03-3	0.52	56.87	0.51	1.38	n.a.	46.36	105.64
GNP03-4	0.57	55.91	0.48	1.55	n.a.	45.75	104.26
GNP03-5	0.61	55.56	0.55	1.62	n.a.	45.60	103.94
GNP03-6	0.57	56.02	0.42	1.35	n.a.	45.67	104.03
GNP03-7	0.50	57.45	0.41	1.21	n.a.	46.63	106.20
GNP03-8	0.54	54.73	0.48	1.32	n.a.	44.65	101.72
GNP03-9	0.56	54.05	0.48	1.36	n.a.	44.16	100.61
GNP03-10	0.49	54.45	0.48	1.28	n.a.	44.35	101.05
GNP03-11	0.51	54.37	0.55	1.23	n.a.	44.32	100.98
GNP03-12	0.47	54.36	0.49	1.16	n.a.	44.19	100.67
GNP03-13	0.52	54.69	0.45	1.22	n.a.	44.52	101.40
GNP03-14	0.53	54.41	0.46	1.37	n.a.	44.40	101.17
GNP03-15	0.54	55.07	0.37	1.34	n.a.	44.86	102.18
GNP03-16	0.58	54.40	0.54	1.36	n.a.	44.49	101.37
GNP03-17	0.01	57.66	0.14	0.11	n.a.	45.42	103.34
GNP03-18	0.00	57.65	0.00	0.03	n.a.	45.26	102.94
GNP03-19	0.04	57.65	0.08	0.10	n.a.	45.40	103.27
GNP03-20	0.00	58.00	0.00	0.03	n.a.	45.54	103.57

n.a. = not analyzed

**A12: GNP 05**

	<b>Oxide wt.% (*CO2 from stoichiometry)</b>						
	MGO	CAO	MNO	FEO	PBO	CO2 *	TOTAL
GNP05-1	9.57	1.37	0.14	48.57	n.a.	41.36	101.01
GNP05-2	10.97	1.49	0.16	46.01	n.a.	41.43	100.06
GNP05-3	12.51	4.03	0.14	41.91	n.a.	42.58	101.17
GNP05-4	11.64	4.17	0.24	41.26	n.a.	41.41	98.72
GNP05-5	10.59	4.50	0.09	42.48	n.a.	41.17	98.83
GNP05-6	9.87	2.40	0.15	46.15	n.a.	41.02	99.59
GNP05-7	9.63	2.46	0.17	46.48	n.a.	41.02	99.76
GNP05-8	12.96	4.14	0.07	40.55	n.a.	42.28	100.00
GNP05-9	14.63	1.77	0.10	41.17	n.a.	42.65	100.32
GNP05-10	9.64	2.49	0.20	45.72	n.a.	40.61	98.66
GNP05-11	3.11	4.32	0.10	53.06	n.a.	39.35	99.94
GNP05-12	2.03	2.96	0.02	56.69	n.a.	39.28	100.98
GNP05-13	12.03	2.79	0.20	43.70	n.a.	42.22	100.94
GNP05-14	7.64	2.33	0.29	48.57	n.a.	40.10	98.93
GNP05-15	9.37	2.37	0.55	47.56	n.a.	41.57	101.42
GNP05-16	13.28	0.95	0.18	43.93	n.a.	42.27	100.61
GNP05-17	14.91	1.30	0.12	41.85	n.a.	43.01	101.19
GNP05-18	14.77	1.33	0.18	41.81	n.a.	42.89	100.98
GNP05-19	16.72	2.13	0.06	38.18	n.a.	43.35	100.44
GNP05-20	7.05	1.09	0.04	50.90	n.a.	39.76	98.84

n.a. = not analyzed



**A13: GNP 06**

	<b>Oxide wt.% (*CO2 from stoichiometry)</b>						
	MGO	CAO	MNO	FEO	PBO	CO2 *	TOTAL
GNP06-1	5.36	6.09	0.26	47.84	n.d.	40.10	99.65
GNP06-2	4.72	6.89	0.28	48.20	n.d.	40.26	100.35
GNP06-3	4.17	6.55	0.06	48.80	n.d.	39.62	99.20
GNP06-4	9.86	7.96	0.27	40.63	n.d.	42.07	100.79
GNP06-5	9.63	7.32	0.33	40.66	n.d.	41.37	99.31
GNP06-6	10.56	7.37	0.20	40.17	n.d.	42.05	100.35
GNP06-7	10.75	7.09	0.34	40.72	n.d.	42.46	101.36
GNP06-8	10.42	7.20	0.22	40.38	n.d.	41.90	100.12
GNP06-9	10.83	7.32	0.34	40.08	n.d.	42.33	100.90
GNP06-10	0.14	55.86	0.51	0.43	n.d.	44.57	101.51
GNP06-11	0.14	55.56	0.60	0.47	n.d.	44.42	101.19
GNP06-12	0.29	54.71	0.88	0.75	n.d.	44.26	100.89
GNP06-13	0.31	55.17	0.74	0.69	n.d.	44.52	101.43
GNP06-14	0.15	55.35	0.65	0.59	n.d.	44.37	101.11
GNP06-15	0.18	55.13	0.52	0.58	n.d.	44.14	100.55
GNP06-16	0.39	54.77	0.70	0.99	n.d.	44.45	101.30
GNP06-17	0.36	54.77	0.64	0.87	n.d.	44.31	100.95
GNP06-18	9.80	6.44	0.30	42.99	n.d.	42.27	101.80
GNP06-19	10.03	7.28	0.28	40.99	n.d.	41.95	100.53
GNP06-20	0.10	55.66	0.60	0.54	n.d.	44.49	101.39

n.d. = not detected

**A14: GNP 07**

	<b>Oxide wt.% (*CO2 from stoichiometry)</b>						
	MGO	CAO	MNO	FEO	PBO	CO2 *	TOTAL
GNP07-1	0.32	55.80	0.28	0.61	n.a.	44.69	101.70
GNP07-2	0.38	55.53	0.23	0.75	n.a.	44.60	101.49
GNP07-3	0.34	55.48	0.29	0.64	n.a.	44.48	101.23
GNP07-4	0.38	55.44	0.27	0.65	n.a.	44.49	101.23
GNP07-5	0.59	54.66	0.30	0.95	n.a.	44.31	100.81
GNP07-6	0.35	55.14	0.23	0.53	n.a.	44.12	100.37
GNP07-7	0.39	54.50	0.26	0.59	n.a.	43.72	99.46
GNP07-8	0.37	55.65	0.29	0.66	n.a.	44.66	101.63
GNP07-9	0.38	55.82	0.21	0.57	n.a.	44.70	101.68
GNP07-10	0.27	55.81	0.28	0.69	n.a.	44.69	101.74
GNP07-11	0.35	55.70	0.26	0.59	n.a.	44.62	101.52
GNP07-12	0.31	55.42	0.23	0.56	n.a.	44.32	100.84
GNP07-13	0.32	55.36	0.27	0.57	n.a.	44.31	100.83
GNP07-14	0.49	54.20	0.28	0.72	n.a.	43.69	99.38
GNP07-15	0.37	53.98	0.24	0.88	n.a.	43.46	98.93
GNP07-16	0.34	55.37	0.35	0.73	n.a.	44.49	101.28
GNP07-17	0.30	55.53	0.28	0.62	n.a.	44.46	101.19
GNP07-18	0.48	54.95	0.21	1.02	n.a.	44.40	101.06
GNP07-19	0.37	55.30	0.30	0.71	n.a.	44.42	101.10
GNP07-20	0.39	55.32	0.37	0.76	n.a.	44.54	101.38

n.a. = not analyzed

**A15: GNP 09**

	<b>Oxide wt.% (*CO2 from stoichiometry)</b>						
	MGO	CAO	MNO	FEO	PBO	CO2 *	TOTAL
GNP09-1	0.15	55.62	0.56	0.47	n.a.	44.45	101.25
GNP09-2	0.08	56.06	0.30	0.19	n.a.	44.39	101.02
GNP09-3	0.31	54.67	0.73	0.67	n.a.	44.11	100.49
GNP09-4	0.66	53.95	0.24	1.73	n.a.	44.27	100.85
GNP09-5	0.83	53.59	0.31	1.75	n.a.	44.23	100.71
GNP09-6	0.78	54.20	0.25	1.66	n.a.	44.56	101.45
GNP09-7	0.54	54.08	0.18	1.56	n.a.	44.10	100.46
GNP09-8	0.91	53.54	0.35	1.89	n.a.	44.39	101.08
GNP09-9	0.54	54.17	0.30	1.32	n.a.	44.10	100.43
GNP09-10	0.69	54.15	0.24	1.84	n.a.	44.53	101.45
GNP09-11	0.79	53.73	0.33	1.87	n.a.	44.38	101.10
GNP09-12	0.88	53.66	0.26	1.87	n.a.	44.38	101.05
GNP09-13	0.75	54.31	0.22	1.66	n.a.	44.60	101.54
GNP09-14	0.45	54.83	0.33	1.14	n.a.	44.43	101.18
GNP09-15	0.78	53.68	0.41	1.71	n.a.	44.28	100.86
GNP09-16	0.79	53.96	0.28	1.60	n.a.	44.36	100.99
GNP09-17	0.66	54.16	0.21	1.71	n.a.	44.40	101.14
GNP09-18	0.57	54.66	0.22	1.45	n.a.	44.54	101.44
GNP09-19	0.58	54.19	0.22	1.53	n.a.	44.24	100.76
GNP09-20	0.63	54.50	0.30	1.50	n.a.	44.56	101.49

n.a. = not analyzed

**A16: GNP 11**

	<b>Oxide wt.% (*CO2 from stoichiometry)</b>						
	MGO	CAO	MNO	FEO	PBO	CO2 *	TOTAL
GNP11-1	0.39	54.90	0.69	0.82	n.a.	44.44	101.24
GNP11-2	0.65	54.67	0.35	1.32	n.a.	44.64	101.63
GNP11-3	0.70	54.65	0.27	1.52	n.a.	44.75	101.89
GNP11-4	0.73	54.46	0.33	1.55	n.a.	44.69	101.76
GNP11-5	11.53	32.12	0.68	11.62	n.a.	45.34	101.29
GNP11-6	12.97	30.25	0.46	11.95	n.a.	45.51	101.14
GNP11-7	13.04	30.66	0.59	12.29	n.a.	46.20	102.78
GNP11-8	13.40	30.37	0.57	11.90	n.a.	46.11	102.35
GNP11-9	0.70	54.34	0.31	1.79	n.a.	44.70	101.84
GNP11-10	0.62	54.67	0.29	1.64	n.a.	44.77	101.99
GNP11-11	7.81	40.79	0.71	6.51	n.a.	44.97	100.79
GNP11-12	13.06	30.40	0.60	12.61	n.a.	46.22	102.89
GNP11-13	13.24	30.56	0.53	12.27	n.a.	46.29	102.89
GNP11-14	0.49	54.03	0.57	1.39	n.a.	44.14	100.62
GNP11-15	0.42	54.42	0.53	1.13	n.a.	44.19	100.69
GNP11-16	0.43	54.93	0.52	1.21	n.a.	44.64	101.73
GNP11-17	0.45	54.74	0.50	1.14	n.a.	44.46	101.29
GNP11-18	0.27	54.34	0.83	2.31	n.a.	44.87	102.62
GNP11-19	0.54	54.87	0.72	1.51	n.a.	45.02	102.66
GNP11-20	0.58	54.66	0.67	1.78	n.a.	45.04	102.73

n.a. = not analyzed

**A17: VNP 02**

	<b>Oxide wt.% (*CO2 from stoichiometry)</b>						
	MGO	CAO	MNO	FEO	PBO	CO2 *	TOTAL
VNP02-1	11.94	0.66	1.85	44.53	n.d.	41.98	100.96
VNP02-2	11.48	7.98	2.45	35.99	n.d.	42.37	100.30
VNP02-3	10.50	0.66	2.17	46.73	n.d.	41.95	102.01
VNP02-4	10.58	0.63	2.24	46.00	n.d.	41.64	101.20
VNP02-5	11.63	0.27	1.89	44.78	n.d.	41.53	100.16
VNP02-6	13.87	29.24	1.46	9.76	0.18	45.01	99.52
VNP02-7	3.88	0.96	4.19	48.67	4.43	38.28	100.41
VNP02-8	9.46	1.54	2.43	45.90	n.d.	41.17	100.55
VNP02-9	11.20	4.30	1.95	40.36	0.82	41.70	100.33

n.d. = not detected